PHYSICAL REVIEW D **85,** 092002 (2012)

Study of jets produced in association with a W boson in pp collisions at $\sqrt{s} = 7$ TeV with the ATLAS detector

G. Aad *et al.**
(ATLAS Collaboration)

(Received 5 January 2012; published 2 May 2012)

We report a study of final states containing a W boson and hadronic jets, produced in proton-proton collisions at a center-of-mass energy of 7 TeV. The data were collected with the ATLAS detector at the CERN LHC and comprise the full 2010 data sample of 36 pb^{-1}. Cross sections are determined using both the electron and muon decay modes of the W boson and are presented as a function of inclusive jet multiplicity, N_{jet}, for up to five jets. At each multiplicity, cross sections are presented as a function of jet transverse momentum, the scalar sum of the transverse momenta of the charged lepton, missing transverse momentum, and all jets, the invariant mass spectra of jets, and the rapidity distributions of various combinations of leptons and final-state jets. The results, corrected for all detector effects and for all backgrounds such as diboson and top quark pair production, are compared with particle-level predictions from perturbative QCD. Leading-order multiparton event generators, normalized to the next-to-next-to-leading-order total cross section for inclusive W-boson production, describe the data reasonably well for all measured inclusive jet multiplicities. Next-to-leading-order calculations from MCFM, studied here for $N_{\text{jet}} \leq 2$, and BLACKHAT-SHERPA, studied here for $N_{\text{jet}} \leq 4$, are found to be mostly in good agreement with the data.

DOI: 10.1103/PhysRevD.85.092002 PACS numbers: 12.38.Qk, 13.85.Hd, 13.85.Qk, 13.87.Ce

I. INTRODUCTION

The study of massive vector boson production in association with one or more jets is an important test of quantum chromodynamics (QCD). These final states are also a significant background to studies of standard model processes such as $t\bar{t}$, diboson, and single-top production, as well as to searches for the Higgs boson and for physics beyond the standard model. Thus, measurements of the cross section and kinematic properties, and comparisons with theoretical predictions, are of significant interest. Measurements of W + jets production in proton-antiproton collisions at $\sqrt{s} = 1.96$ TeV have been reported by the CDF and D0 Collaborations [1,2] and for $\sqrt{s} = 7$ TeV proton-proton collisions by the CMS Collaboration [3]. Measurements of jets produced in association with a Z boson were also performed using $p\bar{p}$ collisions at $\sqrt{s} = 1.96$ TeV [4–6] and pp collisions at $\sqrt{s} = 7$ TeV [3,7]. The study presented here is complementary to the measurement of the transverse momentum distribution of W bosons conducted by the ATLAS Collaboration [8].

This paper reports a measurement at the CERN Large Hadron Collider (LHC) of the W + jets cross section for proton-proton (pp) collisions at a center-of-mass energy ($\sqrt{s}$) of 7 TeV, using the ATLAS detector. The measurement is based on the full 2010 data sample, corresponding to an integrated luminosity of approximately 36 pb^{-1}. It is an extension of an earlier ATLAS measurement of both the electron and muon decay modes of the W boson based on 1.3 pb^{-1} [9]. Compared to the earlier result, uncertainties in both the jet energy scale and luminosity are reduced, acceptance for the jets is expanded, and event reconstruction and simulation are improved. The improved reconstruction brings better alignment of the detector systems and reduction of backgrounds in the electron channel.

The results have been corrected for all known detector effects and are quoted in a specific range of jet and lepton kinematics, fully covered by the detector acceptance. This avoids model-dependent extrapolations and facilitates comparisons with theoretical predictions. Theoretical calculations at next-to-leading order (NLO) in perturbative QCD (pQCD) have been computed inclusively for up to four jets [10,11] and are compared with the data.

II. THE ATLAS DETECTOR

ATLAS uses a right-handed coordinate system with its origin at the nominal pp interaction point (IP) in the center of the detector and the z-axis along the beam pipe. The x-axis points from the IP to the center of the LHC ring, and the y-axis points upward. Cylindrical coordinates (r, ϕ) are used in the transverse plane, ϕ being the azimuthal angle around the beam pipe. The pseudorapidity is defined in terms of the polar angle θ as $\eta = -\ln[\tan(\theta/2)]$ and the rapidity is defined as $y = \ln[(E + p_z)/(E - p_z)]/2$. The separation between final-state particles is defined as $\Delta R = \sqrt{(\Delta y)^2 + (\Delta\phi)^2}$ and is Lorentz invariant under boosts along the z-axis.

*Full author list given at the end of the article.

The ATLAS detector [12,13] consists of an inner tracking system (inner detector, or ID) surrounded by a thin superconducting solenoid providing a 2T magnetic field, electromagnetic and hadronic calorimeters, and a muon spectrometer (MS). The ID consists of pixel and silicon microstrip detectors, surrounded by a transition radiation tracker. The electromagnetic calorimeter is a liquid-argon and lead detector, split into barrel ($|\eta| < 1.475$) and end cap ($1.375 < |\eta| < 3.2$) regions. Hadron calorimetry is based on two different detector technologies. The barrel ($|\eta| < 0.8$) and extended barrel ($0.8 < |\eta| < 1.7$) calorimeters are composed of scintillator and steel, while the hadronic end cap calorimeters ($1.5 < |\eta| < 3.2$) utilize liquid-argon and copper. The forward calorimeters ($3.1 < |\eta| < 4.9$) are instrumented with liquid-argon/copper and liquid-argon/tungsten, providing electromagnetic and hadronic energy measurements, respectively. The MS is based on three large superconducting toroids arranged with an eight-fold azimuthal coil symmetry around the calorimeters, and a system of three stations of chambers for triggering and for precise track measurements.

III. DATA AND ONLINE EVENT SELECTION

The data for this analysis were collected during LHC operation in 2010 with proton-proton interactions at a center-of-mass energy of 7 TeV. The collisions occurred within pairs of bunches of up to $\sim 1.1 \times 10^{11}$ protons per bunch. The bunches were configured in trains with a time separation between bunches of 150 ns and a longer separation between trains. Data were collected with up to 348 colliding bunch pairs per beam revolution. This configuration led to a peak instantaneous luminosity of up to $2.1 \times 10^{32}\ \mathrm{cm}^{-2}\,\mathrm{s}^{-1}$ that corresponds to an average of 3.8 inelastic collisions per bunch crossing. Typical values were lower as the luminosity degraded during the data-taking fills which lasted up to 20 hours. On average, the data contain 2.1 inelastic collisions per bunch crossing.

Application of beam, detector, and data-quality requirements resulted in a total integrated luminosity of 36 pb^{-1}. The uncertainty on the luminosity is 3.4% [14,15]. The integrated luminosities for the data samples associated with the electron and muon decay modes of the W boson were calculated separately and differ by 1.7%.

Events were selected online if they satisfied either the electron or muon criteria described below. Criteria for electron and muon identification, as well as for event selection, followed closely those of the previous 1.3 pb^{-1} W + jets cross-section analysis [9].

For this analysis, the following kinematic requirements were imposed on events in order to enter the selected sample:

(i) $p_{\mathrm{T}}^{\ell} > 20$ GeV (ℓ = electron or muon),
(ii) $|\eta^e| < 2.47$ (except $1.37 < |\eta^e| < 1.52$) or $|\eta^\mu| < 2.4$,
(iii) $E_{\mathrm{T}}^{\mathrm{miss}} > 25$ GeV (missing transverse momentum),
(iv) $m_{\mathrm{T}}(W) > 40$ GeV,
(v) $p_{\mathrm{T}}^{\mathrm{jet}} > 30$ GeV,
(vi) $|y^{\mathrm{jet}}| < 4.4$ and $\Delta R(\ell, \mathrm{jet}) > 0.5$.

These selection criteria differ slightly from the fiducial acceptance to which measured cross sections are finally corrected, which is described in Sec. V F. The transverse momenta of the leptons and neutrinos from $W \to e\nu$ and $W \to \mu\nu$ decays are denoted as p_{T}^{ℓ} and p_{T}^{ν}, respectively. The transverse momentum of the neutrino is determined as $E_{\mathrm{T}}^{\mathrm{miss}}$, the missing transverse momentum, from the requirement that the total transverse momentum of all final-state particles is a zero vector. The calculation of $E_{\mathrm{T}}^{\mathrm{miss}}$ and the transverse mass of the W, $m_{\mathrm{T}}(W)$, are discussed later in Sec. V B.

All measured cross sections are corrected for any detection losses within these regions. The lower bound $p_{\mathrm{T}}^{\mathrm{jet}} > 30$ GeV is chosen to facilitate comparisons with other experiments and with next-to-leading-order QCD predictions. The Appendix shows analogous results with $p_{\mathrm{T}}^{\mathrm{jet}} > 20$ GeV in order to facilitate validation of the QCD description in Monte Carlo generators and future theoretical developments in this area.

A. Electron selection

In the electron channel, events were selected online using two different triggers depending on the instantaneous luminosity. The tighter trigger requirement corresponds to 99.1% of the data and is a subset of the looser one. It required the presence of at least one electromagnetic cluster in the calorimeter with transverse energy above 15 GeV in the region of $|\eta| < 2.5$. The final selection requirements were applied by the online event filter [12] and the kinematic variables correspond closely to those in the offline analysis described in Sec. V C.

The impact of the trigger efficiency was small for electrons with $E_{\mathrm{T}} > 20$ GeV, as required in this analysis. The efficiency was measured using $Z \to ee$ decays identified in the experimental data. It was found to be $99.0 \pm 0.5\%$ and constant over the full kinematic region of this measurement [16,17].

B. Muon selection

In the muon channel, events were selected online using a trigger that required the presence of a muon candidate reconstructed in both the muon spectrometer and inner detector, consistent with having originated from the interaction region. The candidate was required to have $p_{\mathrm{T}} > 10$ GeV or $p_{\mathrm{T}} > 13$ GeV (depending on the data-taking period) and $|\eta| < 2.4$. The higher threshold was used to collect most of the data. As in the electron case, these requirements were imposed in the online event filter and were less stringent than those applied offline. The offline selection is documented later in Sec. V D. The average trigger efficiency was measured to be $\sim 85\%$ including the reduced geometrical acceptance in the central region.

IV. SIMULATED EVENT SAMPLES

Simulated event samples were used for most background estimates, for the correction of the signal yield for detector effects and for comparisons of results to theoretical expectations. The detector simulation [18] was performed using GEANT4 [19]. The simulated event samples are summarized in Table I for signal simulations and Table II for the background simulations. The ALPGEN and MC@NLO samples were interfaced to HERWIG for parton shower and fragmentation processes and to JIMMY v4.31 [37] for underlying event simulation. Similarly, JIMMY was used for the underlying event simulation in the diboson samples produced with HERWIG. The ACERMC $t\bar{t}$ samples were showered with PYTHIA where the default settings for initial-state radiation (ISR) and final-state radiation (FSR) were altered [38]. The parameterization of the factorization scale used for the matrix-element (ME) calculation in the ALPGEN samples was chosen to be $Q_0^2 = m_V^2 + \sum_{\text{partons}}(p_{\text{T}}^2)$, where m_V is the mass of a W or Z boson and the decay products of the boson are not included in the sum [23]. The parton-jet matching was performed at $p_{\text{T}}^{\text{jet}} = 20$ GeV with the MLM matching scheme [39] using jets from the cone clustering algorithm with $R = 0.7$. The default renormalization and factorization scales were used in the SHERPA samples and the parton-jet matching was performed at $p_{\text{T}}^{\text{jet}} = 30$ GeV using the Catani-Krauss-Kuhn-Webber (CKKW) matching scheme [40,41]. Parton density functions (PDFs) were: CTEQ6L1 [42] for the ALPGEN samples and the parton showering and underlying event in the POWHEG samples interfaced to PYTHIA; MRST2007LO* [43] for PYTHIA, ACERMC, and the diboson samples; and CTEQ6.6M [28] for MC@NLO, SHERPA, and the NLO matrix-element calculations in POWHEG. The radiation of photons from charged leptons was treated in HERWIG and PYTHIA using PHOTOS v2.15.4 [44]. TAUOLA v1.0.2 [45] was used for τ lepton decays. The underlying event tunes were the ATLAS MC10 tunes: ATLAS underlying event tune #1 (AUET1) [46] for the HERWIG, ALPGEN, and MC@NLO samples; ATLAS minimum bias 1 (AMBT1) [47] for PYTHIA, ACERMC, and POWHEG samples. These two tunes were derived using pp collisions at $\sqrt{s} = 7$ TeV produced at the LHC. The samples generated with SHERPA used the

TABLE I. Samples of simulated signal events used in this analysis. The W samples are normalized to the inclusive next-to-next-to-leading order (NNLO) cross section of 10.46 nb calculated with FEWZ [20] using the MSTW2008 PDF set [21]. For PYTHIA, the inclusive W sample is based on a $2 \rightarrow 1$ matrix element merged with a $2 \rightarrow 2$ matrix element and a leading-logarithmic parton shower. Details of PDF sets, final-state photon radiation, and underlying event tunes are given in the text.

Physics process	Generator
W inclusive ($W \rightarrow \ell\nu$; $\ell = e, \mu, \tau$)	PYTHIA 6.4.21 [22]
W + jets ($W \rightarrow \ell\nu$; $\ell = e, \mu$; $0 \leq N_{\text{parton}} \leq 5$)	ALPGEN 2.13 [23]
W + jets ($W \rightarrow \ell\nu$; $\ell = e, \mu$; $0 \leq N_{\text{parton}} \leq 5$)	SHERPA 1.3.1 [24]

TABLE II. Samples of simulated background events used in this analysis. The Z + jets samples were normalized using the inclusive cross sections from FEWZ [20] code that utilized MSTW2008 PDF set [21]. The $t\bar{t}$ cross section is given at next-to-leading order (plus next-to-next-to-leading-log). The dijet cross sections are given at leading order in pQCD. For these samples, the variable $\hat{p}_{\text{T}}$ is the average p_{T} of the two outgoing partons from the hard-scattering process before modification by initial- and final-state radiation and the underlying event. Details of PDF sets, final-state photon radiation, and underlying event tunes are given in the text.

Physics process	Generator	$\sigma \cdot$ BR (nb)
Z + jets ($Z \rightarrow \ell\ell$; $\ell = e, \mu$; $m_{\ell\ell} > 40$ GeV; $0 \leq N_{\text{parton}} \leq 5$)	ALPGEN 2.13 [23]	1.07 NNLO [20]
$Z \rightarrow \tau\tau$ ($m_{\ell\ell} > 60$ GeV)	PYTHIA 6.4.21 [22]	0.989 NNLO [20]
$t\bar{t}$	POWHEG-HVQ v1.01 patch 4 [25]	0.165 NLO + NNLL [26]
$t\bar{t}$	ACERMC 3.7 [31]	0.165 NLO + NNLL [26]
Single-top $t \rightarrow \ell\nu q$ (s-channel)	MC@NLO 3.3.1 [32,33]	4.3×10^{-4} NLO [34]
Single-top $t \rightarrow \ell\nu q$ (t-channel)	MC@NLO 3.3.1 [32,33]	6.34×10^{-3} NLO [34]
Single-top (Wt)	MC@NLO 3.3.1 [32,35]	13.1×10^{-3} NLO [34]
WW	HERWIG 6.510 [36]	44.9×10^{-3} NLO [34]
WZ ($m_Z > 60$ GeV)	HERWIG 6.510 [36]	18.5×10^{-3} NLO [34]
ZZ ($m_Z > 60$ GeV)	HERWIG 6.510 [36]	5.96×10^{-3} NLO [34]
Dijet (μ channel, $\hat{p}_{\text{T}} > 8$ GeV, $p_{\text{T}}^{\mu} > 8$ GeV)	PYTHIA 6.4.21 [22]	10.6×10^{6} LO [22]

default underlying event tune determined from lower energy measurements and pp data from the LHC.

Samples were generated with minimum bias interactions overlaid on the hard-scattering event to account for the multiple pp interactions in the same beam crossing (pileup). The minimum bias interactions were simulated with PYTHIA with the AMBT1 tune. These samples were then reweighted so the distribution of the number of primary vertices matched that of the data.

V. OFFLINE EVENT ANALYSIS

Events were selected if they satisfied the criteria described above and had at least one interaction vertex with three or more associated charged particle tracks, located within 200 mm in z from the center of the detector. For these data the luminous region had a typical rms size of $\sim$60 mm in z. The position resolution of reconstructed vertices along z was $\sim$0.1 mm for a vertex with 10 tracks. For the sample of events passing the single-lepton trigger the mean number of interaction vertices was 2.1 per event. The primary vertex was taken as the one with the largest Σp_{T}^2 of associated tracks. Events with significant noise in the calorimeters, cosmic rays, and beam-induced background were rejected [48].

A. Jet selection

Jets were reconstructed from energy observed in the calorimeter cells using the anti-k_{t} algorithm [49] with a radius parameter $R = 0.4$ [48]. Since the volume of individual cells is small compared to the volume of the electromagnetic and hadronic energy showers, cells were grouped into clusters depending on their signal size relative to noise [50]. These clusters formed the input to the jet reconstruction. Since a jet involves many clusters a mass can be calculated and the jet rapidity rather than pseudorapidity was determined.

To account for the difference in calorimeter response between electrons and hadrons of the same energy, and to correct for other experimental effects, a p_{T} and η-dependent factor, derived from simulated events, was applied to each jet to provide an average energy-scale correction [48]. Jets were required to have a rapidity $|y| < 4.4$ and $p_{\mathrm{T}} > 30$ GeV. To ensure a reliable energy measurement all jets within $\Delta R < 0.5$ of an electron or muon (that passed the lepton identification requirements) were explicitly not considered, regardless of the jet p_{T} or rapidity, but the event itself was retained. Jets consistent with detector noise, cosmic rays, or beam halo were rejected [48]. The jet rejection requirement was more stringent than that applied to events.

To suppress jets arising from additional pp interactions a parameter called the jet-vertex fraction (JVF) was calculated for each jet in the event. After associating tracks to jets by requiring $\Delta R < 0.4$ between tracks and a jet, the JVF was computed for each jet as the scalar sum of p_{T} of all associated tracks from the primary vertex divided by the total p_{T} associated with that jet from all vertices. The JVF could not be calculated for jets which fell outside the fiducial tracking region ($|\eta| < 2.5$) or which had no matching tracks so these were assigned a value of -1 for accounting purposes. Only jets with the absolute value of the JVF smaller than 0.75 were rejected so that jets with a JVF of -1 were kept. Figure 1 shows the distribution of this parameter for all jets in the $W \rightarrow e\nu$ data and Monte Carlo event samples. The requirement on the JVF is most important for low p_{T} jets and for the data with high instantaneous luminosity.

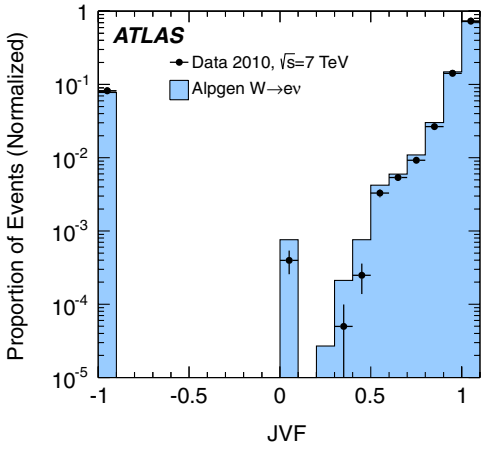

FIG. 1 (color online). Jet-vertex fraction distribution for all jets in the $W \rightarrow e\nu$ sample. The events at -1 correspond to jets where the JVF could not be calculated, while the peak near 0 corresponds to jets from a secondary vertex. For the data 99.1% of the jets pass the requirement that the absolute value of the JVF be greater than 0.75, while for the Monte Carlo sample this rate is 98.8%.

The pileup collisions also add a uniform background of particles to the events and slightly increase the measured jet energies. The jet energy calibration factor described above contains a correction for this effect.

No minimum separation ΔR was required between final-state jets, but the measured jet response changed for separations less than $\Delta R < 0.5$. This distortion in the response was corrected by the event reconstruction efficiency calculation and residual effects enter the estimated systematic uncertainties.

After the application of all jet requirements, the efficiency for reconstructing jets was determined from simulation to be $\sim$97% for jets with $p_{\mathrm{T}} = 30$ GeV, rising to close to 100% for jets above 80 GeV. The uncertainties in the jet energy scale and jet energy resolution were determined in separate studies [48]. The uncertainties in the jet energy scale were 2.5–14%, and depended on the η and p_{T} of the jet. The uncertainty on the jet energy resolution was $\sim$10% for each jet, relative to the nominal resolution which also varied with η and p_{T}.

B. Missing transverse momentum and $m_{\mathrm{T}}(W)$

The calculation of missing transverse momentum ($E_{\mathrm{T}}^{\mathrm{miss}}$) and transverse mass of W bosons ($m_{\mathrm{T}}(W)$) followed the prescription in Refs. [16,51]. $m_{\mathrm{T}}(W)$ was defined by the lepton and neutrino p_{T} and direction as $m_{\mathrm{T}}(W) = \sqrt{2p_{\mathrm{T}}^{\ell}p_{\mathrm{T}}^{\nu}(1-\cos(\phi^{\ell}-\phi^{\nu}))}$, where the (x, y) components of the neutrino momentum were taken to be the same as the corresponding $E_{\mathrm{T}}^{\mathrm{miss}}$ components. $E_{\mathrm{T}}^{\mathrm{miss}}$ was calculated from the energy deposits in calorimeter cells inside three-dimensional clusters [50]. These clusters were then corrected to account for the different response to hadrons compared to electrons or photons, as well as dead material and out-of-cluster energy losses [52]. Only clusters within $|\eta| < 4.5$ were used. In the muon channel, $E_{\mathrm{T}}^{\mathrm{miss}}$ was corrected for the muon momentum and its energy deposit in the calorimeters. Events were required to have $E_{\mathrm{T}}^{\mathrm{miss}} > 25$ GeV and $m_{\mathrm{T}}(W) > 40$ GeV.

C. $W \to e\nu$ + jets final state

Electrons were required to pass the standard ''tight'' electron selection criteria [16,17] with $E_{\mathrm{T}} > 20$ GeV and $|\eta| < 2.47$. Electrons in the transition region between the barrel and end-cap calorimeter ($1.37 < |\eta| < 1.52$) were rejected.

To suppress multijet events containing nonisolated electrons such as those from semileptonic decays of hadrons containing charm and bottom quarks, a calorimeter-based isolation requirement was applied. The transverse energy within a cone of radius $R = 0.2$ around the electron, corrected for contributions from the electron, was required to be less than 4 GeV. This isolation requirement is more than 96% efficient over all jet multiplicities for prompt electrons originating from decays of W bosons and reduces the nonisolated electron background by a factor of 2.

To remove backgrounds from $Z \to ee$ decays, events were also rejected if there was a second electron passing the ''medium'' electron selection criteria [16,17] and the same kinematic selections and isolation requirements as above.

1. Electron channel background estimates

The principal backgrounds in the electron channel arise from multijet QCD events, other leptonic decays of gauge bosons, and, at higher jet multiplicities, $t\bar{t}$ production. The background from gauge bosons includes $W \to \tau\nu$, where the τ lepton decays to an electron and $Z \to ee$, where one electron is not identified and hadronic energy in the event is mismeasured. Leptonic $t\bar{t}$ decays ($t\bar{t} \to b\bar{b}qq'e\nu$), single-top events, and diboson (WW, WZ, ZZ) processes were also evaluated. The number of leptonic background events surviving the above selection requirements was estimated with simulated event samples that were introduced earlier in Sec. IV. Specifically, PYTHIA was used for $W \to \tau\nu$ and $Z \to \tau\tau$ and ALPGEN for the other vector boson samples. The simulated leptonic background samples were normalized to the integrated luminosity of the data using the predicted cross sections shown in Table II. The $t\bar{t}$ background is discussed in more detail later in Sec. V E.

The multijet background in the electron channel has two components, one where a light flavor jet passes the electron selection and additional energy mismeasurement results in large $E_{\mathrm{T}}^{\mathrm{miss}}$, and the other where a bottom or charm hadron decays to an electron. The number of multijet background events was estimated by fitting, for each exclusive jet multiplicity, the $E_{\mathrm{T}}^{\mathrm{miss}}$ distribution in the data (without the $E_{\mathrm{T}}^{\mathrm{miss}}$ selection requirement) to a sum of two templates: one for the multijet background and another which included signal and the leptonic backgrounds. The fits determined the relative normalizations of the two templates for each exclusive jet multiplicity. The shapes for the second template were obtained from simulation and their relative normalization was fixed to the ratio of their predicted cross sections.

The template for the multijet background was obtained from the data because the mechanisms by which a jet fakes an electron are difficult to simulate reliably. The template was derived by loosening some of the electron identification requirements. Two approaches were taken so their results could be compared.

In the first, the requirements on shower shape in the calorimeter were relaxed. The ''loose'' electron identification criteria of Refs. [16,17] were applied to the shower shapes. The track-cluster matching requirements applied in the standard ''tight'' electron selection were still applied but the remaining ''tight'' requirements with respect to the ''medium'' requirements were required to fail [16,17]; the selection favors electron candidates from conversions or from charged hadrons overlapping electromagnetic showers.

In the second method, the requirement that a track matched the energy deposition in the calorimeter was relaxed and loose photon identification requirements were used instead of those of an electron.

To suppress any residual signal contribution, the isolation requirement was also reversed in both methods. A large simulated dijet sample was used to verify that these requirements do not bias the $E_{\mathrm{T}}^{\mathrm{miss}}$ shape of the background templates.

The results of the two methods were compared for each jet multiplicity and agreed within their statistical uncertainties. For the zero-jet bin they agreed to better than 17% with respect to the total number of candidate background events. Residual differences are included in the estimates of systematic uncertainty described below. The range of $E_{\mathrm{T}}^{\mathrm{miss}}$ used to fit the templates was also varied to estimate systematic effects. The first method was used to calculate the central values of the multijet backgrounds for the various jet multiplicities.

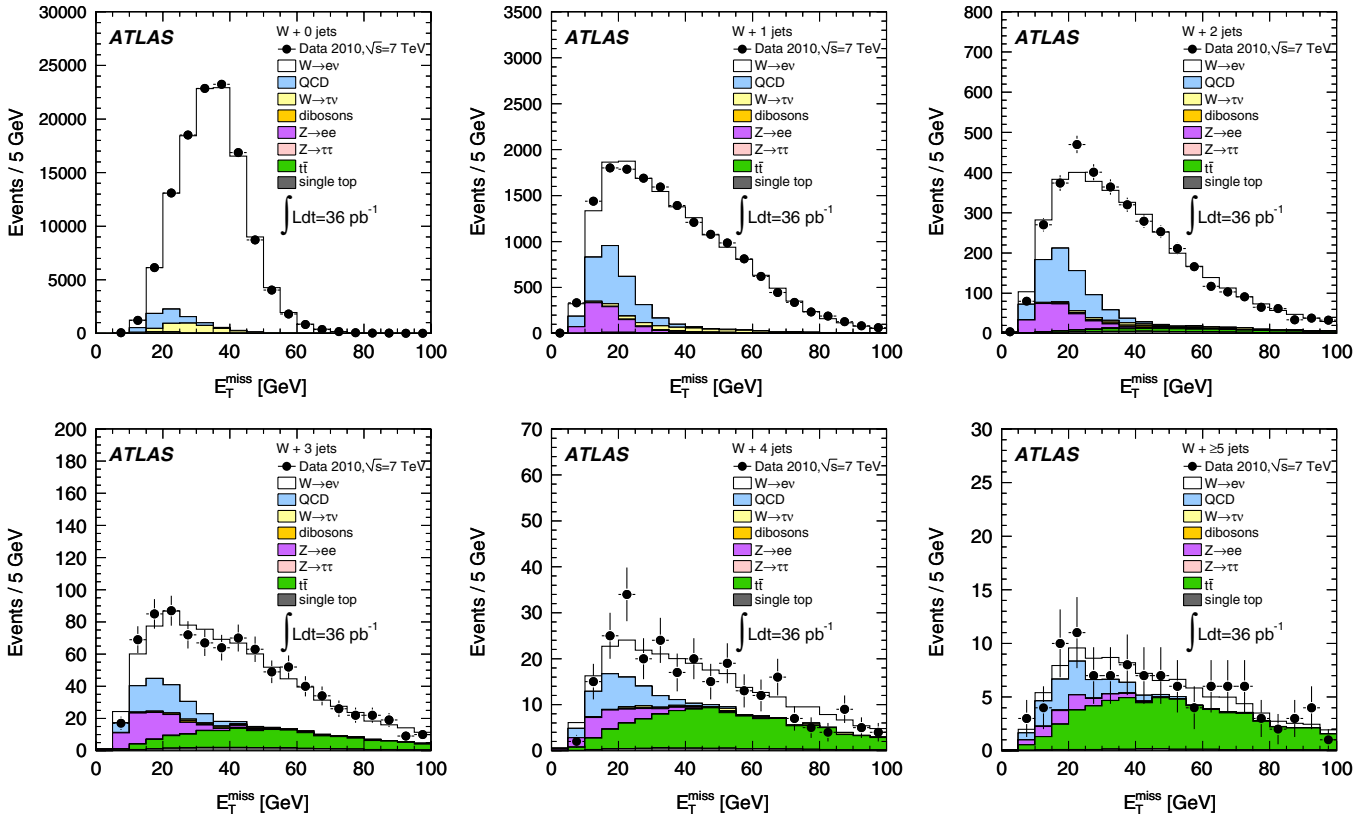

FIG. 2 (color online). Result of the $E_{\mathrm{T}}^{\mathrm{miss}}$ template fits used to obtain an estimate of the multijet background for $W \to e\nu$ events, in bins of exclusive jet multiplicity. The data are shown with the statistical uncertainties only. In this case the multijet template was obtained with relaxed shower shape requirements, as described in the text. The data with ≥ 5 jets are not used for measurements because of low event multiplicity and a poor signal-to-background ratio. The event multiplicity and the ratio were better for $p_{\mathrm{T}}^{\mathrm{jet}} > 20$ GeV. W candidate events were required to have $E_{\mathrm{T}}^{\mathrm{miss}} > 25$ GeV.

The comparisons of the template fits to the $E_{\mathrm{T}}^{\mathrm{miss}}$ distributions are shown in Fig. 2 for the first type of multijet template. Figure 3 shows the final $m_{\mathrm{T}}(W)$ distributions in the various bins of inclusive jet multiplicity.

2. Electron channel systematic uncertainties

The systematic uncertainties for the electron channel are summarized in Table III. The calculation of uncertainty on the number of multijet background events was introduced in Sec. V C 1.

The electron trigger efficiency was measured using $Z \to ee$ events triggered by an object other than the electron under study (tag-and-probe method). A scale factor of $99.5 \pm 0.5\%$ relative to the value predicted by the Monte Carlo simulation was determined. The same event samples were used to determine the electron reconstruction and identification efficiencies relative to the Monte Carlo prediction. The reconstruction efficiencies were consistent with the Monte Carlo values within a systematic uncertainty of 1.5%. Data-driven corrections to the simulated identification efficiencies were characterized by a two-dimensional matrix in η and E_{T}. The $Z \to ee$ events were also used to test the electron identification efficiency for any dependence on accompanying jet activity and none was found.

The measured electron energy scale and resolution were also studied with $Z \to ee$ events. In the data, electron energies were adjusted with an η-dependent correction with typical values of about 2% [17]. The electron energy resolution was similarly tested and adjusted in simulated events. The residual systematic uncertainties are shown in Table III.

D. $W \to \mu\nu$ + jets final state

The muons were required to be reconstructed in both the ID and MS subsystems and to have $p_{\mathrm{T}} > 20$ GeV and $|\eta| < 2.4$. The ID track requirements were those of Ref. [16]. An ID-based muon isolation was applied which required a relative isolation of $\sum p_{\mathrm{T}}^{\mathrm{ID}}/p_{\mathrm{T}}^{\mu} < 0.1$, using a cone size of $\Delta R < 0.2$, where $\sum p_{\mathrm{T}}^{\mathrm{ID}}$ included all ID tracks in the cone except the muon track. To help ensure that the muon is prompt it was required that the transverse impact parameter of the track d_0 and its uncertainty $\sigma(d_0)$ satisfied $|d_0/\sigma(d_0)| < 3$. Also the longitudinal impact

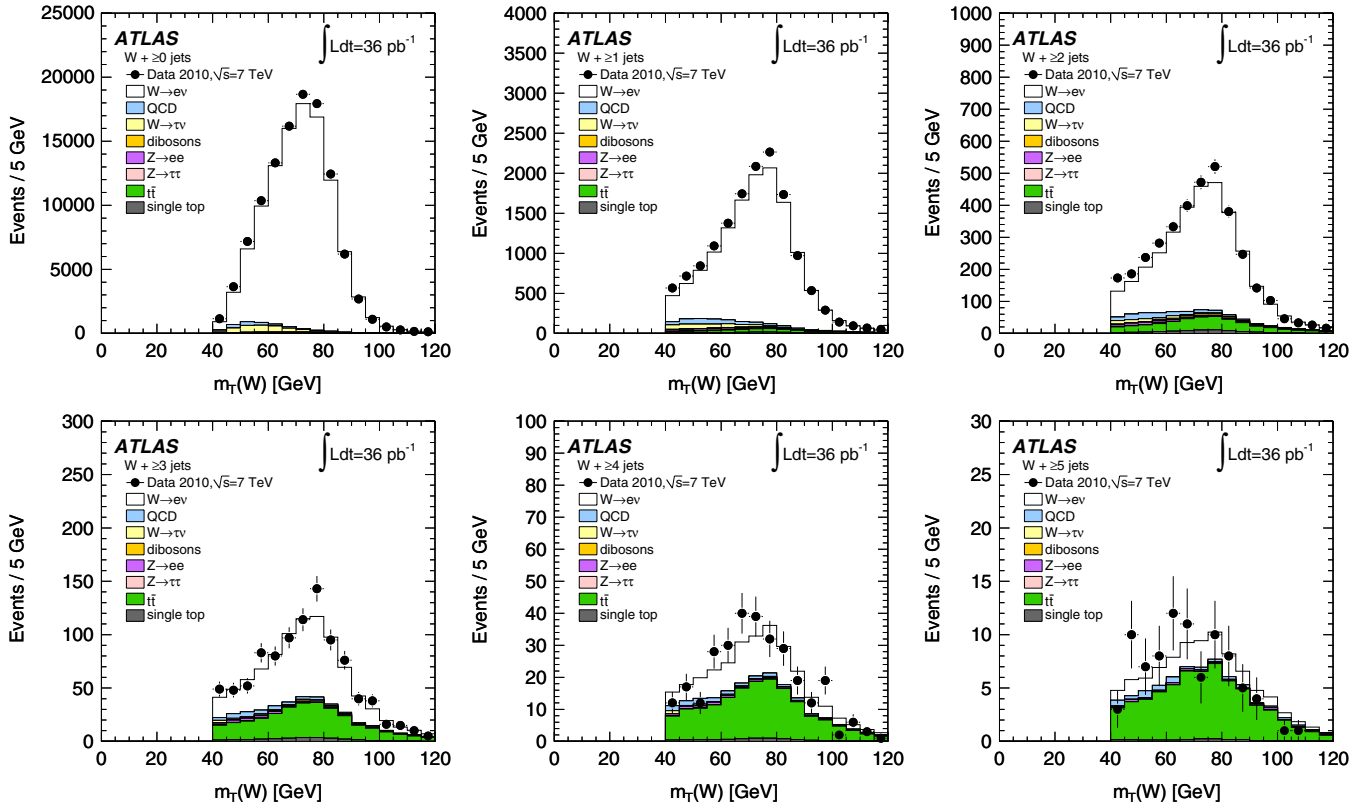

FIG. 3 (color online). Transverse mass distributions $m_{\mathrm{T}}(W)$ for selected $W \to e\nu$ events in bins of inclusive jet multiplicity. MC predictions for the signal and leptonic backgrounds are normalized to luminosity using (N)NLO cross sections and the multijet background is estimated from data (method I).

parameter Δz was required to satisfy $|\Delta z| < 10$ mm to reduce contributions from in-time pileup and cosmic ray muons. These impact parameters were measured with respect to the primary vertex. Events were rejected if there was a second muon passing the same kinematic selections and isolation requirements as above. These muon selection criteria are similar to those applied in Ref. [9].

TABLE III. Summary of relative systematic uncertainties associated with the electron channel.

Quantity	Uncertainty
Trigger efficiency	~0.5%
Electron reconstruction	~1.5%
Electron identification	2–8%[a]
Electron energy scale	0.3–1.6%[a]
Electron energy resolution	<0.6% of the energy
Multijet QCD background	17–100%[b]; difference between the two methods, see Sec. V C 1

[a] $\eta - p_{\mathrm{T}}$ dependent.
[b] Increased with jet multiplicity.

1. Muon channel background estimates

For the muon channel, the main backgrounds arise from semileptonic decays of heavy flavor hadrons in multijet events, other leptonic decays of heavy gauge bosons, and $t\bar{t}$ production. The backgrounds from gauge bosons include $W \to \tau\nu$, where the tau decays to a muon, $Z \to \mu\mu$ where one muon is not identified, $Z \to \tau\tau$, and diboson production. For low jet multiplicities the largest backgrounds are $W \to \tau\nu$ and $Z \to \mu\mu$, while for higher multiplicities $t\bar{t}$ production dominates ($t\bar{t} \to b\bar{b}qq'\mu\nu$). Similarly to the electron channel, the number of leptonic background events surviving the selection criteria was estimated with simulated event samples described in Sec. IV. PYTHIA was used only for inclusive production of $W \to \tau\nu$ and $Z \to \tau\tau$ and ALPGEN for the other vector boson samples. The simulated leptonic background samples were normalized to the integrated luminosity of the data using the predicted NNLO, NLO + NNLL (next-to-next-to-leading logarithm) or NLO cross sections. Discussion of the $t\bar{t}$ background follows in Sec. V E.

The multijet QCD background in the muon channel is dominated by leptonic decays of bottom or charm hadrons in jets where the hadron decay involves a muon and neutrino. The number of background events was estimated by fitting, for each exclusive jet multiplicity, the $E_{\mathrm{T}}^{\mathrm{miss}}$

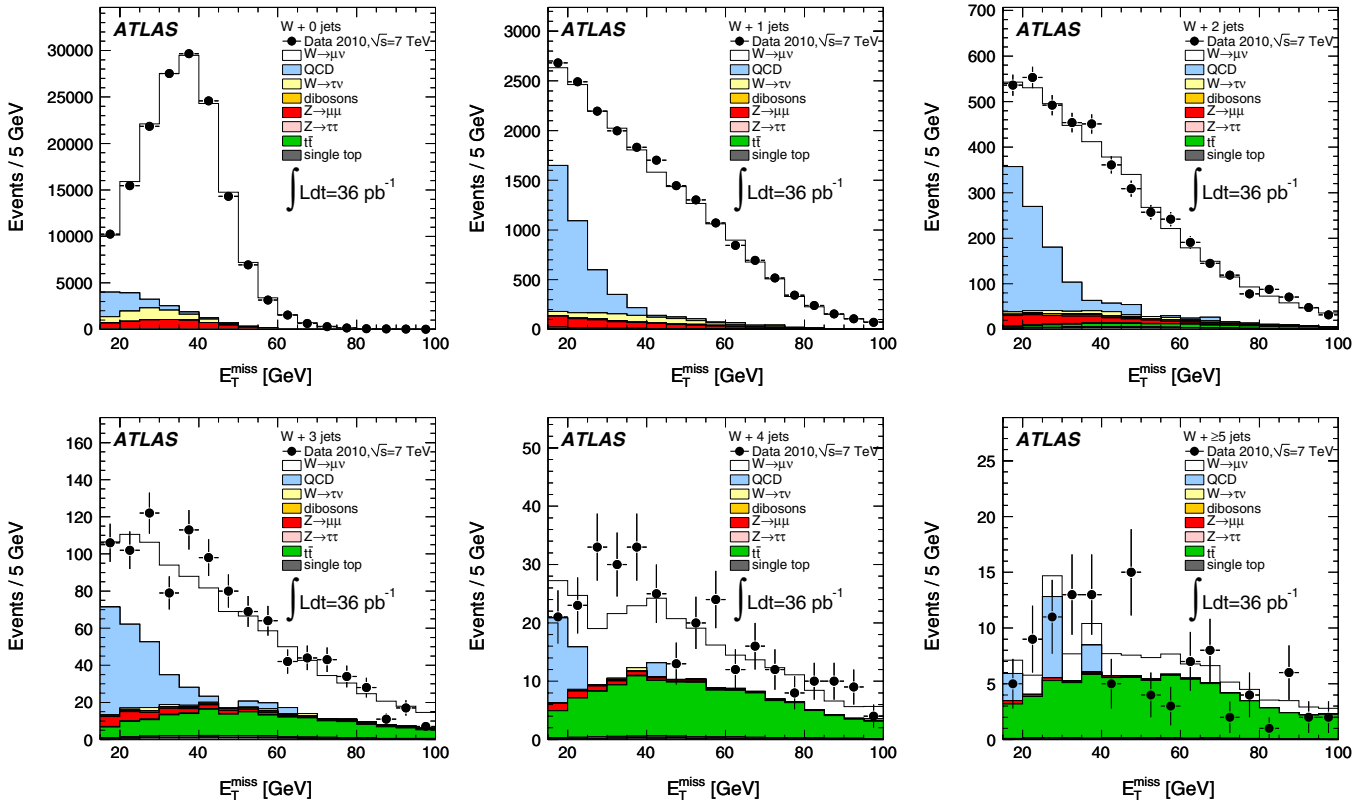

FIG. 4 (color online). Result of the $E_{\mathrm{T}}^{\mathrm{miss}}$ template fits used to obtain an estimate of the multijet background for $W \to \mu\nu$ events with relaxed kinematic requirements, $m_{\mathrm{T}}(W) > 25$ GeV and $E_{\mathrm{T}}^{\mathrm{miss}} > 15$ GeV. Results are shown in bins of exclusive jet multiplicity. In this case the multijet template was obtained with a reversed requirement on the significance of muon's impact parameter. The data with ≥ 5 jets are not used for measurements because of the low event count and a poor signal-to-background ratio.

distribution in the data (with relaxed selection requirements on $E_{\mathrm{T}}^{\mathrm{miss}}$ and $m_{\mathrm{T}}(W)$: $E_{\mathrm{T}}^{\mathrm{miss}} > 15$ GeV and $m_{\mathrm{T}}(W) > 35$ GeV) to a sum of two templates: one for the multijet background and another which included signal and the leptonic backgrounds. The fit determined the relative normalization of the two templates. The shapes for the second template were obtained from simulation and their relative normalization was fixed to the predicted cross sections. The full kinematic selection, $E_{\mathrm{T}}^{\mathrm{miss}} > 25$ GeV and $m_{\mathrm{T}}(W) > 40$ GeV, was imposed on the multijet background samples to convert their normalization coefficients from the relaxed to full selection.

The template for the multijet background was obtained from data by applying all the standard muon selection requirements, except that the requirement on the significance of the transverse impact parameter was reversed to $|d_0/\sigma(d_0)| > 3$. In addition, the impact parameter was required to be within $0.1 < |d_0| < 0.4$ mm. The lower cut on the impact parameter reduces signal $W \to \mu\nu$ events leaking into the background sample. The upper cut on $|d_0|$ was placed to minimize bias from multijet events where an isolated muon is accompanied by a nearby energetic jet; the isolated muons from decays of heavy hadrons tend to have large impact parameters. The background events with a muon and an energetic jet do not survive the standard muon selection due to the stringent requirement on the impact parameter, in conjunction with the isolation cut.

The comparisons of the template fits to the $E_{\mathrm{T}}^{\mathrm{miss}}$ distributions are presented in Fig. 4 for $W \to \mu\nu$ events with the relaxed selection requirements on $E_{\mathrm{T}}^{\mathrm{miss}}$ and $m_{\mathrm{T}}(W)$. Figure 5 shows the final $m_{\mathrm{T}}(W)$ distributions in the various bins of inclusive jet multiplicity for events passing the normal selection requirements.

Another set of templates for the multijet background was obtained using a simulated dijet sample from PYTHIA where the event record was required to contain at least one muon with $p_{\mathrm{T}} > 8$ GeV. The second set of templates was fitted to data in the same manner as the first in order to estimate a systematic uncertainty in the number of multijet background events. The uncertainty increased with the jet multiplicity from 15% for the inclusive W-boson sample up to 76% for events with a W boson and four or more jets.

1. Muon channel systematic uncertainties

The muon trigger efficiencies were measured using a $Z \to \mu\mu$ sample triggered by a muon candidate other than

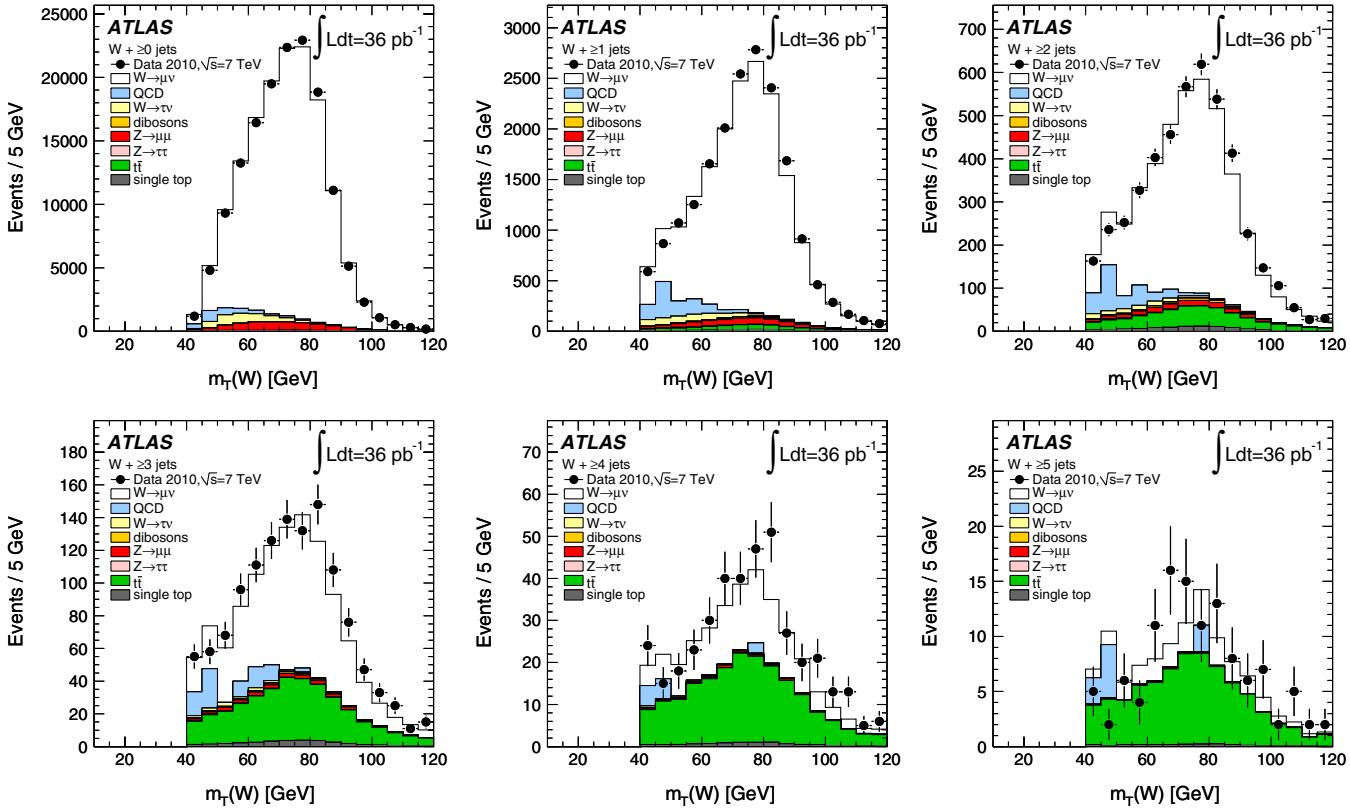

FIG. 5 (color online). Comparison of transverse mass distributions $m_{\mathrm{T}}(W)$ for $W \to \mu\nu$ events. Results are shown in bins of inclusive jet multiplicity for events passing the normal selection requirements. MC predictions for the $W \to \mu\nu$ signal and leptonic backgrounds are normalized to luminosity using (N)NLO cross sections and the multijet background is estimated from data.

the muon under study [16]. Scale factors close to unity, relative to the value predicted by the Monte Carlo simulation, were obtained for the muon triggers. The scale factors were calculated as a function of muon η and p_{T}. The same sample of events was used to determine the muon reconstruction and identification efficiencies as a two-dimensional matrix in η and ϕ [53,54]. The measured efficiencies were used to correct the simulated samples. The average efficiency correction is consistent with unity within a systematic uncertainty of 1.1%.

The measured momentum scale and resolution for the muons were studied with $Z \to \mu\mu$ events [55]. The muon transverse momentum and its resolution were calibrated as a function of η and p_{T}. The systematic uncertainties for the muon channel are summarized in Table IV.

TABLE IV. Summary of relative systematic uncertainties associated with the muon channel.

Quantity	Uncertainty
Trigger efficiency	0.6–0.7%[a]
Muon reconstruction and identification	~1.1%[b]
Muon p_{T} scale	~0.4%[a]
Muon p_{T} resolution	<6%[c]
Multijet QCD background	15–76%[d]; difference between the two templates, see Sec. V D 1

[a] $\eta - p_{\mathrm{T}}$ dependent.
[b] $\eta - \phi$ dependent.
[c] $\eta - p_{\mathrm{T}}$ dependent relative to the measured resolution.
[d] Varies with jet multiplicity.

E. Detector-level comparisons between final states of $W \to e\nu$ + jets and $W \to \mu\nu$ + jets

Observed and expected distributions for several variables have been compared for the electron and muon channels. The observed distributions are shown with statistical uncertainties. The expected distributions are presented with experimental uncertainties that include those described later in Sec. V G in addition to the uncertainties specific to the two channels from Secs. V C 2 and V D 2. Distributions of the inclusive jet multiplicity are shown in Fig. 6. Figures 7–10 show distributions in p_{T} of the first four (highest p_{T}) jets. The rapidity of the first jet is shown in Fig. 11. The difference and sum of the rapidities of the lepton and the first jet are shown in Figs. 12 and 13,

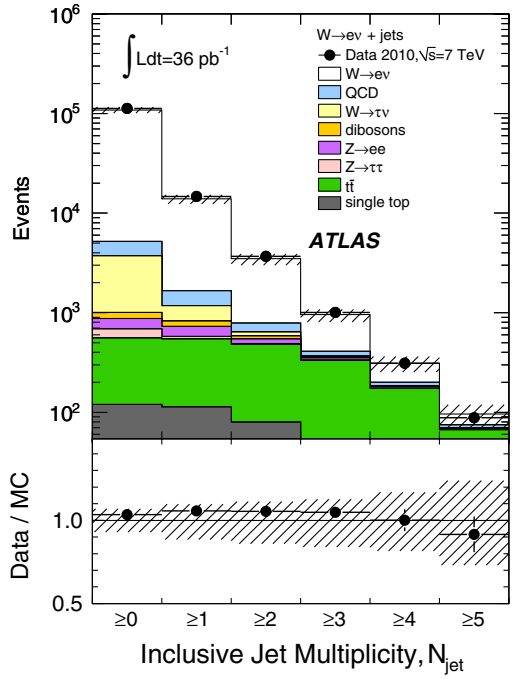

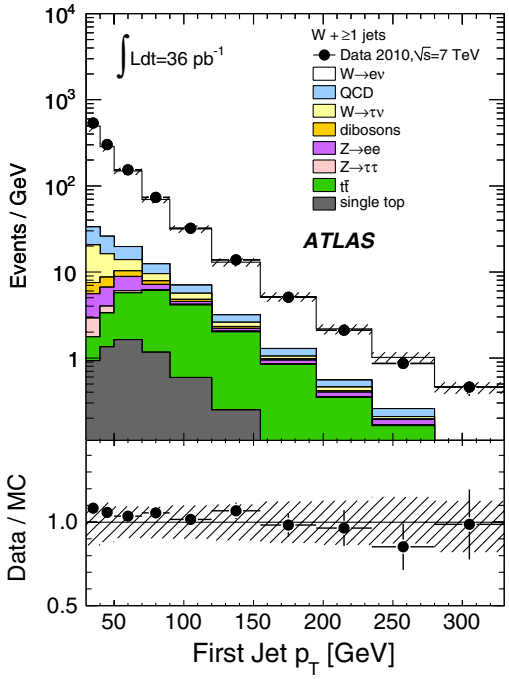

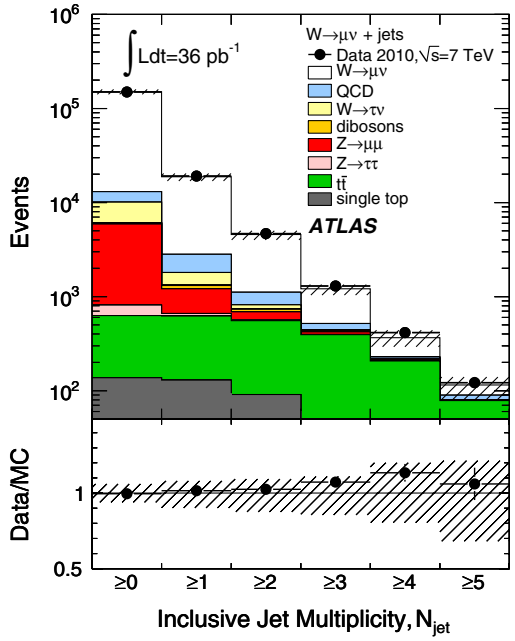

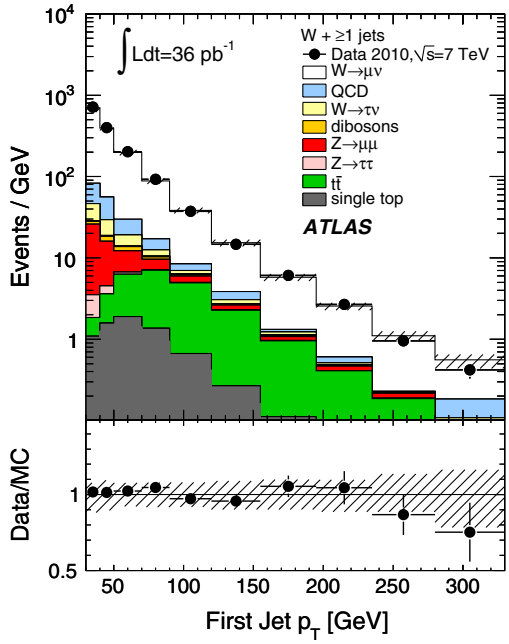

FIG. 6 (color online). The uncorrected inclusive jet multiplicity distribution. The following remarks apply to this and subsequent figures. Top: electron channel. Bottom: muon channel. The signal and leptonic backgrounds are shown using simulations, whereas the multijet background uses the method described in the text. The signal and leptonic backgrounds are normalized to the predicted cross sections. The black-hashed regions illustrate the experimental uncertainties on the predicted distributions.

FIG. 7 (color online). The uncorrected distribution in p_{T} of the jet with the highest p_{T}, in events with one or more jets.

respectively. Variables dependent on the azimuthal and rapidity separations between the first two jets are featured in Figs. 14–16. Overall, a good agreement is seen between measured and predicted distributions. Minor discrepancies appear for jet pairs with large rapidity separation in Figs. 14 and 16. Figure 12 illustrates discrepancies for events with the first jet separated in rapidity from the lepton. Predictions in Figs. 11–13 are found to be sensitive to the choice of PDF.

Top quark pair production is a substantial background to W + jets in events with four or more jets as can be seen in Fig. 6. The predicted $t\bar{t}$ cross section of 165^{+11}_{-16} pb [26] is

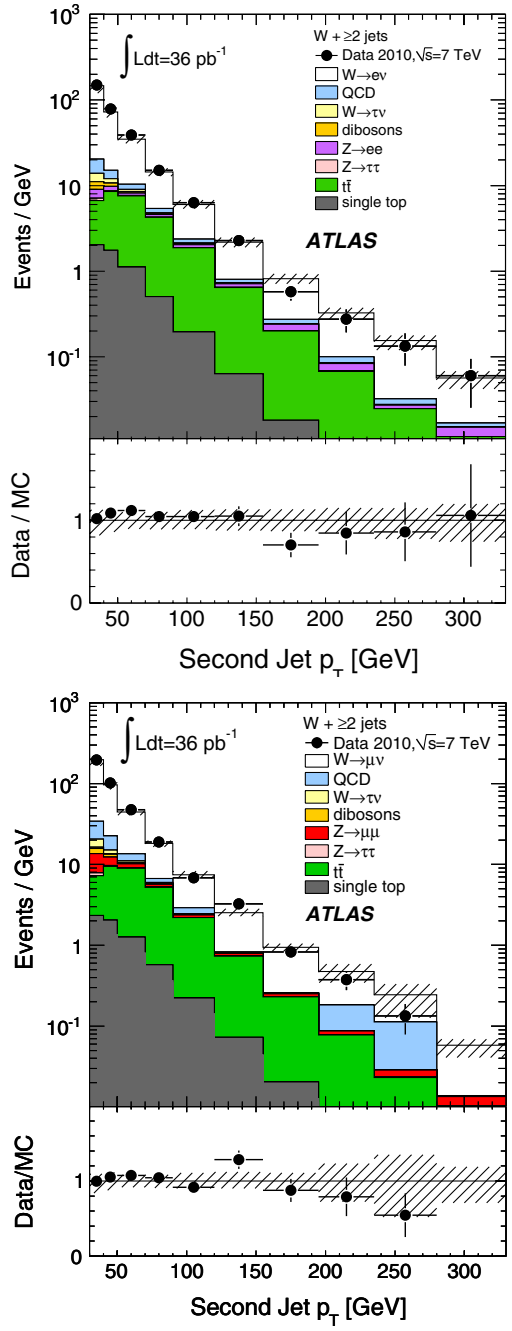

FIG. 8 (color online). The uncorrected distribution in p_{T} of the jet with the second highest p_{T}, in events with two or more jets.

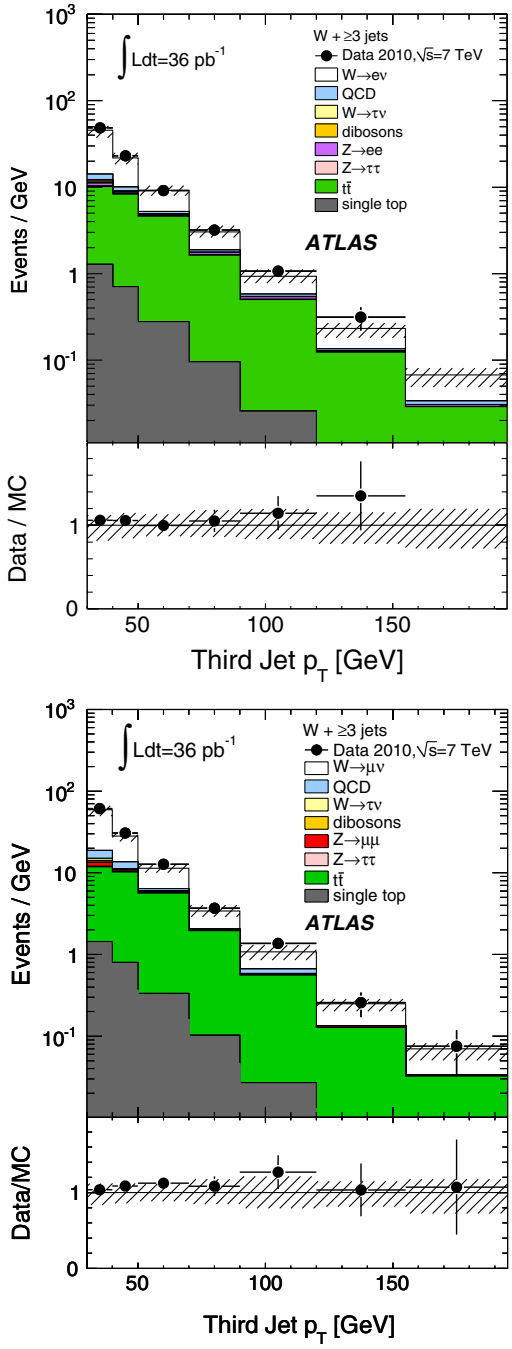

FIG. 9 (color online). The uncorrected distribution in p_{T} of the jet with the third highest p_{T} in events with three or more jets.

fully consistent with the measured value of $171 \pm 20(\mathrm{stat}) \pm 14(\mathrm{syst}) + 8 - 6(\mathrm{lum})$ pb, obtained with the same 2010 data sample [56]. Here the predicted one was used to obtain the cross-section results.

Several kinematic distributions were used to check the normalization of the $t\bar{t}$ component in the channels with a W boson plus four or more jets. These included the rapidity of the charged lepton and the mass of the W-jet system. The normalizations obtained were consistent with the expected value but had a statistical uncertainty too large to usefully constrain the $t\bar{t}$ cross section.

F. Unfolding of efficiency and resolution effects

The yield of signal events was corrected back to the particle level separately for the two lepton channels, taking into account detector acceptance and reconstruction efficiency. The correction was made using an iterative Bayesian method of unfolding [57]. Bin sizes in each

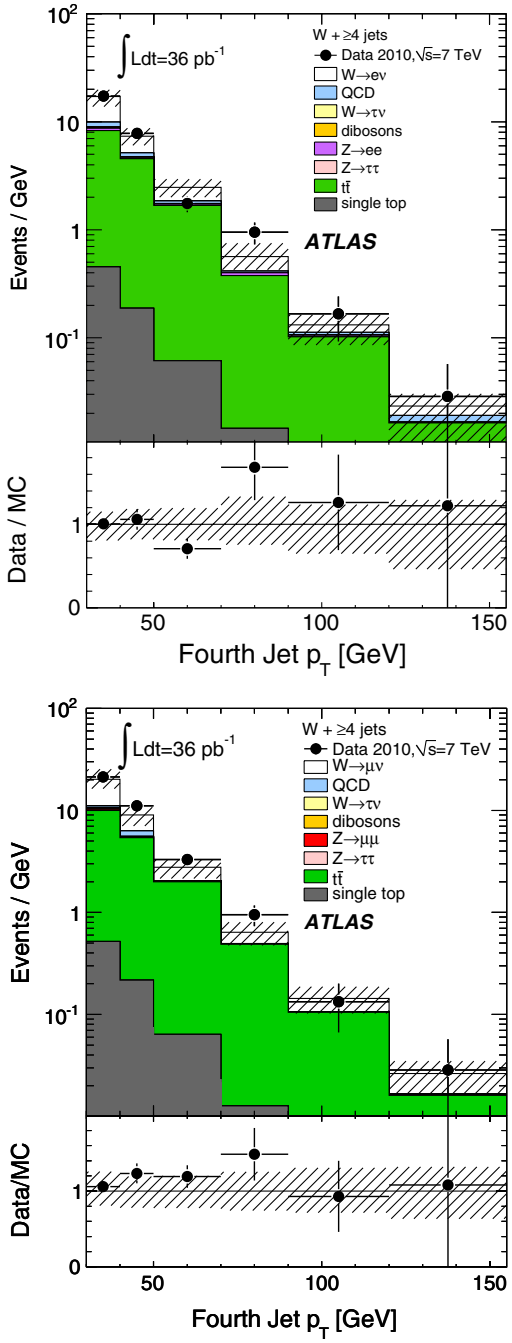

FIG. 10 (color online). The uncorrected distribution in p_{T} of the jet with the fourth highest p_{T}, in events with four or more jets.

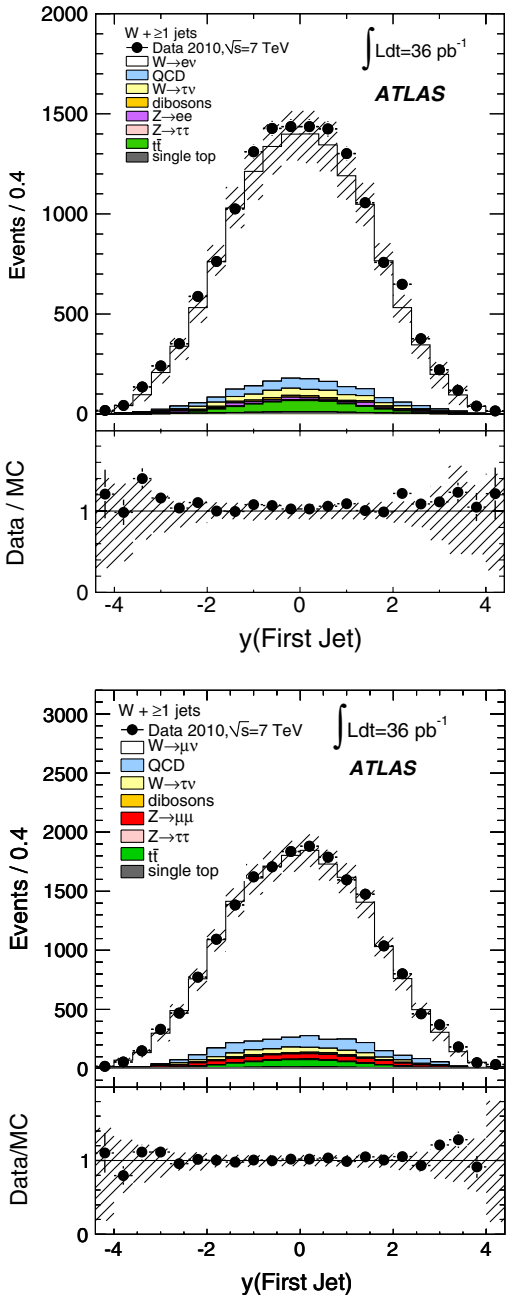

FIG. 11 (color online). The uncorrected distribution in rapidity of the leading jet, y(first jet), in events with one or more jets.

histogram were chosen to be a few times larger than the resolution of the corresponding variable. Migration matrices were computed using the ALPGEN W + jets event generator plus full detector simulation, restricting the events to the common phase space:

(i) $p_{\mathrm{T}}^{\ell} > 20$ GeV (ℓ = electron or muon),
(ii) $|\eta^{\ell}| < 2.5$,
(iii) $p_{\mathrm{T}}^{\nu} > 25$ GeV,
(iv) $m_{\mathrm{T}}(W) > 40$ GeV,
(v) $p_{\mathrm{T}}^{\mathrm{jet}} > 30$ GeV,
(vi) $|y^{\mathrm{jet}}| < 4.4$ and $\Delta R(\ell, \mathrm{jet}) > 0.5$.

The common phase space requirements were applied to generated objects before the detector simulation. In this analysis, particle-level jets were constructed in simulated events by applying the anti-k_{t} jet finder to all final-state particles with a lifetime longer than 10 ps, whether produced directly in the pp collision or from the decay of particles with shorter lifetimes. Neutrinos, electrons, and

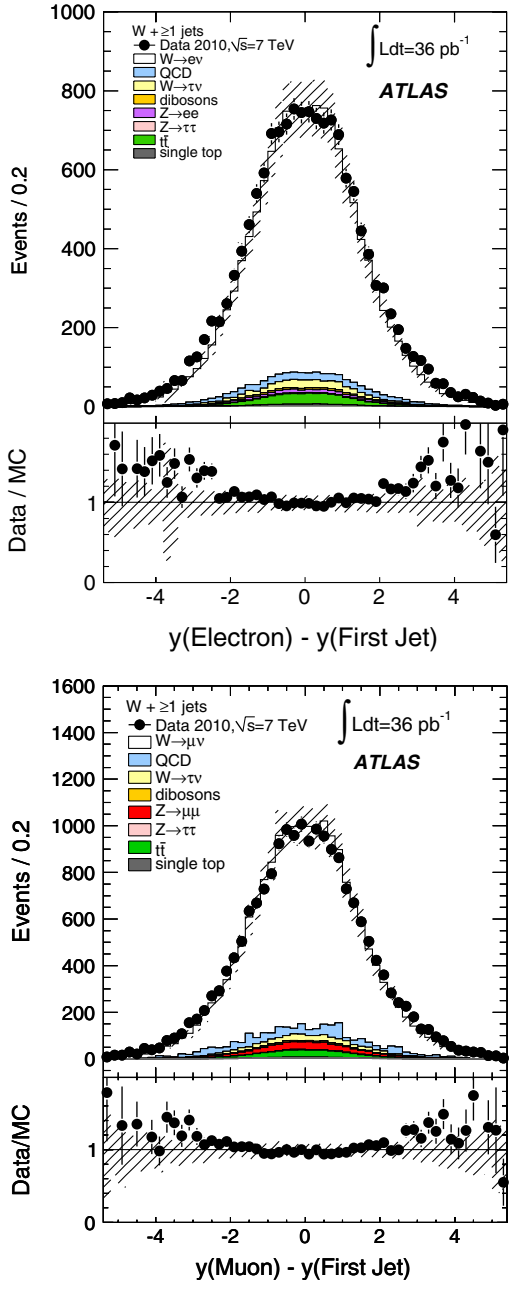

FIG. 12 (color online). The uncorrected distribution in $y(\ell) - y$(first jet), rapidity difference between the lepton and the leading jet, for events with one or more jets.

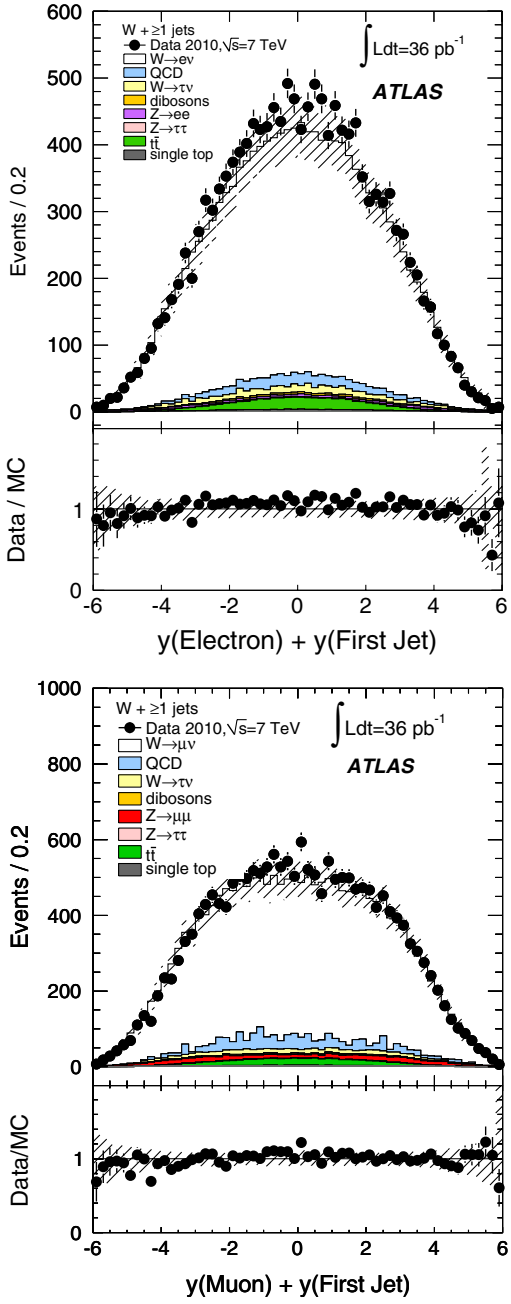

FIG. 13 (color online). The uncorrected distribution in $y(\ell) + y$(first jet), sum of rapidities of the lepton and the leading jet, for events with one or more jets.

muons from decays of the massive W bosons were not used for the jet finding. Final-state QED radiation differs for electrons and muons, and its effects were corrected in the combined cross sections. Fiducial cross sections for each channel were defined using final-state leptons for which collinear radiation in a cone of $R = 0.1$ is added to the lepton four-momentum [58]. This accounts for the most significant effects of collinear QED radiation. A residual correction for large-angle radiation outside this cone is then applied to bring both electrons and muons to the Born level for the combined cross sections. These correction factors range from 0.985 to 0.995 and are similar for both electrons and muons.

Instead of inverting the migration matrix, the unfolded distributions were determined using Bayes' theorem to recalculate the particle-level distributions from the detector-level distributions. The unfolded values were calculated using different numbers of iterations for different bins of a distribution. The standard Bayesian approach treats all bins using the same number of iterations. Fewer

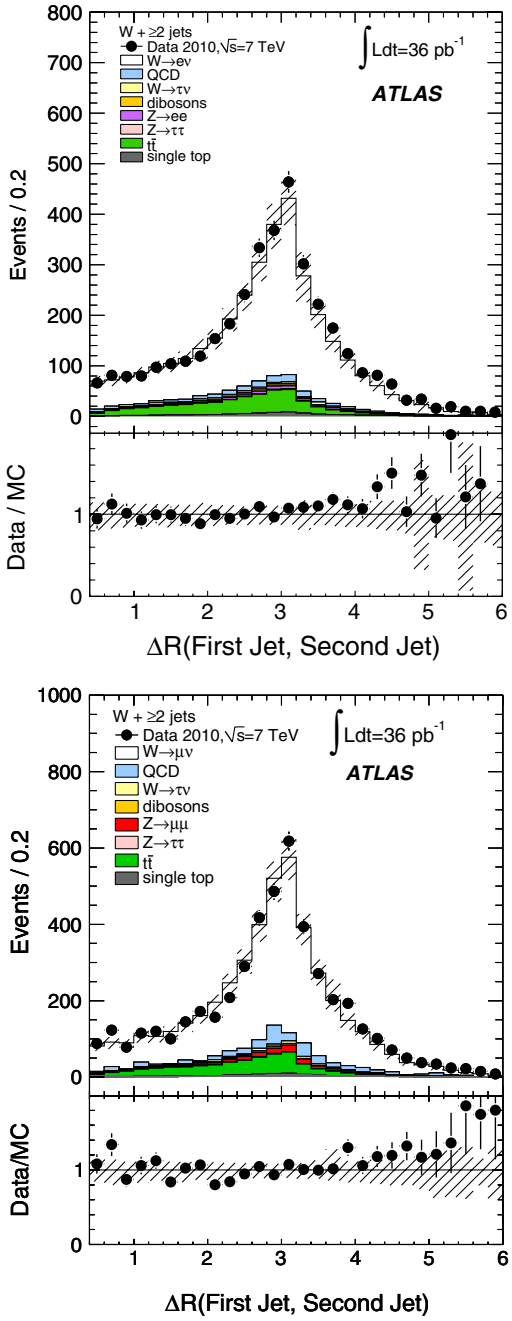

FIG. 14 (color online). The uncorrected distribution as a function of ΔR(first jet, second jet), distance between the first two jets, for events with two or more jets.

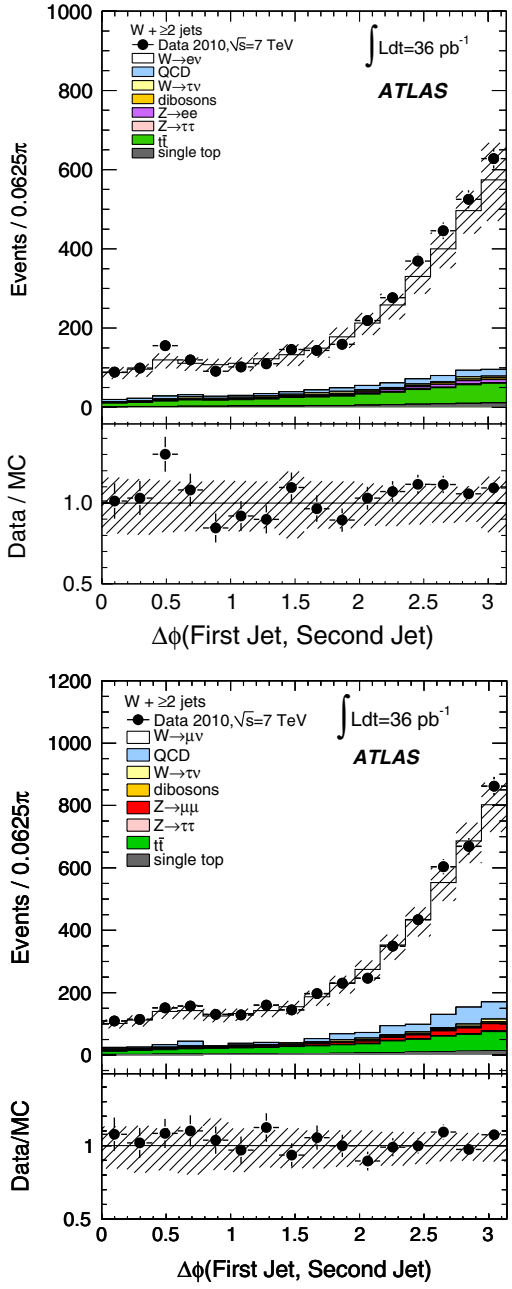

FIG. 15 (color online). The uncorrected distribution as a function of $\Delta\phi$(first jet, second jet), azimuthal separation between the first two jets, for events with two or more jets.

iterations were performed for bins with few events than for bins with large numbers of events to avoid large statistical fluctuations in the tails of the distributions. The number of iterations was limited for a bin once the statistical uncertainty becomes substantially larger than the change due to the last application of the unfolding matrix [59]. Tests with simulated data showed that the iterative Bayesian method was sufficient to recover particle-level distributions. The dominant detector to particle-level corrections in the electron channel come from electron reconstruction efficiency ($\approx 30\%$ correction). In the muon channel, the dominant corrections come from trigger and reconstruction efficiency (corrections of $\approx$ 10–20% and $\approx 10\%$ respectively). The statistical uncertainty on the unfolding was estimated using toy simulations. The systematic uncertainties on the unfolding included the uncertainty on the migration matrix which was estimated by using the alternative SHERPA simulation for W + jets production (see Table I).

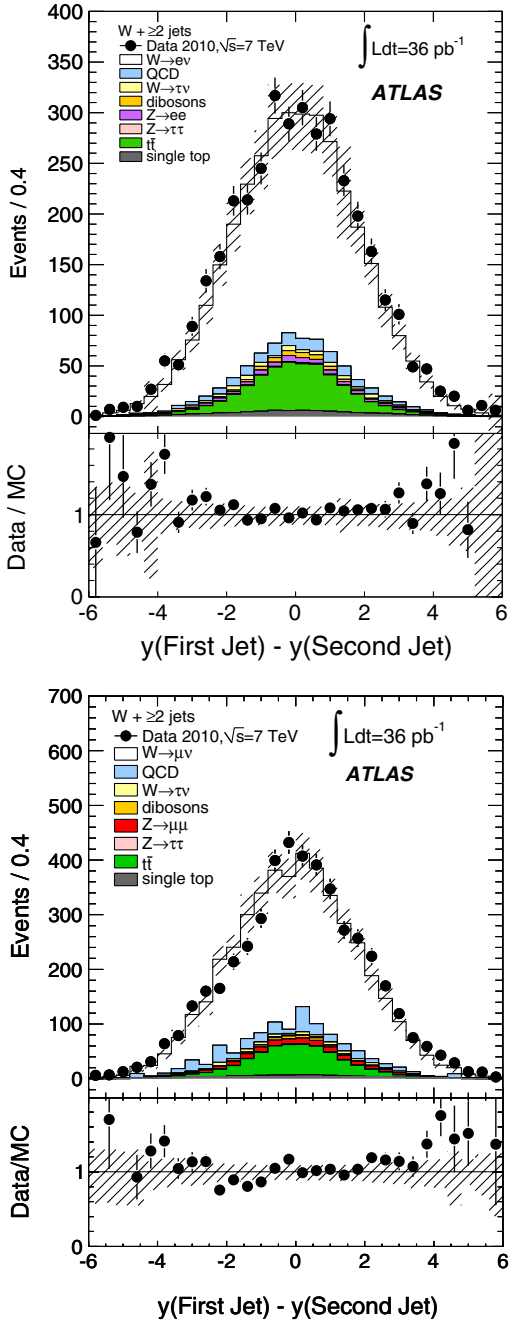

FIG. 16 (color online). The uncorrected distribution as a function of y(first jet) $-$ y(second jet), rapidity separation between the first two jets, for events with two or more jets.

G. Overall systematic uncertainties

In addition to the systematic uncertainties specific to the electron and muon channels documented earlier in Secs. V C 2 and V D 2, respectively, there are a number of common sources of uncertainty. As a brief reminder, the uncertainty on the identification efficiency for electrons results in $+4.0-4.3\%$ variation of the $N_{\text{jet}} \geq 1$ cross section, giving the largest variation among the electron-specific uncertainties. Similarly, the uncertainty on reconstruction and identification efficiency of muons corresponds to a variation of $\pm 1.1\%$ in the $N_{\text{jet}} \geq 1$ cross section and represents the single largest muon-specific uncertainty.

The dominant source of systematic uncertainty in the cross-section measurement for both electron and muon channels is the uncertainty in the jet energy scale [48]. For $N_{\text{jet}} \geq 4$, uncertainties on the predicted $t\bar{t}$ cross section and $t\bar{t}$ shape also become significant and can be as high as 10% and 21%, respectively. The luminosity uncertainty enters primarily through the signal normalization but also has a small effect on the estimation of the leptonic backgrounds.

Uncertainties in the jet energy scale (JES) and jet energy resolution (JER) were determined from data and simulation [48]. The JER uncertainty was 10% of the jet energy resolution [48]. The JES uncertainty varies as a function of jet p_{T} and η, and ranges from $\sim$2.5% at 60 GeV in the central region to $\sim$14% below 30 GeV in the forward regions; the uncertainty increases monotonically with the absolute value of jet pseudorapidity. The uncertainty on the correction of the JES for pileup pp interactions is less than 1.5% per additional interaction for jets with $p_{\text{T}} >$ 50 GeV. To take into account the differences in calorimeter response to quark- and gluon-initiated jets, the uncertainty on the fraction of gluon-initiated jets, the flavor composition [48] was estimated by comparing the fractions in SHERPA and ALPGEN simulations for W + jets production. For jets accompanied by a second jet within $\Delta R <$ 0.7, an additional uncertainty is added to the JES uncertainty; the additional uncertainty is less than 2.8%. To estimate the impact of the JES uncertainty, jet energies in the simulated events were coherently shifted by the JES uncertainty, and the $E_{\text{T}}^{\text{miss}}$ vector was recomputed. In addition, simulated energy clusters in the calorimeters not associated with a jet or electron, such as those coming from the underlying event and pileup interactions, were scaled using a p_{T} and $|\eta|$ dependent uncertainty [16], ranging from $\pm 5.5\%$ for central clusters at $p_{\text{T}} \simeq$ 500 MeV to $\pm 3\%$ at high p_{T}. Similarly the simulated jet energies were smeared by the JER uncertainty and the $E_{\text{T}}^{\text{miss}}$ vector was recomputed. The full analysis was repeated with these variations, and the cross sections were recomputed; the change in the cross section was taken as the systematic uncertainty. The uncertainty on the measured cross sections caused by the uncertainties on the JES and cluster energy scale increases with jet multiplicity from 9% for $N_{\text{jet}} \geq 1$ to 37% for $N_{\text{jet}} \geq 4$. The impact of the JES uncertainty is amplified for events with high jet multiplicities due to the large subtraction of $t\bar{t}$ events, corresponding to $\sim$54% of these events. The simulated jet multiplicity of the top background is sensitive to the JES. The magnification is somewhat smaller when jets are selected with $p_{\text{T}}^{\text{jet}} > 20$ GeV instead of 30 GeV; the JES-related uncertainty on the $N_{\text{jet}} \geq 4$ cross section is up to 29%.

The uncertainty due to jets originating from pileup interactions and the influence of the JVF selection requirement includes the efficiency of the requirement and how well the rate of pileup jets is modeled in the simulation. As a conservative estimate, the percentage of jets in the data removed by the JVF requirement is applied as the uncertainty. This results in a 1.5% uncertainty for jets with $p_{\mathrm{T}} < 40$ GeV with a resulting uncertainty on the cross section of 1% for $N_{\mathrm{jet}} \geq 1$.

Other uncertainties which were considered include the jet reconstruction efficiency and biases in the procedure for correcting for detector effects (by comparing correction factors obtained with ALPGEN to those obtained with SHERPA). Their effect on the cross section was found to be smaller than the uncertainties described before. All of these systematic uncertainties were also applied to the estimates of the multijet and leptonic backgrounds in both electron and muon channels. In addition, for the leptonic backgrounds the uncertainty in the NNLO cross sections was taken to be 5% for W/Z production as in Ref. [16]. The $t\bar{t}$ cross-section uncertainty was taken to be $^{+7}_{-10}$ % [26]. The uncertainty on the shapes of the $t\bar{t}$ distributions was estimated using ACERMC simulations where rates of ISR and FSR were altered with respect to the default settings. Samples with altered ISR were used to estimate the shape uncertainty since their impact on measured cross sections was the largest among these samples. The procedure has been used for ATLAS measurements involving top pair production [56].

The systematic uncertainties in the cross-section measurement are summarized in Table V for $N_{\mathrm{jet}} \geq 1$ and $N_{\mathrm{jet}} \geq 4$; most of the uncertainties are approximately

TABLE V. Summary of systematic uncertainties on the cross sections. The uncertainties are shown for $N_{\mathrm{jet}} \geq 1$ and $N_{\mathrm{jet}} \geq 4$. The sign convention for the JES and lepton energy scale uncertainties is such that a positive change in the energy scale results in an increase in the jet or lepton energy observed in the data.

$W \rightarrow e\nu$ channel

Effect	Range	Cross-section uncertainty (%) $N_{\mathrm{jet}} \geq 1$	Cross-section uncertainty (%) $N_{\mathrm{jet}} \geq 4$
Jet and cluster energy scales	2.5–14% (dependent on jet η and p_{T})	+9.0, −6.6	+37, −35
Jet energy resolution	∼10% on each jet (dependent on jet η and p_{T})	±1.6	±6
Electron trigger	±0.5%	+0.6, −0.5	±1
Electron reconstruction	±1.5%	+1.7, −1.6	±4
Electron identification	±2–8% (dependent on electron η and p_{T})	+4.3, −4.0	+10, −9
Electron energy scale	±0.3–1.6% (dependent on η and p_{T})	±0.6	+1, −3
Electron energy resolution	<0.6% of the energy	±0.0	<1
Pileup removal requirement	∼1.5% in lowest jet p_{T} bin	±1.1	±3
Multijet QCD background shape	from template variation	±0.7	±11
Unfolding	ALPGEN vs SHERPA	±1.5	±6
Luminosity	±3.4%	+3.8, −3.6	+9, −8
NNLO cross section for W/Z	±5%	±0.2	<1
NLO cross section for $t\bar{t}$	+7 − 10%	±0.3	±10
Simulated $t\bar{t}$ shape	from samples with more or less ISR	±0.1	+12, −21

$W \rightarrow \mu\nu$ channel

Effect	Range	Cross-section uncertainty (%) $N_{\mathrm{jet}} \geq 1$	Cross-section uncertainty (%) $N_{\mathrm{jet}} \geq 4$
Jet and cluster energy scales	2.5–14% (dependent on jet η and p_{T})	+8.2, −6.2	+33, −26
Jet energy resolution	10% on each jet (dependent on jet η and p_{T})	±1.5	±5
Muon trigger	±0.7% (± 0.6%) in barrel (end cap)	±0.6	±1
Muon reconstruction and identification	±1.1%	±1.1	±2
Muon momentum scale	±0.4%	+0.2, −0.3	<1
Muon momentum resolution	±6%	±0.1	<1
Pileup removal requirement	∼1.5% in lowest jet p_{T} bin	±1.0	±3
Multijet QCD background shape	from template variation	+0.8	−20
Unfolding	ALPGEN vs SHERPA	±0.2	<1
Luminosity	±3.4%	+3.7, −3.5	±7
NNLO cross section for W/Z	±5%	±0.4	<1
NLO cross section for $t\bar{t}$	+7 − 10%	+0.4, −0.3	+10, −7
Simulated $t\bar{t}$ shape	from samples with more or less ISR	<0.1	+13, −15

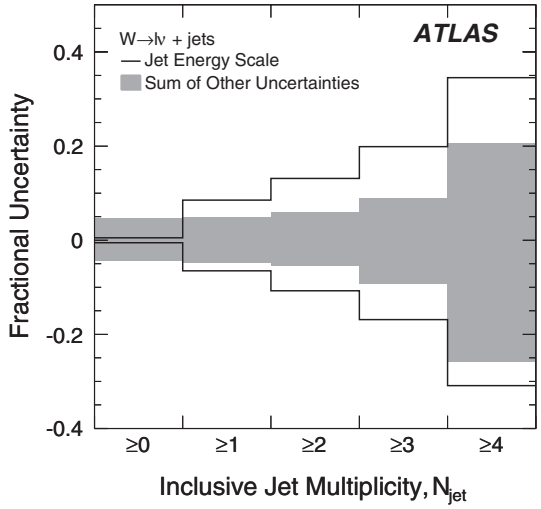

FIG. 17. Systematic uncertainties on the cross section as a function of the inclusive jet multiplicity. The uncertainty due to the jet energy scale is bounded by the two black lines. The quadratic sum of the other systematic uncertainties is presented as the shaded area. The uncertainties are for the sum of the electron and muon cross sections.

independent of the jet multiplicity, except for the uncertainty due to the jet energy scale and resolution, multijet background shape, $t\bar{t}$ production, and pileup jet removal. The uncertainty due to the jet energy scale dominates for events with at least one jet as illustrated in Fig. 17.

In the cross-section ratio measurement, $\sigma(W+ \geq N_{\text{jet}})/\sigma(W+ \geq N_{\text{jet}} - 1)$, the uncertainty due to the jet energy scale uncertainty remains the dominant effect, amounting to approximately 5–20% on the ratio. The luminosity uncertainty does not completely cancel in the ratio because the background estimates are affected by the luminosity uncertainty and the background levels vary as a function of jet multiplicity.

VI. NEXT-TO-LEADING-ORDER QCD PREDICTIONS

The MCFM v5.8 [34] and BLACKHAT-SHERPA [11] predictions were obtained with the same jet algorithm and same kinematic selection requirements applied to the data. In both cases, renormalization and factorization scales were set to $H_{\text{T}}/2$, where H_{T} is the scalar sum of the p_{T} of all the partons and of the lepton and neutrino from the W-decay. The PDFs used for MCFM were CTEQ6L1 [42] and CTEQ6.6M [28] for the LO and NLO calculations, respectively. For BLACKHAT-SHERPA CTEQ6.6M was used for both LO and NLO calculations.

The systematic uncertainty in the MCFM and BLACKHAT-SHERPA cross section due to renormalization and factorization scales were estimated by varying the scales by factors of two, up and down, in all combinations. The ratio of one scale to the other was kept within the range 0.5 to 2.0 to avoid the effects of large logarithms of the scale ratios in some kinematic regions. The cross-section ratio, $\sigma(W+ \geq N_{\text{jet}})/\sigma(W+ \geq N_{\text{jet}} - 1)$, was recalculated for each variation of the scales and the resulting uncertainty was determined using the recalculated values. Overall, the asynchronous variations of scales resulted in bigger deviations from the nominal values than the synchronous variations. The upper and lower uncertainties were taken as the maximum deviations from the nominal value.

Following the PDF4LHC recommendations [60], PDF uncertainties were computed by summing in quadrature the dependence on each of the 22 eigenvectors characterizing the CTEQ6.6 PDF set; the uncertainty in α_{s} was also taken into account. The uncertainties were scaled to a confidence level (C.L.) of 68%. Two alternative PDF sets, MSTW2008 [21], with its set of 68% C.L. eigenvectors, and NNPDF2.0 [61], were also examined. The error envelope of CTEQ6.6 was found to contain nearly all variations due to the two alternative PDF sets. The uncertainties due to the scale variations were substantially larger than those due to PDFs.

As a cross-check, cross sections from BLACKHAT-SHERPA and MCFM were compared for events with up to two jets, and found to be nearly identical. Therefore, only distributions from BLACKHAT-SHERPA were compared to the measured cross sections.

Bin-by-bin corrections for non-pQCD effects, hadronization and underlying event, were computed using simulated W + jets samples for each predicted distribution for the NLO cross sections. The corrections were taken to be the ratios of the distributions for particle-level jets to the distributions for parton-level jets, where the sample for parton-level jets was produced with the underlying event turned off. To calculate the central values, samples from ALPGEN v2.13 were showered with HERWIG v6.510 and JIMMY v4.31 set to the AUET2 tune [62]. The systematic uncertainty on the non-pQCD corrections was evaluated by comparing the central values to corrections from samples where ALPGEN was showered with PYTHIA v6.4.21 set to the AMBT1 [47] event generator tune. The corrections and their uncertainties were applied to all the NLO predictions presented in the paper.

VII. CROSS-SECTION RESULTS

The measured W + jets cross sections were calculated in the limited kinematic region defined in Sec. V F. All cross sections were multiplied by the leptonic branching ratio, $\text{Br}(W \rightarrow \ell\nu)$.

The cross sections for the $W \rightarrow e\nu$ and $W \rightarrow \mu\nu$ channels were calculated separately and then compared. The two sets of cross sections were found in good agreement within their uncorrelated uncertainties. The systematic uncertainties specific to the individual channels were considered fully uncorrelated and the common systematic uncertainties fully correlated. Results for the electron and muon channels were combined using three passes of the best linear unbiased

estimator (BLUE) technique [63–65]. Three iterations were required to compute the upper systematic uncertainty, the central value, and the lower systematic uncertainty. The combination improved uncertainties and fluctuations in the tails of the measured distributions.

Particle-level expectations from ALPGEN and SHERPA simulations as well as a calculation using BLACKHAT-SHERPA were compared to the measured cross sections. PYTHIA is shown only for selected distributions that are given as a function of corrected jet multiplicity. As PYTHIA features LO matrix-element accuracy for events with up to one jet, it does not provide a good description of the data for jet multiplicities greater than one. The ALPGEN, PYTHIA, and SHERPA predictions were normalized to the NNLO inclusive W-boson production cross section. The version of BLACKHAT-SHERPA used here provides NLO predictions at parton level for W-boson production with $N_{\text{jet}} \leq 4$. No additional normalization was applied to the BLACKHAT-SHERPA predictions.

The measured W + jets cross sections and the cross-section ratios are shown as a function of the corrected jet multiplicity in Figs. 18 and 19. The cross section is shown

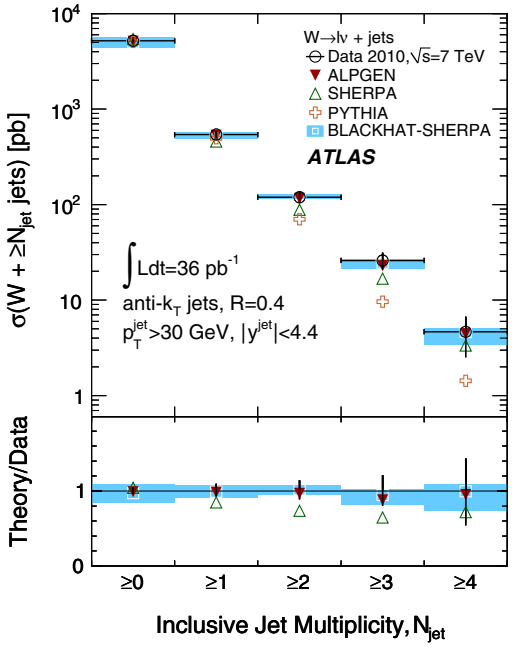

FIG. 18 (color online). W + jets cross-section results as a function of corrected jet multiplicity. The following remarks apply to this and subsequent figures unless specific comments are provided. The cross sections are quoted in the kinematic region described in Sec. V F. For the data, the statistical uncertainties are shown with a tick on the vertical bars, and the combined statistical and systematic uncertainties are shown with the full error bar. Also shown are predictions from ALPGEN, SHERPA, PYTHIA, and BLACKHAT-SHERPA, and the ratio of theoretical predictions to data (PYTHIA is not shown in the ratio). The distributions from SHERPA, PYTHIA, and ALPGEN were normalized to the NNLO total W-boson production cross section.

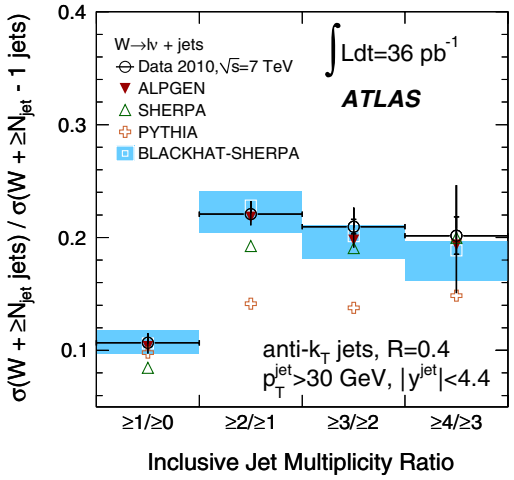

FIG. 19 (color online). W + jets cross-section ratio results as a function of corrected jet multiplicity.

as a function of the p_{T} of the first jet for $N_{\text{jet}} \geq 1$ to $N_{\text{jet}} \geq 4$ events separately in Fig. 20, the second jet for $N_{\text{jet}} \geq 2$ to $N_{\text{jet}} \geq 4$ events separately in Fig. 21, the third jet for $N_{\text{jet}} \geq 3$ and $N_{\text{jet}} \geq 4$ events separately in Fig. 22, and the

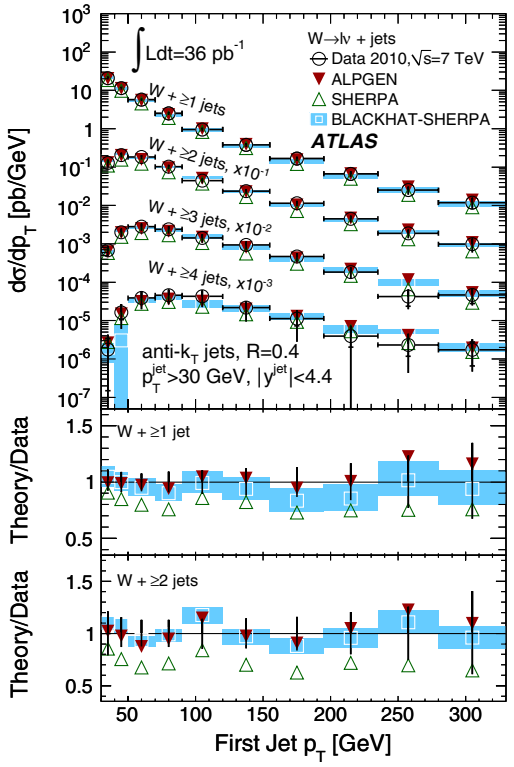

FIG. 20 (color online). W + jets cross section as a function of the p_{T} of the first jet in the event. The p_{T} of the first jet is shown separately for events with ≥ 1 jet to ≥ 4 jet. The ≥ 2 jet, ≥ 3 jet, and ≥ 4 jet distributions have been scaled down by factors of 10, 100, and 1000, respectively. Shown are predictions from ALPGEN, SHERPA, and BLACKHAT-SHERPA, and the ratio of theoretical predictions to data for ≥ 1 jet and ≥ 2 jet events.

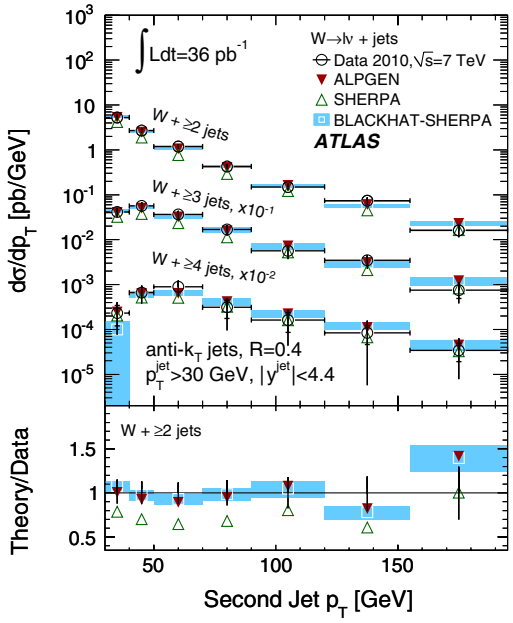

FIG. 21 (color online). W + jets cross section as a function of the p_{T} of the second jet in the event. The p_{T} of the second jet is shown separately for events with ≥ 2 jet to ≥ 4 jet. The ≥ 3 jet and ≥ 4 jet distributions have been scaled down by factors of 10 and 100, respectively. Shown are predictions from ALPGEN, SHERPA, and BLACKHAT-SHERPA, and the ratio of theoretical predictions to data for ≥ 2 jet events.

fourth jet for $N_{\mathrm{jet}} \geq 4$ events in Fig. 23. The jets are ordered from the highest to lowest p_{T}. The differential cross section as a function of H_{T} is shown for $N_{\mathrm{jet}} \geq 1$ to $N_{\mathrm{jet}} \geq 4$ in Fig. 24. Here H_{T} is defined as a scalar sum over p_{T} of the lepton, neutrino ($E_{\mathrm{T}}^{\mathrm{miss}}$), and all jets in the event. H_{T} is often used to set the renormalization and factorization scales in fixed-order calculations and is

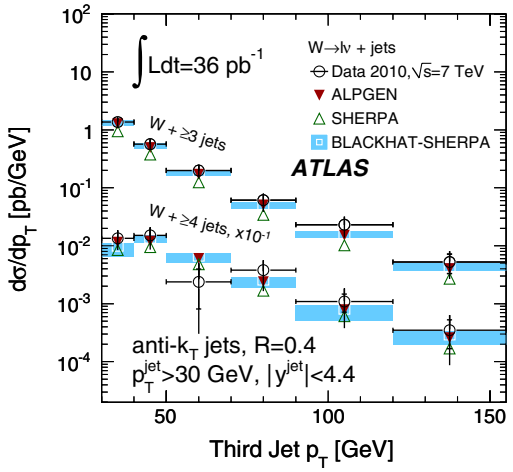

FIG. 22 (color online). W + jets cross section as a function of the p_{T} of the third jet in the event. The p_{T} of the third jet is shown separately for events with ≥ 3 jet and ≥ 4 jet. The ≥ 4 jet distribution has been scaled down by a factor of 10. Shown are predictions from ALPGEN, SHERPA, and BLACKHAT-SHERPA.

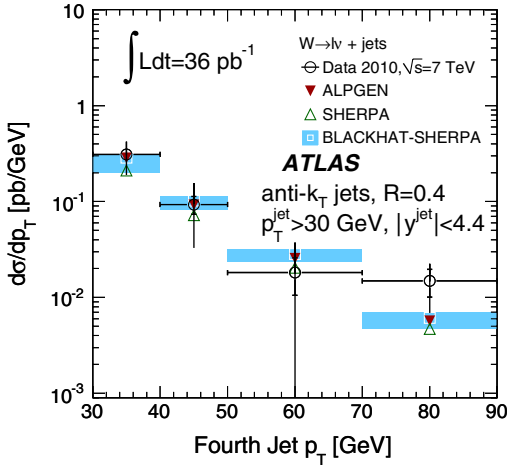

FIG. 23 (color online). W + jets cross section as a function of the p_{T} of the fourth jet in the event. The distributions are for events with ≥ 4 jet. Shown are predictions from ALPGEN, SHERPA, and BLACKHAT-SHERPA.

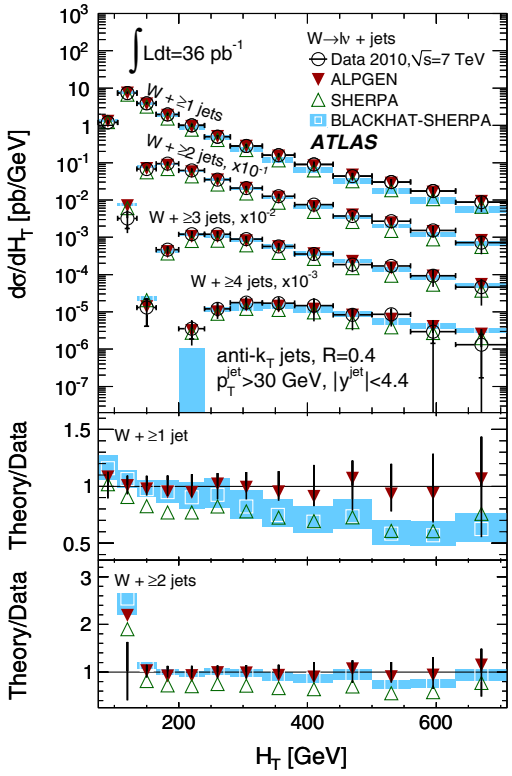

FIG. 24 (color online). W + jets cross section as a function of H_{T}, shown separately for ≥ 1 jets to ≥ 4 jets. The ≥ 2 jet, ≥ 3 jet, and ≥ 4 jet distributions have been scaled down by factors of 10, 100, and 1000, respectively. Shown are predictions from ALPGEN, SHERPA, and BLACKHAT-SHERPA, and the ratio of theoretical predictions to data for ≥ 1 jet and ≥ 2 jet events. The apparent discrepancy between the data and BLACKHAT-SHERPA predictions is discussed in the text.

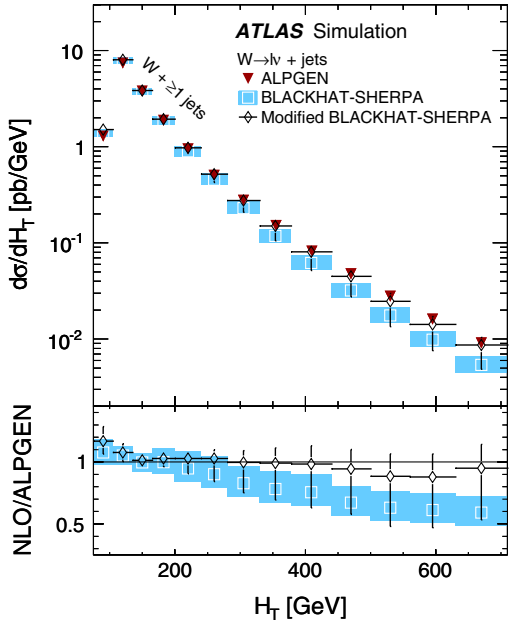

FIG. 25 (color online). W + jets cross section as a function of H_{T}, shown for final states with ≥ 1 jets. The cross sections are quoted in the kinematic region described in Sec. V F. Shown are predictions from ALPGEN, BLACKHAT-SHERPA, and modified BLACKHAT-SHERPA and the ratio of these NLO theoretical predictions to ALPGEN. The BLACKHAT-SHERPA predictions were modified by introducing higher-order NLO terms with two, three, and four real emissions to the $N_{\mathrm{jet}} \geq 1$ distribution. The distribution from ALPGEN was normalized to the NNLO total W-boson production cross section.

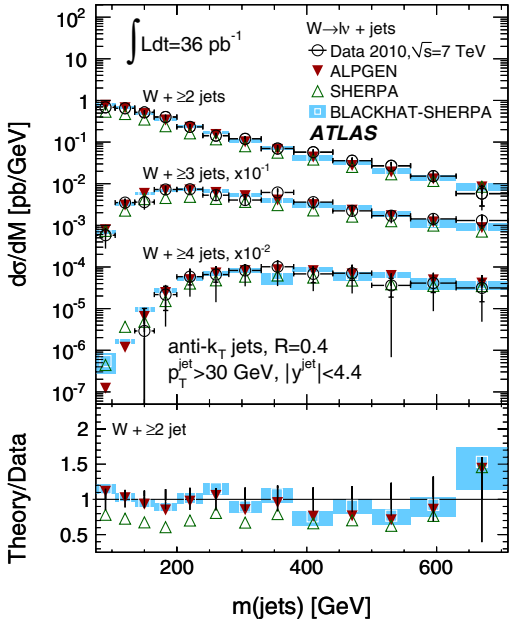

FIG. 26 (color online). W + jets cross section as a function of m(jets), shown separately for ≥ 2 jets to ≥ 4 jets. The ≥ 3 jet and ≥ 4 jet distributions have been scaled down by factors of 10 and 100, respectively. Shown are predictions from ALPGEN, SHERPA, and BLACKHAT-SHERPA, and the ratio of theoretical predictions to data for ≥ 2 jet events.

therefore an interesting variable to compare between data and predictions.

The measured H_{T} distribution for events with one or more jets is not well described by the BLACKHAT-SHERPA prediction. The prediction is calculated inclusively, at NLO, for events with a W boson and one or more jets: because of the limited order of the calculation, matrix elements with three or more real emissions of final-state partons are not included in the calculation. In contrast, ALPGEN, where LO matrix-element terms with up to five final-state partons are utilized, describes the data well. The data themselves are, as stated above, inclusive of all higher jet multiplicities. A modified treatment of BLACKHAT-SHERPA prediction was introduced, where higher-order NLO terms with two, three, and four real emissions were also added to the $N_{\mathrm{jet}} \geq 1$ distribution: this is shown in Fig. 25. The higher-order terms were combined by matching them exclusively in jet multiplicity by counting parton jets with $p_{\mathrm{T}} > 30$ GeV. The matching scheme is required to reduce double-counting of cross sections. This case illustrates the challenges of comparing NLO calculations to complex inclusive jet variables like H_{T}. In Fig. 26 the cross sections are shown as a function of the invariant mass, m(jets), of the first two, three, and four jets for events

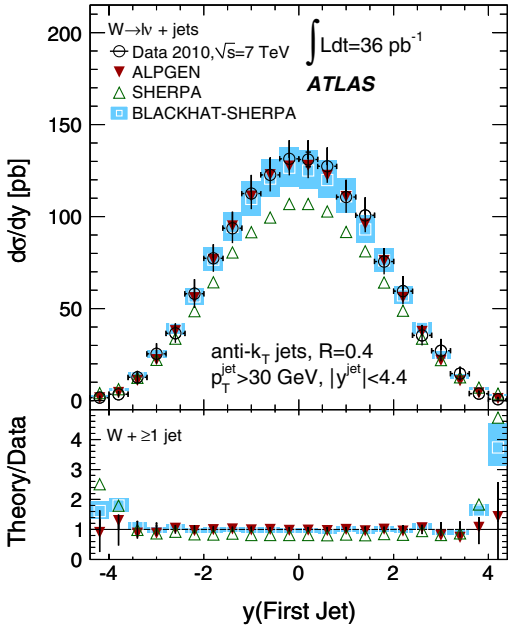

FIG. 27 (color online). W + jets cross section as a function of y(first jet) for events with ≥ 1 jets. Shown are predictions from ALPGEN, SHERPA, and BLACKHAT-SHERPA, and the ratio of theoretical predictions to data. The apparent discrepancy between the data and BLACKHAT-SHERPA predictions is described in the text.

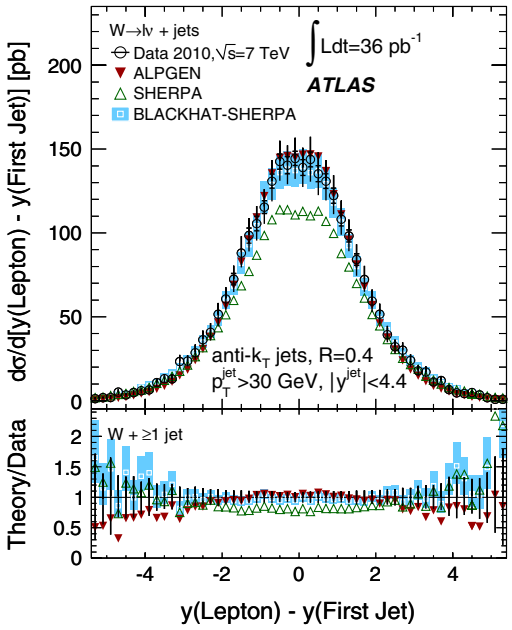

FIG. 28 (color online). W + jets cross section as a function of $y(\ell) - y$(first jet) for events with ≥ 1 jets. Shown are predictions from ALPGEN, SHERPA, and BLACKHAT-SHERPA, and the ratio of theoretical predictions to data.

with $N_{\text{jet}} \geq 2$, $N_{\text{jet}} \geq 3$, and $N_{\text{jet}} \geq 4$, respectively. The invariant mass of the multijet system is also considered for the renormalization and factorization scales in fixed-order pQCD calculations. Overall, these distributions constitute a set of tests for factorization and renormalization scales used in calculations of α_s; the ALPGEN samples demonstrate a better agreement with data than SHERPA due to differences in the scales and PDFs described in Sec. IV.

Distributions dependent on rapidities of the leptons and the first jet are shown in Figs. 27–29 for y(first jet), $y(\ell) - y$(first jet), and $y(\ell) + y$(first jet), respectively. These distributions are sensitive to PDFs used for calculations of LO and NLO matrix elements. Predictions from BLACKHAT-SHERPA and SHERPA were produced with CTEQ6.6M, a NLO PDF, while ALPGEN used CTEQ6L1, a LO PDF. The shape of the distributions from SHERPA were found to be similar to BLACKHAT-SHERPA. ALPGEN gave a different description of the $y(\ell) - y$(first jet) distribution. The deviations observed between the data and BLACKHAT-SHERPA at high jet rapidities in Fig. 27 may be caused by insufficient knowledge of the gluon PDFs at high x.

Lastly, distances between the first two jets are explored in Figs. 30–32 by defining the distance as ΔR(firstjet, secondjet), y(first jet) $-$ y(second jet), and $\Delta\phi$(first jet, second jet), respectively. This set of measurements offers a test of hard parton radiation at large angles and of matrix element to parton shower matching schemes. The majority of jets are modeled via the ME calculation for the jet pairs with large angular separation, when ΔR and $\Delta\phi$ are close to π. Collinear radiation at small angular separation, when ΔR is small, is produced mainly via the parton shower. Overall, ALPGEN and

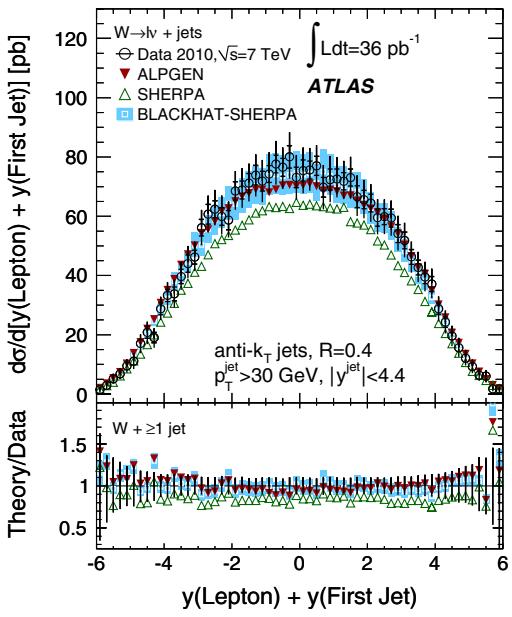

FIG. 29 (color online). W + jets cross section as a function of $y(\ell) + y$(first jet) for events with ≥ 1 jets. Shown are predictions from ALPGEN, SHERPA, and BLACKHAT-SHERPA, and the ratio of theoretical predictions to data.

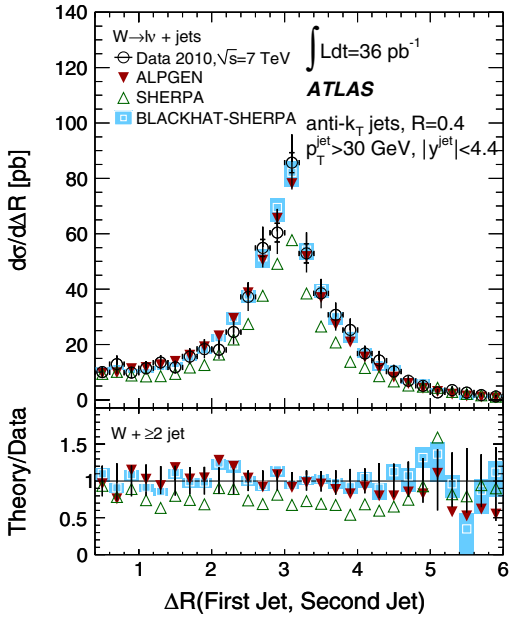

FIG. 30 (color online). W + jets cross section as a function of ΔR(first jet, second jet) for events with ≥ 2 jets. Shown are predictions from ALPGEN, SHERPA, and BLACKHAT-SHERPA, and the ratio of theoretical predictions to data.

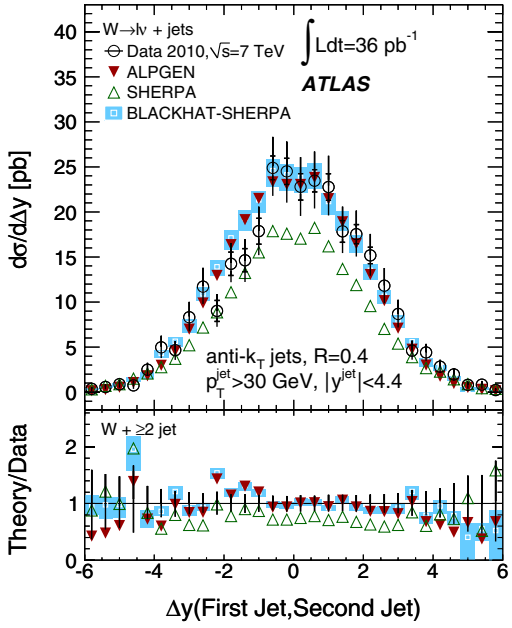

FIG. 31 (color online). W + jets cross section as a function of y(first jet) − y(second jet) for events with ≥ 2 jets. Shown are predictions from ALPGEN, SHERPA, and BLACKHAT-SHERPA, and the ratio of theoretical predictions to data.

BLACKHAT-SHERPA demonstrate good agreement with the data while SHERPA deviates due to the differences in PDFs, α_s, and factorization scales.

All distributions were also produced with the selection requirement on $p_{\mathrm{T}}^{\mathrm{jet}}$ reduced from 30 GeV to 20 GeV. The results for the softer threshold are given in the Appendix. The softer threshold makes the cross sections more sensitive to the non-pQCD and experimental effects, especially for forward jets.

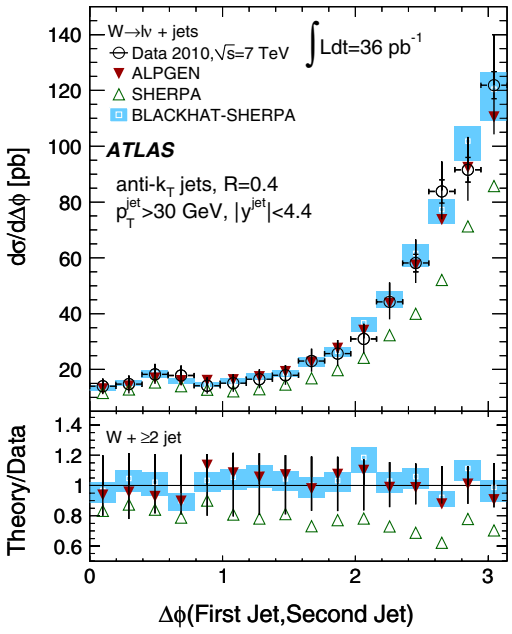

FIG. 32 (color online). W + jets cross section as a function of $\Delta\phi$(first jet, second jet) for events with ≥ 2 jets. Shown are predictions from ALPGEN, SHERPA, and BLACKHAT-SHERPA, and the ratio of theoretical predictions to data.

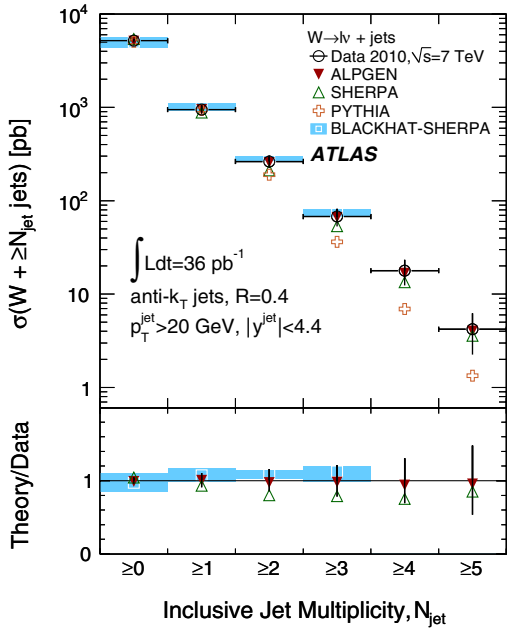

FIG. 33 (color online). W + jets cross-section results as a function of corrected jet multiplicity. The following remarks apply to this and subsequent figures unless specific comments are given. The cross sections are quoted in the restricted kinematic region described in Sec. V F, except here $p_{\mathrm{T}}^{\mathrm{jet}} > 20$ GeV. For the data, the statistical uncertainties are shown with a tick on the vertical bars, and the combined statistical and systematic uncertainties are shown with the full error bar. Also shown are predictions from ALPGEN, SHERPA, PYTHIA and BLACKHAT-SHERPA, and the ratio of theoretical predictions to data (PYTHIA is not shown in the ratio). The distributions from SHERPA, PYTHIA and ALPGEN were normalized to the NNLO total W-boson production cross section.

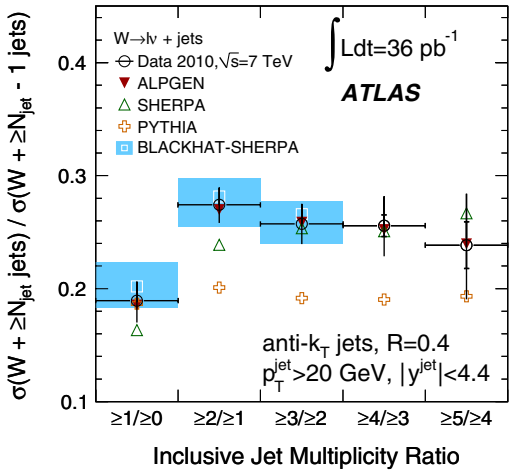

FIG. 34 (color online). W + jets cross-section ratio results as a function of corrected jet multiplicity.

All these cross sections accompanied by the non-pQCD and QED corrections are available in HEPDATA.

VIII. CONCLUSIONS

This paper presents a measurement of the W + jets cross section as a function of jet multiplicity in pp collisions at $\sqrt{s} = 7$ TeV in both electron and muon decay modes of the W boson, based on an integrated luminosity of 36 pb^{-1}. The ratios of cross sections $\sigma(W+ \geq N_{\text{jet}})/\sigma(W+ \geq N_{\text{jet}} - 1)$ have been calculated for inclusive jet multiplicities, N_{jet}, that range between 1–4 for the $p_{\text{T}}^{\text{jet}} > 30$ GeV jet threshold and between 1–5 for the $p_{\text{T}}^{\text{jet}} > 20$ GeV threshold. Measurements are also presented of the p_{T} distribution of the first through fourth jets in the event, of the invariant masses of two or more jets, of the distances between the lepton and the first jet, of the distances between the first two jets, and of the H_{T} distribution. The results have been corrected for all detector effects and are quoted in an ATLAS-specific range of jet and lepton kinematics. This range is almost fully covered by the detector acceptance, so as to avoid model-dependent extrapolations and to facilitate the comparison with theoretical predictions. Good agreement is observed between the predictions from the multiparton matrix-element generator ALPGEN and the measured distributions. At the same time, SHERPA demonstrates a slightly worse agreement with the experimental results than ALPGEN. The paper features the first comparison between the NLO predictions and the LHC data for events with a W boson and four jets. Calculations based on NLO matrix elements in MCFM (available for jet multiplicities $N_{\text{jet}} \leq 2$) and in BLACKHAT-SHERPA (available for jet multiplicities $N_{\text{jet}} \leq 4$) are generally in good agreement with the data; deviations are observed in the $d\sigma(W+ \geq \text{jet})/dH_{\text{T}}$ distribution at large H_{T} and in the tails of $d\sigma/dy(\text{jet})$ and $d\sigma/d(y(\ell) - y(\text{jet}))$ distributions.

ACKNOWLEDGMENTS

We are grateful to the BLACKHAT-SHERPA Collaboration and Daniel Maitre for all their help. We thank CERN for the very successful operation of the LHC, as well as the support staff from our institutions without whom ATLAS could not be operated efficiently. We acknowledge the support of ANPCyT, Argentina; YerPhI, Armenia; ARC, Australia; BMWF, Austria; ANAS, Azerbaijan; SSTC, Belarus; CNPq and FAPESP, Brazil; NSERC, NRC, and CFI, Canada; CERN; CONICYT, Chile; CAS, MOST, and NSFC, China; COLCIENCIAS, Colombia; MSMT CR, MPO CR, and VSC CR, Czech Republic; DNRF, DNSRC, and Lundbeck Foundation, Denmark; ARTEMIS, European Union; IN2P3-CNRS, CEA-DSM/IRFU, France; GNAS, Georgia; BMBF, DFG, HGF, MPG, and AvH Foundation, Germany; GSRT, Greece; ISF, MINERVA, GIF, DIP, and Benoziyo Center, Israel; INFN, Italy; MEXT and JSPS, Japan; CNRST, Morocco; FOM and NWO, Netherlands; RCN, Norway; MNiSW, Poland; GRICES and FCT, Portugal; MERYS (MECTS), Romania; MES of Russia and ROSATOM, Russian Federation; JINR; MSTD, Serbia; MSSR, Slovakia; ARRS and MVZT, Slovenia; DST/NRF, South Africa; MICINN, Spain; SRC and Wallenberg Foundation, Sweden; SER, SNSF, and Cantons of Bern and Geneva, Switzerland; NSC, Taiwan; TAEK, Turkey; STFC, the Royal Society and Leverhulme Trust, United Kingdom; DOE and NSF, United States of America. The crucial computing support from all WLCG partners is acknowledged gratefully, in particular, from CERN and the ATLAS Tier-1 facilities at TRIUMF (Canada), NDGF (Denmark, Norway, Sweden), CC-IN2P3 (France), KIT/GridKA (Germany), INFN-CNAF (Italy), NL-T1 (Netherlands), PIC (Spain), ASGC (Taiwan), RAL (UK), and BNL (USA) and in the Tier-2 facilities worldwide.

APPENDIX: RESULTS FOR A JET THRESHOLD OF $p_{\text{T}} > 20$ GeV

In Figs. 33–46, we present results for jets selected with a 20 GeV threshold in p_{T}. The distributions are the same variables as for jets with the 30 GeV threshold shown in Sec. VII except that the data with $N_{\text{jet}} \geq 5$ were used for physics conclusions; the 20 GeV threshold improved the

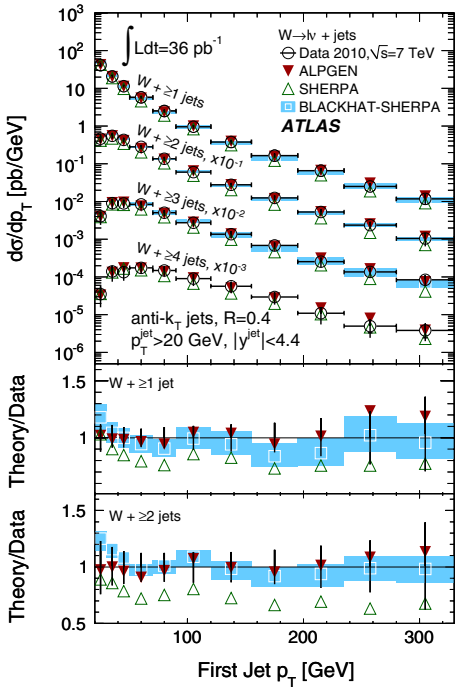

FIG. 35 (color online). W + jets cross section as a function of the p_{T} of the first jet in the event. The p_{T} of the first jet is shown separately for events with ≥ 1 jet to ≥ 4 jet. The ≥ 2 jet, ≥ 3 jet, and ≥ 4 jet distributions have been scaled down by factors of 10, 100, and 1000, respectively. Shown are predictions from ALPGEN, SHERPA, and BLACKHAT-SHERPA, and the ratio of theoretical predictions to data for ≥ 1 jet and ≥ 2 jet events.

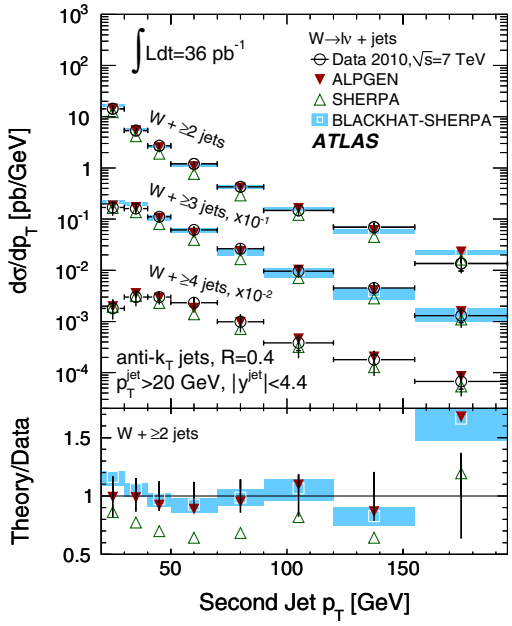

FIG. 36 (color online). W + jets cross section as a function of the p_{T} of the second jet in the event. The p_{T} of the second jet is shown separately for events with ≥ 2 jet to ≥ 4 jet. The ≥ 3 jet and ≥ 4 jet distributions have been scaled down by factors of 10 and 100, respectively. Shown are predictions from ALPGEN, SHERPA, and BLACKHAT-SHERPA, and the ratio of theoretical predictions to data for ≥ 2 jet events.

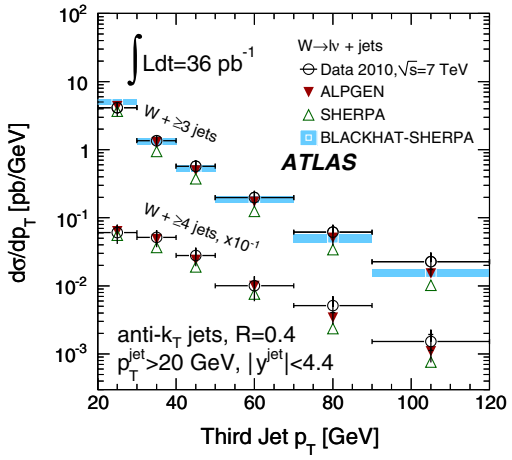

FIG. 37 (color online). W + jets cross section as a function of the p_{T} of the third jet in the event. The p_{T} of the third jet is shown separately for events with ≥ 3 jet and ≥ 4 jet. The ≥ 4 jet distribution has been scaled down by a factor of 10. Shown are predictions from ALPGEN, SHERPA, and BLACKHAT-SHERPA.

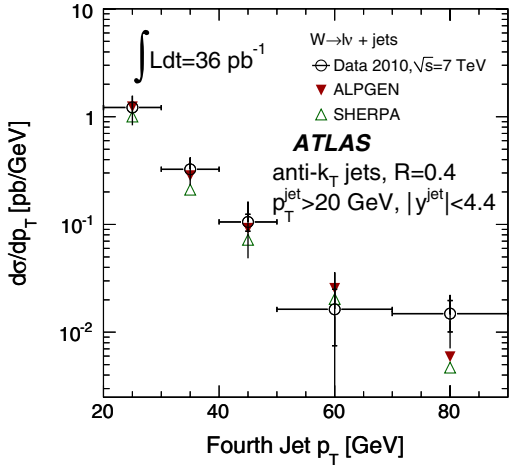

FIG. 38 (color online). W + jets cross section as a function of the p_{T} of the fourth jet in the event. The distributions are for events with ≥ 4 jet. Shown are predictions from ALPGEN and SHERPA.

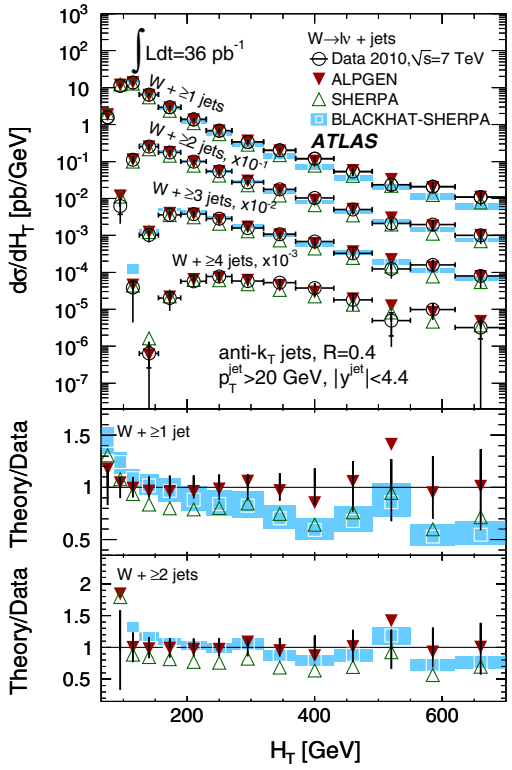

FIG. 39 (color online). W + jets cross section as a function of H_{T}, shown separately for ≥ 1 jets to ≥ 4 jets. The ≥ 2 jet, ≥ 3 jet, and ≥ 4 jet distributions have been scaled down by factors of 10, 100, and 1000, respectively. Shown are predictions from ALPGEN, SHERPA, and BLACKHAT-SHERPA, and the ratio of theoretical predictions to data for ≥ 1 jet and ≥ 2 jet events.

signal-to-background ratio and event count. The softer threshold makes the cross sections more sensitive to the non-pQCD and experimental effects such as the underlying event model, multiple parton interactions, parton fragmentation, hadronization, and pileup pp interactions. The corrections accounting for the non-pQCD effects, that were applied to BLACKHAT-SHERPA calculations, increased monotonically with the absolute value of jet rapidity from $\sim$1.0 up to $\sim$2.4. The uncertainties on the corrections are also larger in the forward region.

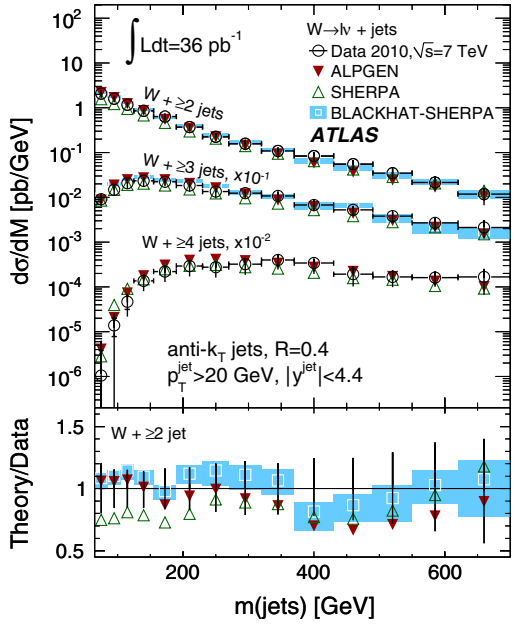

FIG. 40 (color online). W + jets cross section as a function of m(jets), shown separately for ≥ 2 jets to ≥ 4 jets. The ≥ 3 jet and ≥ 4 jet distributions have been scaled down by factors of 10 and 100, respectively. Shown are predictions from ALPGEN, SHERPA, and BLACKHAT-SHERPA, and the ratio of theoretical predictions to data for ≥ 2 jet events.

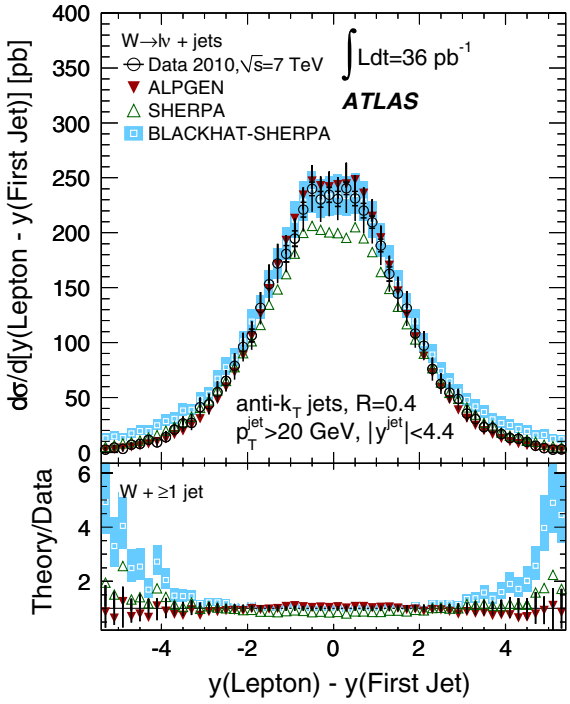

FIG. 42 (color online). W + jets cross section as a function of $y(\ell) - y$(first jet) for events with ≥ 1 jets. Shown are predictions from ALPGEN, SHERPA, and BLACKHAT-SHERPA, and the ratio of theoretical predictions to data.

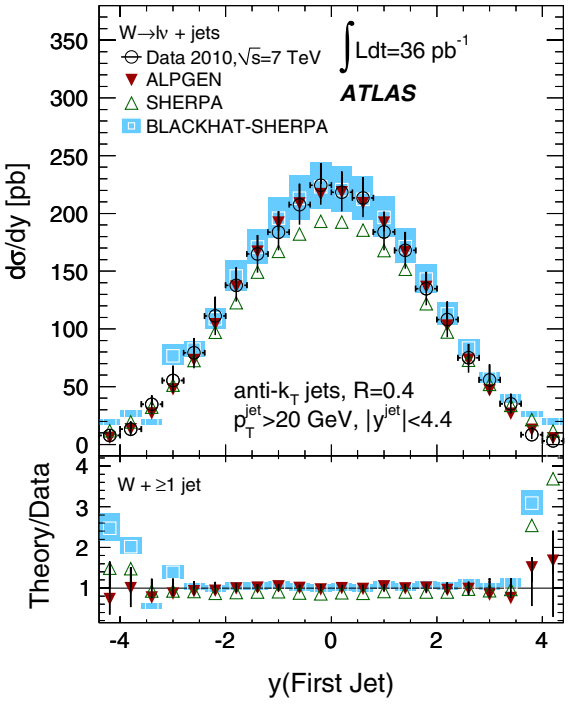

FIG. 41 (color online). W + jets cross section as a function of y(first jet) for events with ≥ 1 jets. Shown are predictions from ALPGEN, SHERPA, and BLACKHAT-SHERPA, and the ratio of theoretical predictions to data.

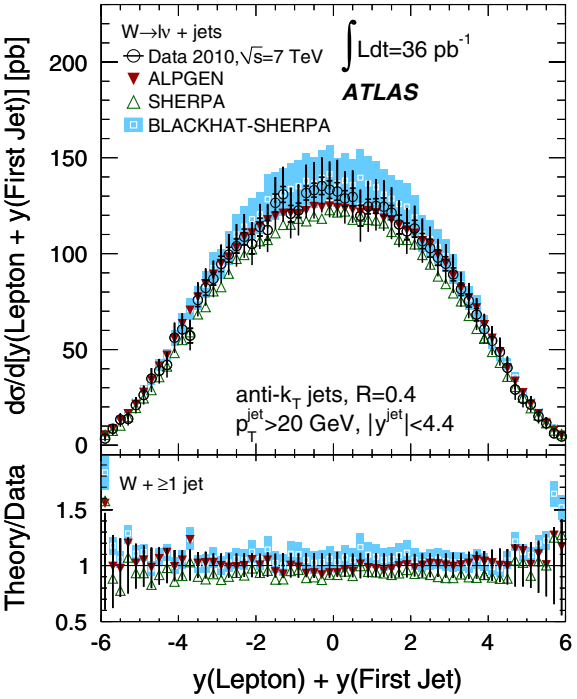

FIG. 43 (color online). W + jets cross section as a function of $y(\ell) + y$(first jet) for events with ≥ 1 jets. Shown are predictions from ALPGEN, SHERPA, and BLACKHAT-SHERPA, and the ratio of theoretical predictions to data.

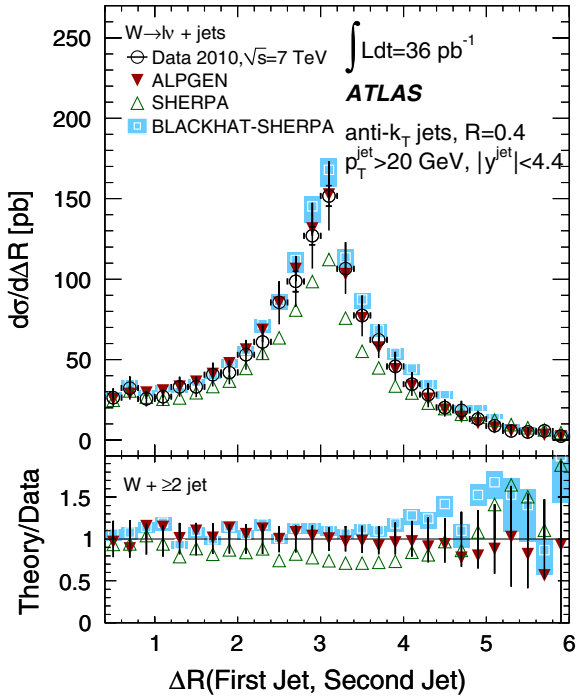

FIG. 44 (color online). W + jets cross section as a function of ΔR(firstjet, secondjet) for events with ≥ 2 jets. Shown are predictions from ALPGEN, SHERPA, and BLACKHAT-SHERPA, and the ratio of theoretical predictions to data.

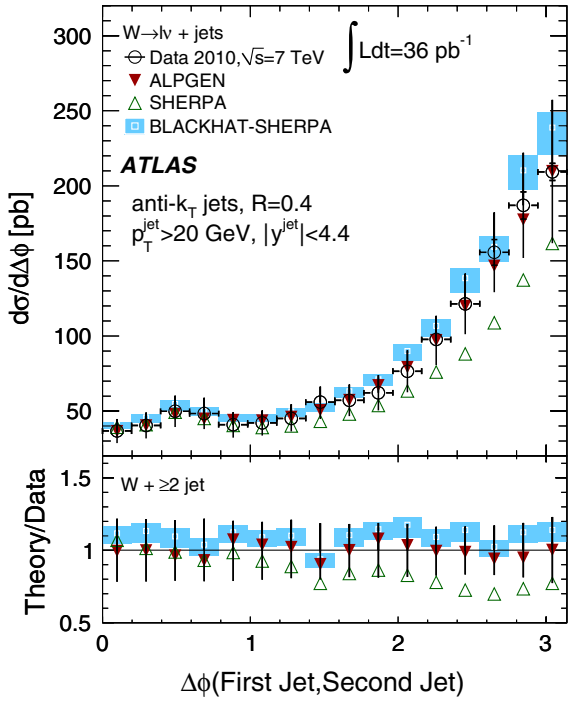

FIG. 46 (color online). W + jets cross section as a function of $\Delta\phi$(first jet, second jet) for events with ≥ 2 jets. Shown are predictions from ALPGEN, SHERPA, and BLACKHAT-SHERPA, and the ratio of theoretical predictions to data.

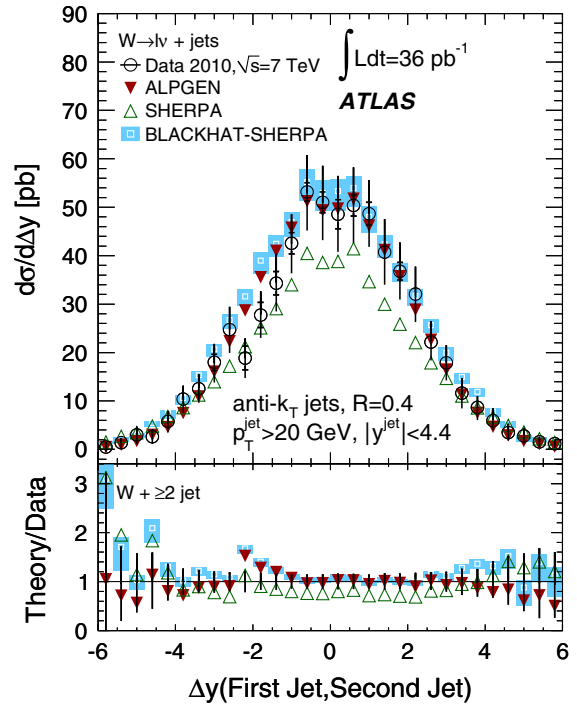

FIG. 45 (color online). W + jets cross section as a function of y(first jet) − y(second jet) for events with ≥ 2 jets. Shown are predictions from ALPGEN, SHERPA, and BLACKHAT-SHERPA, and the ratio of theoretical predictions to data.

[1] CDF Collaboration, Phys. Rev. D **77**, 011108 (2008).
[2] D0 Collaboration, Phys. Lett. B **705**, 200 (2011).
[3] CMS Collaboration, arXiv:1110.3226.
[4] D0 Collaboration, Phys. Lett. B **678**, 45 (2009).
[5] D0 Collaboration, Phys. Lett. B **682**, 370 (2010).
[6] CDF Collaboration, Phys. Rev. Lett. **100**, 102001 (2008).
[7] G. Aad *et al.* (ATLAS Collaboration), Phys. Rev. D **85**, 032009 (2012).
[8] G. Aad *et al.* (ATLAS Collaboration), Phys. Rev. D **85**, 012005 (2012).
[9] ATLAS Collaboration, Phys. Lett. B **698**, 325 (2011).
[10] R. K. Ellis *et al.*, Phys. Rev. D **80**, 094002 (2009).
[11] C. F. Berger, Z. Bern, L. J. Dixon, F. Febres Cordero, D. Forde, T. Gleisberg, H. Ita, D. A. Kosower, and D. Maître, Phys. Rev. Lett. **106**, 092001 (2011).
[12] ATLAS Collaboration, JINST **3**, S08003 (2008).
[13] ATLAS Collaboration, Report No. CERN-OPEN-2008-020, 2009.
[14] ATLAS Collaboration, Report No. ATLAS-CONF-2011-011, 2011.
[15] ATLAS Collaboration, Eur. Phys. J. C **71**, 1630 (2011).
[16] ATLAS Collaboration, Phys. Rev. D **85**, 072004 (2012).
[17] G. Aad *et al.* (ATLAS Collaboration), Eur. Phys. J. C **72**, 1909 (2012).
[18] ATLAS Collaboration, Eur. Phys. J. C **70**, 823 (2010).
[19] S. Agostinelli *et al.*, Nucl. Instrum. Methods Phys. Res., Sect. A **506**, 250 (2003).
[20] K. Melnikov and F. Petriello, Phys. Rev. D **74**, 114017 (2006).

[21] A. D. Martin, W. J. Stirling, R. S. Thorne, and G. Watt, Eur. Phys. J. C **63**, 189 (2009).
[22] T. Sjöstrand, S. Mrenna, and P. Skands, J. High Energy Phys. 05 (2006) 026.
[23] M. L. Mangano *et al.*, J. High Energy Phys. 07 (2003) 001.
[24] T. Gleisberg *et al.*, J. High Energy Phys. 02 (2009) 007.
[25] S. Frixione, P. Nason, and C. Oleari, J. High Energy Phys. 11 (2007) 070.
[26] The cross section for the inclusive $t\bar{t}$ production was calculated with Hathor [27] with $m_{\text{top}} = 172.5$ GeV, CTEQ6.6 [28], with PDF and scale uncertainties added linearly [29,30].
[27] M. Aliev, H. Lacker, U. Langenfeld, S. Moch, P. Uwer, and M. Wiedermann, Comput. Phys. Commun. **182**, 1034 (2011).
[28] P. M. Nadolsky *et al.*, Phys. Rev. D **78**, 013004 (2008).
[29] S. Moch and P. Uwer, Phys. Rev. D **78**, 034003 (2008).
[30] M. Beneke, M. Czakon, P. Falgari, A. Mitov, and C. Schwinn, Phys. Lett. B **690**, 483 (2010).
[31] B. P. Kersevan and E. Richter-Was, arXiv:hep-ph/0405247.
[32] S. Frixione and B. R. Webber, J. High Energy Phys. 06 (2002) 029.
[33] S. Frixione, E. Laenen, P. Motylinski, and B. R. Webber, J. High Energy Phys. 03 (2006) 092.
[34] J. M. Campbell, R. K. Ellis, and D. L. Rainwater, Phys. Rev. D **68**, 094021 (2003).
[35] S. Frixione, E. Laenen, P. Motylinski, B. R. Webber, and C. D. White, J. High Energy Phys. 07 (2008) 029.
[36] G. Corcella *et al.*, J. High Energy Phys. 01 (2001) 010.
[37] J. M. Butterworth, J. R. Forshaw, and M. H. Seymour, Z. Phys. C **72**, 637 (1996).
[38] The ISR and FSR rates were increased or decreased individually or simultaneously. To decrease ISR, parameters PARP(67) and PARP(64) were adjusted from 4 and 1 to 0.5 and 4, respectively. They were set to 6 and 0.25 to increase ISR. Similarly, parameters PARP(72) and PARJ (82) were switched from 0.192 GeV and 1 GeV to 0.096 GeV and 2 GeV to decrease FSR and to 0.384 GeV and 0.5 GeV to increase FSR.
[39] M. L. Mangano, M. Moretti, F. Piccinini, and M. Treccani, J. High Energy Phys. 01 (2007) 013.
[40] S. Catani, F. Krauss, R. Kuhn, and B. R. Webber, J. High Energy Phys. 11 (2001) 063.
[41] F. Krauss, J. High Energy Phys. 08 (2002) 015.
[42] J. Pumplin *et al.*, J. High Energy Phys. 07 (2002) 012.
[43] A. Sherstnev and R. S. Thorne, Eur. Phys. J. C **55**, 553 (2008).
[44] P. Golonka and Z. Was, Eur. Phys. J. C **45**, 97 (2006).
[45] N. Davidson *et al.*, Comput. Phys. Commun. **183**, 821 (2012).
[46] ATLAS Collaboration, Report No. ATL-PHYS-PUB-2010-014, 2010.
[47] ATLAS Collaboration, Report No. ATLAS-CONF-2010-031, 2010.
[48] ATLAS Collaboration, arXiv:1112.6426.
[49] M. Cacciari, G. P. Salam, and G. Soyez, J. High Energy Phys. 04 (2008) 063.
[50] W. Lampl *et al.*, Report No. ATL-LARG-PUB-2008-002, 2008.
[51] ATLAS Collaboration, Eur. Phys. J. C **72**, 1844 (2012).
[52] T. Barillari *et al.*, Report No. ATL-LARG-PUB-2009-001, 2009.
[53] ATLAS Collaboration, Report No. ATLAS-CONF-2011-008, 2011.
[54] ATLAS Collaboration, Report No. ATLAS-CONF-2011-063, 2011.
[55] ATLAS Collaboration, Report No. ATLAS-CONF-2011-046, 2011.
[56] ATLAS Collaboration, Phys. Lett. B **707**, 459 (2012).
[57] G. D'Agostini, Nucl. Instrum. Methods Phys. Res., Sect. A **362**, 487 (1995).
[58] J. M. Butterworth *et al.*, arXiv:1003.1643.
[59] The iterative procedure was stopped when the statistical uncertainty was 5 times larger than the last change in the unfolded value.
[60] M. Botje, J. Butterworth, A. Cooper-Sarkar, A. de Roeck, J. Feltesse *et al.*, arXiv:1101.0538.
[61] R. D. Ball, L. Del Debbio, S. Forte, A. Guffanti, J. I. Latorre *et al.*, Nucl. Phys. B **838**,136 (2010).
[62] ATLAS Collaboration, Report No. ATL-PHYS-PUB-2011-008, 2011.
[63] L. Lyons, D. Gibaut, and P. Clifford, Nucl. Instrum. Methods Phys. Res., Sect. A **270**, 110 (1988).
[64] A. Valassi, Nucl. Instrum. Methods Phys. Res., Sect. A **500**, 391 (2003).
[65] R. C. Group, C. I. Ciobanu, K. Lannon, and C. Plager, arXiv:0809.4670.

G. Aad,[47] B. Abbott,[110] J. Abdallah,[11] A. A. Abdelalim,[48] A. Abdesselam,[117] O. Abdinov,[10] B. Abi,[111] M. Abolins,[87] H. Abramowicz,[152] H. Abreu,[114] E. Acerbi,[88a,88b] B. S. Acharya,[163a,163b] L. Adamczyk,[37] D. L. Adams,[24] T. N. Addy,[55] J. Adelman,[174] M. Aderholz,[98] S. Adomeit,[97] P. Adragna,[74] T. Adye,[128] S. Aefsky,[22] J. A. Aguilar-Saavedra,[123b,b] M. Aharrouche,[80] S. P. Ahlen,[21] F. Ahles,[47] A. Ahmad,[147] M. Ahsan,[40] G. Aielli,[132a,132b] T. Akdogan,[18a] T. P. A. Åkesson,[78] G. Akimoto,[154] A. V. Akimov,[93] A. Akiyama,[66] M. S. Alam,[1] M. A. Alam,[75] J. Albert,[168] S. Albrand,[54] M. Aleksa,[29] I. N. Aleksandrov,[64] F. Alessandria,[88a] C. Alexa,[25a] G. Alexander,[152] G. Alexandre,[48] T. Alexopoulos,[9] M. Alhroob,[20] M. Aliev,[15] G. Alimonti,[88a] J. Alison,[119] M. Aliyev,[10] P. P. Allport,[72] S. E. Allwood-Spiers,[52] J. Almond,[81] A. Aloisio,[101a,101b] R. Alon,[170] A. Alonso,[78] B. Alvarez Gonzalez,[87] M. G. Alviggi,[101a,101b] K. Amako,[65] P. Amaral,[29] C. Amelung,[22] V. V. Ammosov,[127] A. Amorim,[123a,c] G. Amorós,[166] N. Amram,[152] C. Anastopoulos,[29] L. S. Ancu,[16] N. Andari,[114] T. Andeen,[34] C. F. Anders,[20] G. Anders,[57a] K. J. Anderson,[30] A. Andreazza,[88a,88b] V. Andrei,[57a] M-L. Andrieux,[54] X. S. Anduaga,[69] A. Angerami,[34] F. Anghinolfi,[29] A. Anisenkov,[106] N. Anjos,[123a] A. Annovi,[46] A. Antonaki,[8]

M. Antonelli,[46] A. Antonov,[95] J. Antos,[143b] F. Anulli,[131a] S. Aoun,[82] L. Aperio Bella,[4] R. Apolle,[117,d] G. Arabidze,[87] I. Aracena,[142] Y. Arai,[65] A. T. H. Arce,[44] J. P. Archambault,[28] S. Arfaoui,[82] J-F. Arguin,[14] E. Arik,[18a,a] M. Arik,[18a] A. J. Armbruster,[86] O. Arnaez,[80] C. Arnault,[114] A. Artamonov,[94] G. Artoni,[131a,131b] D. Arutinov,[20] S. Asai,[154] R. Asfandiyarov,[171] S. Ask,[27] B. Åsman,[145a,145b] L. Asquith,[5] K. Assamagan,[24] A. Astbury,[168] A. Astvatsatourov,[51] B. Aubert,[4] E. Auge,[114] K. Augsten,[126] M. Aurousseau,[144a] G. Avolio,[162] R. Avramidou,[9] D. Axen,[167] C. Ay,[53] G. Azuelos,[92,e] Y. Azuma,[154] M. A. Baak,[29] G. Baccaglioni,[88a] C. Bacci,[133a,133b] A. M. Bach,[14] H. Bachacou,[135] K. Bachas,[29] G. Bachy,[29] M. Backes,[48] M. Backhaus,[20] E. Badescu,[25a] P. Bagnaia,[131a,131b] S. Bahinipati,[2] Y. Bai,[32a] D. C. Bailey,[157] T. Bain,[157] J. T. Baines,[128] O. K. Baker,[174] M. D. Baker,[24] S. Baker,[76] E. Banas,[38] P. Banerjee,[92] Sw. Banerjee,[171] D. Banfi,[29] A. Bangert,[149] V. Bansal,[168] H. S. Bansil,[17] L. Barak,[170] S. P. Baranov,[93] A. Barashkou,[64] A. Barbaro Galtieri,[14] T. Barber,[47] E. L. Barberio,[85] D. Barberis,[49a,49b] M. Barbero,[20] D. Y. Bardin,[64] T. Barillari,[98] M. Barisonzi,[173] T. Barklow,[142] N. Barlow,[27] B. M. Barnett,[128] R. M. Barnett,[14] A. Baroncelli,[133a] G. Barone,[48] A. J. Barr,[117] F. Barreiro,[79] J. Barreiro Guimarães da Costa,[56] P. Barrillon ,[114] R. Bartoldus,[142] A. E. Barton,[70] V. Bartsch,[148] R. L. Bates,[52] L. Batkova,[143a] J. R. Batley,[27] A. Battaglia,[16] M. Battistin,[29] F. Bauer,[135] H. S. Bawa,[142,f] S. Beale,[97] B. Beare,[157] T. Beau,[77] P. H. Beauchemin,[160] R. Beccherle,[49a] P. Bechtle,[20] H. P. Beck,[16] S. Becker,[97] M. Beckingham,[137] K. H. Becks,[173] A. J. Beddall,[18c] A. Beddall,[18c] S. Bedikian,[174] V. A. Bednyakov,[64] C. P. Bee,[82] M. Begel,[24] S. Behar Harpaz,[151] P. K. Behera,[62] M. Beimforde,[98] C. Belanger-Champagne,[84] P. J. Bell,[48] W. H. Bell,[48] G. Bella,[152] L. Bellagamba,[19a] F. Bellina,[29] M. Bellomo,[29] A. Belloni,[56] O. Beloborodova,[106,g] K. Belotskiy,[95] O. Beltramello,[29] S. Ben Ami,[151] O. Benary,[152] D. Benchekroun,[134a] C. Benchouk,[82] M. Bendel,[80] N. Benekos,[164] Y. Benhammou,[152] J. A. Benitez Garcia,[158b] D. P. Benjamin,[44] M. Benoit,[114] J. R. Bensinger,[22] K. Benslama,[129] S. Bentvelsen,[104] D. Berge,[29] E. Bergeaas Kuutmann,[41] N. Berger,[4] F. Berghaus,[168] E. Berglund,[104] J. Beringer,[14] P. Bernat,[76] R. Bernhard,[47] C. Bernius,[24] T. Berry,[75] C. Bertella,[82] A. Bertin,[19a,19b] F. Bertinelli,[29] F. Bertolucci,[121a,121b] M. I. Besana,[88a,88b] N. Besson,[135] S. Bethke,[98] W. Bhimji,[45] R. M. Bianchi,[29] M. Bianco,[71a,71b] O. Biebel,[97] S. P. Bieniek,[76] K. Bierwagen,[53] J. Biesiada,[14] M. Biglietti,[133a] H. Bilokon,[46] M. Bindi,[19a,19b] S. Binet,[114] A. Bingul,[18c] C. Bini,[131a,131b] C. Biscarat,[176] U. Bitenc,[47] K. M. Black,[21] R. E. Blair,[5] J.-B. Blanchard,[114] G. Blanchot,[29] T. Blazek,[143a] C. Blocker,[22] J. Blocki,[38] A. Blondel,[48] W. Blum,[80] U. Blumenschein,[53] G. J. Bobbink,[104] V. B. Bobrovnikov,[106] S. S. Bocchetta,[78] A. Bocci,[44] C. R. Boddy,[117] M. Boehler,[41] J. Boek,[173] N. Boelaert,[35] S. Böser,[76] J. A. Bogaerts,[29] A. Bogdanchikov,[106] A. Bogouch,[89,a] C. Bohm,[145a] V. Boisvert,[75] T. Bold,[37] V. Boldea,[25a] N. M. Bolnet,[135] M. Bona,[74] V. G. Bondarenko,[95] M. Bondioli,[162] M. Boonekamp,[135] G. Boorman,[75] C. N. Booth,[138] S. Bordoni,[77] C. Borer,[16] A. Borisov,[127] G. Borissov,[70] I. Borjanovic,[12a] S. Borroni,[86] K. Bos,[104] D. Boscherini,[19a] M. Bosman,[11] H. Boterenbrood,[104] D. Botterill,[128] J. Bouchami,[92] J. Boudreau,[122] E. V. Bouhova-Thacker,[70] D. Boumediene,[33] C. Bourdarios,[114] N. Bousson,[82] A. Boveia,[30] J. Boyd,[29] I. R. Boyko,[64] N. I. Bozhko,[127] I. Bozovic-Jelisavcic,[12b] J. Bracinik,[17] A. Braem,[29] P. Branchini,[133a] G. W. Brandenburg,[56] A. Brandt,[7] G. Brandt,[117] O. Brandt,[53] U. Bratzler,[155] B. Brau,[83] J. E. Brau,[113] H. M. Braun,[173] B. Brelier,[157] J. Bremer,[29] R. Brenner,[165] S. Bressler,[170] D. Breton,[114] D. Britton,[52] F. M. Brochu,[27] I. Brock,[20] R. Brock,[87] T. J. Brodbeck,[70] E. Brodet,[152] F. Broggi,[88a] C. Bromberg,[87] J. Bronner,[98] G. Brooijmans,[34] W. K. Brooks,[31b] G. Brown,[81] H. Brown,[7] P. A. Bruckman de Renstrom,[38] D. Bruncko,[143b] R. Bruneliere,[47] S. Brunet,[60] A. Bruni,[19a] G. Bruni,[19a] M. Bruschi,[19a] T. Buanes,[13] Q. Buat,[54] F. Bucci,[48] J. Buchanan,[117] N. J. Buchanan,[2] P. Buchholz,[140] R. M. Buckingham,[117] A. G. Buckley,[45] S. I. Buda,[25a] I. A. Budagov,[64] B. Budick,[107] V. Büscher,[80] L. Bugge,[116] O. Bulekov,[95] M. Bunse,[42] T. Buran,[116] H. Burckhart,[29] S. Burdin,[72] T. Burgess,[13] S. Burke,[128] E. Busato,[33] P. Bussey,[52] C. P. Buszello,[165] F. Butin,[29] B. Butler,[142] J. M. Butler,[21] C. M. Buttar,[52] J. M. Butterworth,[76] W. Buttinger,[27] S. Cabrera Urbán,[166] D. Caforio,[19a,19b] O. Cakir,[3a] P. Calafiura,[14] G. Calderini,[77] P. Calfayan,[97] R. Calkins,[105] L. P. Caloba,[23a] R. Caloi,[131a,131b] D. Calvet,[33] S. Calvet,[33] R. Camacho Toro,[33] P. Camarri,[132a,132b] M. Cambiaghi,[118a,118b] D. Cameron,[116] L. M. Caminada,[14] S. Campana,[29] M. Campanelli,[76] V. Canale,[101a,101b] F. Canelli,[30,h] A. Canepa,[158a] J. Cantero,[79] L. Capasso,[101a,101b] M. D. M. Capeans Garrido,[29] I. Caprini,[25a] M. Caprini,[25a] D. Capriotti,[98] M. Capua,[36a,36b] R. Caputo,[80] C. Caramarcu,[24] R. Cardarelli,[132a] T. Carli,[29] G. Carlino,[101a] L. Carminati,[88a,88b] B. Caron,[84] S. Caron,[47] G. D. Carrillo Montoya,[171] A. A. Carter,[74] J. R. Carter,[27] J. Carvalho,[123a,i] D. Casadei,[107] M. P. Casado,[11] M. Cascella,[121a,121b] C. Caso,[49a,49b,a] A. M. Castaneda Hernandez,[171] E. Castaneda-Miranda,[171] V. Castillo Gimenez,[166] N. F. Castro,[123a] G. Cataldi,[71a] F. Cataneo,[29] A. Catinaccio,[29] J. R. Catmore,[29] A. Cattai,[29] G. Cattani,[132a,132b] S. Caughron,[87] D. Cauz,[163a,163c] P. Cavalleri,[77] D. Cavalli,[88a] M. Cavalli-Sforza,[11] V. Cavasinni,[121a,121b] F. Ceradini,[133a,133b] A. S. Cerqueira,[23b] A. Cerri,[29] L. Cerrito,[74] F. Cerutti,[46] S. A. Cetin,[18b]

F. Cevenini,[101a,101b] A. Chafaq,[134a] D. Chakraborty,[105] K. Chan,[2] B. Chapleau,[84] J. D. Chapman,[27] J. W. Chapman,[86] E. Chareyre,[77] D. G. Charlton,[17] V. Chavda,[81] C. A. Chavez Barajas,[29] S. Cheatham,[84] S. Chekanov,[5] S. V. Chekulaev,[158a] G. A. Chelkov,[64] M. A. Chelstowska,[103] C. Chen,[63] H. Chen,[24] S. Chen,[32c] T. Chen,[32c] X. Chen,[171] S. Cheng,[32a] A. Cheplakov,[64] V. F. Chepurnov,[64] R. Cherkaoui El Moursli,[134e] V. Chernyatin,[24] E. Cheu,[6] S. L. Cheung,[157] L. Chevalier,[135] G. Chiefari,[101a,101b] L. Chikovani,[50a] J. T. Childers,[57a] A. Chilingarov,[70] G. Chiodini,[71a] M. V. Chizhov,[64] G. Choudalakis,[30] S. Chouridou,[136] I. A. Christidi,[76] A. Christov,[47] D. Chromek-Burckhart,[29] M. L. Chu,[150] J. Chudoba,[124] G. Ciapetti,[131a,131b] K. Ciba,[37] A. K. Ciftci,[3a] R. Ciftci,[3a] D. Cinca,[33] V. Cindro,[73] M. D. Ciobotaru,[162] C. Ciocca,[19a] A. Ciocio,[14] M. Cirilli,[86] M. Citterio,[88a] M. Ciubancan,[25a] A. Clark,[48] P. J. Clark,[45] W. Cleland,[122] J. C. Clemens,[82] B. Clement,[54] C. Clement,[145a,145b] R. W. Clifft,[128] Y. Coadou,[82] M. Cobal,[163a,163c] A. Coccaro,[49a,49b] J. Cochran,[63] P. Coe,[117] J. G. Cogan,[142] J. Coggeshall,[164] E. Cogneras,[176] J. Colas,[4] A. P. Colijn,[104] N. J. Collins,[17] C. Collins-Tooth,[52] J. Collot,[54] G. Colon,[83] P. Conde Muiño,[123a] E. Coniavitis,[117] M. C. Conidi,[11] M. Consonni,[103] V. Consorti,[47] S. Constantinescu,[25a] C. Conta,[118a,118b] F. Conventi,[101a,j] J. Cook,[29] M. Cooke,[14] B. D. Cooper,[76] A. M. Cooper-Sarkar,[117] K. Copic,[14] T. Cornelissen,[173] M. Corradi,[19a] F. Corriveau,[84,k] A. Cortes-Gonzalez,[164] G. Cortiana,[98] G. Costa,[88a] M. J. Costa,[166] D. Costanzo,[138] T. Costin,[30] D. Côté,[29] R. Coura Torres,[23a] L. Courneyea,[168] G. Cowan,[75] C. Cowden,[27] B. E. Cox,[81] K. Cranmer,[107] F. Crescioli,[121a,121b] M. Cristinziani,[20] G. Crosetti,[36a,36b] R. Crupi,[71a,71b] S. Crépé-Renaudin,[54] C.-M. Cuciuc,[25a] C. Cuenca Almenar,[174] T. Cuhadar Donszelmann,[138] M. Curatolo,[46] C. J. Curtis,[17] C. Cuthbert,[149] P. Cwetanski,[60] H. Czirr,[140] Z. Czyczula,[174] S. D'Auria,[52] M. D'Onofrio,[72] A. D'Orazio,[131a,131b] P. V. M. Da Silva,[23a] C. Da Via,[81] W. Dabrowski,[37] T. Dai,[86] C. Dallapiccola,[83] M. Dam,[35] M. Dameri,[49a,49b] D. S. Damiani,[136] H. O. Danielsson,[29] D. Dannheim,[98] V. Dao,[48] G. Darbo,[49a] G. L. Darlea,[25b] C. Daum,[104] W. Davey,[20] T. Davidek,[125] N. Davidson,[85] R. Davidson,[70] E. Davies,[117,d] M. Davies,[92] A. R. Davison,[76] Y. Davygora,[57a] E. Dawe,[141] I. Dawson,[138] J. W. Dawson,[5,a] R. K. Daya-Ishmukhametova,[22] K. De,[7] R. de Asmundis,[101a] S. De Castro,[19a,19b] P. E. De Castro Faria Salgado,[24] S. De Cecco,[77] J. de Graat,[97] N. De Groot,[103] P. de Jong,[104] C. De La Taille,[114] H. De la Torre,[79] B. De Lotto,[163a,163c] L. de Mora,[70] L. De Nooij,[104] D. De Pedis,[131a] A. De Salvo,[131a] U. De Sanctis,[163a,163c] A. De Santo,[148] J. B. De Vivie De Regie,[114] S. Dean,[76] W. J. Dearnaley,[70] R. Debbe,[24] C. Debenedetti,[45] D. V. Dedovich,[64] J. Degenhardt,[119] M. Dehchar,[117] C. Del Papa,[163a,163c] J. Del Peso,[79] T. Del Prete,[121a,121b] T. Delemontex,[54] M. Deliyergiyev,[73] A. Dell'Acqua,[29] L. Dell'Asta,[21] M. Della Pietra,[101a,j] D. della Volpe,[101a,101b] M. Delmastro,[4] N. Delruelle,[29] P. A. Delsart,[54] C. Deluca,[147] S. Demers,[174] M. Demichev,[64] B. Demirkoz,[11,l] J. Deng,[162] S. P. Denisov,[127] D. Derendarz,[38] J. E. Derkaoui,[134d] F. Derue,[77] P. Dervan,[72] K. Desch,[20] E. Devetak,[147] P. O. Deviveiros,[104] A. Dewhurst,[128] B. DeWilde,[147] S. Dhaliwal,[157] R. Dhullipudi,[24,m] A. Di Ciaccio,[132a,132b] L. Di Ciaccio,[4] A. Di Girolamo,[29] B. Di Girolamo,[29] S. Di Luise,[133a,133b] A. Di Mattia,[171] B. Di Micco,[29] R. Di Nardo,[46] A. Di Simone,[132a,132b] R. Di Sipio,[19a,19b] M. A. Diaz,[31a] F. Diblen,[18c] E. B. Diehl,[86] J. Dietrich,[41] T. A. Dietzsch,[57a] S. Diglio,[85] K. Dindar Yagci,[39] J. Dingfelder,[20] C. Dionisi,[131a,131b] P. Dita,[25a] S. Dita,[25a] F. Dittus,[29] F. Djama,[82] T. Djobava,[50b] M. A. B. do Vale,[23c] A. Do Valle Wemans,[123a] T. K. O. Doan,[4] M. Dobbs,[84] R. Dobinson,[29,a] D. Dobos,[29] E. Dobson,[29,n] J. Dodd,[34] C. Doglioni,[117] T. Doherty,[52] Y. Doi,[65,a] J. Dolejsi,[125] I. Dolenc,[73] Z. Dolezal,[125] B. A. Dolgoshein,[95,a] T. Dohmae,[154] M. Donadelli,[23d] M. Donega,[119] J. Donini,[33] J. Dopke,[29] A. Doria,[101a] A. Dos Anjos,[171] M. Dosil,[11] A. Dotti,[121a,121b] M. T. Dova,[69] J. D. Dowell,[17] A. D. Doxiadis,[104] A. T. Doyle,[52] Z. Drasal,[125] J. Drees,[173] N. Dressnandt,[119] H. Drevermann,[29] C. Driouichi,[35] M. Dris,[9] J. Dubbert,[98] S. Dube,[14] E. Duchovni,[170] G. Duckeck,[97] A. Dudarev,[29] F. Dudziak,[63] M. Dührssen,[29] I. P. Duerdoth,[81] L. Duflot,[114] M-A. Dufour,[84] M. Dunford,[29] H. Duran Yildiz,[3a] R. Duxfield,[138] M. Dwuznik,[37] F. Dydak,[29] M. Düren,[51] W. L. Ebenstein,[44] J. Ebke,[97] S. Eckweiler,[80] K. Edmonds,[80] C. A. Edwards,[75] N. C. Edwards,[52] W. Ehrenfeld,[41] T. Ehrich,[98] T. Eifert,[29] G. Eigen,[13] K. Einsweiler,[14] E. Eisenhandler,[74] T. Ekelof,[165] M. El Kacimi,[134c] M. Ellert,[165] S. Elles,[4] F. Ellinghaus,[80] K. Ellis,[74] N. Ellis,[29] J. Elmsheuser,[97] M. Elsing,[29] D. Emeliyanov,[128] R. Engelmann,[147] A. Engl,[97] B. Epp,[61] A. Eppig,[86] J. Erdmann,[53] A. Ereditato,[16] D. Eriksson,[145a] J. Ernst,[1] M. Ernst,[24] J. Ernwein,[135] D. Errede,[164] S. Errede,[164] E. Ertel,[80] M. Escalier,[114] C. Escobar,[122] X. Espinal Curull,[11] B. Esposito,[46] F. Etienne,[82] A. I. Etienvre,[135] E. Etzion,[152] D. Evangelakou,[53] H. Evans,[60] L. Fabbri,[19a,19b] C. Fabre,[29] R. M. Fakhrutdinov,[127] S. Falciano,[131a] Y. Fang,[171] M. Fanti,[88a,88b] A. Farbin,[7] A. Farilla,[133a] J. Farley,[147] T. Farooque,[157] S. M. Farrington,[117] P. Farthouat,[29] P. Fassnacht,[29] D. Fassouliotis,[8] B. Fatholahzadeh,[157] A. Favareto,[88a,88b] L. Fayard,[114] S. Fazio,[36a,36b] R. Febbraro,[33] P. Federic,[143a] O. L. Fedin,[120] W. Fedorko,[87] M. Fehling-Kaschek,[47] L. Feligioni,[82] D. Fellmann,[5] C. Feng,[32d] E. J. Feng,[30] A. B. Fenyuk,[127] J. Ferencei,[143b] J. Ferland,[92] W. Fernando,[108] S. Ferrag,[52] J. Ferrando,[52] V. Ferrara,[41] A. Ferrari,[165]

P. Ferrari,[104] R. Ferrari,[118a] A. Ferrer,[166] M. L. Ferrer,[46] D. Ferrere,[48] C. Ferretti,[86] A. Ferretto Parodi,[49a,49b] M. Fiascaris,[30] F. Fiedler,[80] A. Filipčič,[73] A. Filippas,[9] F. Filthaut,[103] M. Fincke-Keeler,[168] M. C. N. Fiolhais,[123a,i] L. Fiorini,[166] A. Firan,[39] G. Fischer,[41] P. Fischer,[20] M. J. Fisher,[108] M. Flechl,[47] I. Fleck,[140] J. Fleckner,[80] P. Fleischmann,[172] S. Fleischmann,[173] T. Flick,[173] L. R. Flores Castillo,[171] M. J. Flowerdew,[98] M. Fokitis,[9] T. Fonseca Martin,[16] J. Fopma,[117] D. A. Forbush,[137] A. Formica,[135] A. Forti,[81] D. Fortin,[158a] J. M. Foster,[81] D. Fournier,[114] A. Foussat,[29] A. J. Fowler,[44] K. Fowler,[136] H. Fox,[70] P. Francavilla,[121a,121b] S. Franchino,[118a,118b] D. Francis,[29] T. Frank,[170] M. Franklin,[56] S. Franz,[29] M. Fraternali,[118a,118b] S. Fratina,[119] S. T. French,[27] F. Friedrich,[43] R. Froeschl,[29] D. Froidevaux,[29] J. A. Frost,[27] C. Fukunaga,[155] E. Fullana Torregrosa,[29] J. Fuster,[166] C. Gabaldon,[29] O. Gabizon,[170] T. Gadfort,[24] S. Gadomski,[48] G. Gagliardi,[49a,49b] P. Gagnon,[60] C. Galea,[97] E. J. Gallas,[117] V. Gallo,[16] B. J. Gallop,[128] P. Gallus,[124] K. K. Gan,[108] Y. S. Gao,[142,f] V. A. Gapienko,[127] A. Gaponenko,[14] F. Garberson,[174] M. Garcia-Sciveres,[14] C. García,[166] J. E. García Navarro,[166] R. W. Gardner,[30] N. Garelli,[29] H. Garitaonandia,[104] V. Garonne,[29] J. Garvey,[17] C. Gatti,[46] G. Gaudio,[118a] O. Gaumer,[48] B. Gaur,[140] L. Gauthier,[135] I. L. Gavrilenko,[93] C. Gay,[167] G. Gaycken,[20] J-C. Gayde,[29] E. N. Gazis,[9] P. Ge,[32d] C. N. P. Gee,[128] D. A. A. Geerts,[104] Ch. Geich-Gimbel,[20] K. Gellerstedt,[145a,145b] C. Gemme,[49a] A. Gemmell,[52] M. H. Genest,[97] S. Gentile,[131a,131b] M. George,[53] S. George,[75] P. Gerlach,[173] A. Gershon,[152] C. Geweniger,[57a] H. Ghazlane,[134b] N. Ghodbane,[33] B. Giacobbe,[19a] S. Giagu,[131a,131b] V. Giakoumopoulou,[8] V. Giangiobbe,[11] F. Gianotti,[29] B. Gibbard,[24] A. Gibson,[157] S. M. Gibson,[29] L. M. Gilbert,[117] V. Gilewsky,[90] D. Gillberg,[28] A. R. Gillman,[128] D. M. Gingrich,[2,e] J. Ginzburg,[152] N. Giokaris,[8] M. P. Giordani,[163c] R. Giordano,[101a,101b] F. M. Giorgi,[15] P. Giovannini,[98] P. F. Giraud,[135] D. Giugni,[88a] M. Giunta,[92] P. Giusti,[19a] B. K. Gjelsten,[116] L. K. Gladilin,[96] C. Glasman,[79] J. Glatzer,[47] A. Glazov,[41] K. W. Glitza,[173] G. L. Glonti,[64] J. R. Goddard,[74] J. Godfrey,[141] J. Godlewski,[29] M. Goebel,[41] T. Göpfert,[43] C. Goeringer,[80] C. Gössling,[42] T. Göttfert,[98] S. Goldfarb,[86] T. Golling,[174] S. N. Golovnia,[127] A. Gomes,[123a,c] L. S. Gomez Fajardo,[41] R. Gonçalo,[75] J. Goncalves Pinto Firmino Da Costa,[41] L. Gonella,[20] A. Gonidec,[29] S. Gonzalez,[171] S. González de la Hoz,[166] G. Gonzalez Parra,[11] M. L. Gonzalez Silva,[26] S. Gonzalez-Sevilla,[48] J. J. Goodson,[147] L. Goossens,[29] P. A. Gorbounov,[94] H. A. Gordon,[24] I. Gorelov,[102] G. Gorfine,[173] B. Gorini,[29] E. Gorini,[71a,71b] A. Gorišek,[73] E. Gornicki,[38] S. A. Gorokhov,[127] V. N. Goryachev,[127] B. Gosdzik,[41] M. Gosselink,[104] M. I. Gostkin,[64] I. Gough Eschrich,[162] M. Gouighri,[134a] D. Goujdami,[134c] M. P. Goulette,[48] A. G. Goussiou,[137] C. Goy,[4] S. Gozpinar,[22] I. Grabowska-Bold,[37] P. Grafström,[29] K-J. Grahn,[41] F. Grancagnolo,[71a] S. Grancagnolo,[15] V. Grassi,[147] V. Gratchev,[120] N. Grau,[34] H. M. Gray,[29] J. A. Gray,[147] E. Graziani,[133a] O. G. Grebenyuk,[120] T. Greenshaw,[72] Z. D. Greenwood,[24,m] K. Gregersen,[35] I. M. Gregor,[41] P. Grenier,[142] J. Griffiths,[137] N. Grigalashvili,[64] A. A. Grillo,[136] S. Grinstein,[11] Y. V. Grishkevich,[96] J.-F. Grivaz,[114] M. Groh,[98] E. Gross,[170] J. Grosse-Knetter,[53] J. Groth-Jensen,[170] K. Grybel,[140] V. J. Guarino,[5] D. Guest,[174] C. Guicheney,[33] A. Guida,[71a,71b] S. Guindon,[53] H. Guler,[84,o] J. Gunther,[124] B. Guo,[157] J. Guo,[34] A. Gupta,[30] Y. Gusakov,[64] V. N. Gushchin,[127] A. Gutierrez,[92] P. Gutierrez,[110] N. Guttman,[152] O. Gutzwiller,[171] C. Guyot,[135] C. Gwenlan,[117] C. B. Gwilliam,[72] A. Haas,[142] S. Haas,[29] C. Haber,[14] H. K. Hadavand,[39] D. R. Hadley,[17] P. Haefner,[98] F. Hahn,[29] S. Haider,[29] Z. Hajduk,[38] H. Hakobyan,[175] D. Hall,[117] J. Haller,[53] K. Hamacher,[173] P. Hamal,[112] M. Hamer,[53] A. Hamilton,[144b] S. Hamilton,[160] H. Han,[32a] L. Han,[32b] K. Hanagaki,[115] K. Hanawa,[159] M. Hance,[14] C. Handel,[80] P. Hanke,[57a] J. R. Hansen,[35] J. B. Hansen,[35] J. D. Hansen,[35] P. H. Hansen,[35] P. Hansson,[142] K. Hara,[159] G. A. Hare,[136] T. Harenberg,[173] S. Harkusha,[89] D. Harper,[86] R. D. Harrington,[45] O. M. Harris,[137] K. Harrison,[17] J. Hartert,[47] F. Hartjes,[104] T. Haruyama,[65] A. Harvey,[55] S. Hasegawa,[100] Y. Hasegawa,[139] S. Hassani,[135] M. Hatch,[29] D. Hauff,[98] S. Haug,[16] M. Hauschild,[29] R. Hauser,[87] M. Havranek,[20] B. M. Hawes,[117] C. M. Hawkes,[17] R. J. Hawkings,[29] D. Hawkins,[162] T. Hayakawa,[66] T. Hayashi,[159] D. Hayden,[75] H. S. Hayward,[72] S. J. Haywood,[128] E. Hazen,[21] M. He,[32d] S. J. Head,[17] V. Hedberg,[78] L. Heelan,[7] S. Heim,[87] B. Heinemann,[14] S. Heisterkamp,[35] L. Helary,[4] C. Heller,[97] M. Heller,[29] S. Hellman,[145a,145b] D. Hellmich,[20] C. Helsens,[11] R. C. W. Henderson,[70] M. Henke,[57a] A. Henrichs,[53] A. M. Henriques Correia,[29] S. Henrot-Versille,[114] F. Henry-Couannier,[82] C. Hensel,[53] T. Henß,[173] C. M. Hernandez,[7] Y. Hernández Jiménez,[166] R. Herrberg,[15] A. D. Hershenhorn,[151] G. Herten,[47] R. Hertenberger,[97] L. Hervas,[29] N. P. Hessey,[104] E. Higón-Rodriguez,[166] D. Hill,[5,a] J. C. Hill,[27] N. Hill,[5] K. H. Hiller,[41] S. Hillert,[20] S. J. Hillier,[17] I. Hinchliffe,[14] E. Hines,[119] M. Hirose,[115] F. Hirsch,[42] D. Hirschbuehl,[173] J. Hobbs,[147] N. Hod,[152] M. C. Hodgkinson,[138] P. Hodgson,[138] A. Hoecker,[29] M. R. Hoeferkamp,[102] J. Hoffman,[39] D. Hoffmann,[82] M. Hohlfeld,[80] M. Holder,[140] S. O. Holmgren,[145a] T. Holy,[126] J. L. Holzbauer,[87] Y. Homma,[66] T. M. Hong,[119] L. Hooft van Huysduynen,[107] T. Horazdovsky,[126] C. Horn,[142] S. Horner,[47] J-Y. Hostachy,[54] S. Hou,[150] M. A. Houlden,[72] A. Hoummada,[134a] J. Howarth,[81] D. F. Howell,[117]

I. Hristova,[15] J. Hrivnac,[114] I. Hruska,[124] T. Hryn'ova,[4] P. J. Hsu,[80] S.-C. Hsu,[14] G. S. Huang,[110] Z. Hubacek,[126] F. Hubaut,[82] F. Huegging,[20] T. B. Huffman,[117] E. W. Hughes,[34] G. Hughes,[70] R. E. Hughes-Jones,[81] M. Huhtinen,[29] P. Hurst,[56] M. Hurwitz,[14] U. Husemann,[41] N. Huseynov,[64,p] J. Huston,[87] J. Huth,[56] G. Iacobucci,[48] G. Iakovidis,[9] M. Ibbotson,[81] I. Ibragimov,[140] R. Ichimiya,[66] L. Iconomidou-Fayard,[114] J. Idarraga,[114] P. Iengo,[101a] O. Igonkina,[104] Y. Ikegami,[65] M. Ikeno,[65] Y. Ilchenko,[39] D. Iliadis,[153] N. Ilic,[157] D. Imbault,[77] M. Imori,[154] T. Ince,[20] J. Inigo-Golfin,[29] P. Ioannou,[8] M. Iodice,[133a] A. Irles Quiles,[166] C. Isaksson,[165] A. Ishikawa,[66] M. Ishino,[67] R. Ishmukhametov,[39] C. Issever,[117] S. Istin,[18a] A. V. Ivashin,[127] W. Iwanski,[38] H. Iwasaki,[65] J. M. Izen,[40] V. Izzo,[101a] B. Jackson,[119] J. N. Jackson,[72] P. Jackson,[142] M. R. Jaekel,[29] V. Jain,[60] K. Jakobs,[47] S. Jakobsen,[35] J. Jakubek,[126] D. K. Jana,[110] E. Jankowski,[157] E. Jansen,[76] H. Jansen,[29] A. Jantsch,[98] M. Janus,[20] G. Jarlskog,[78] L. Jeanty,[56] K. Jelen,[37] I. Jen-La Plante,[30] P. Jenni,[29] A. Jeremie,[4] P. Jež,[35] S. Jézéquel,[4] M. K. Jha,[19a] H. Ji,[171] W. Ji,[80] J. Jia,[147] Y. Jiang,[32b] M. Jimenez Belenguer,[41] G. Jin,[32b] S. Jin,[32a] O. Jinnouchi,[156] M. D. Joergensen,[35] D. Joffe,[39] L. G. Johansen,[13] M. Johansen,[145a,145b] K. E. Johansson,[145a] P. Johansson,[138] S. Johnert,[41] K. A. Johns,[6] K. Jon-And,[145a,145b] G. Jones,[81] R. W. L. Jones,[70] T. W. Jones,[76] T. J. Jones,[72] O. Jonsson,[29] C. Joram,[29] P. M. Jorge,[123a] J. Joseph,[14] T. Jovin,[12b] X. Ju,[171] C. A. Jung,[42] V. Juranek,[124] P. Jussel,[61] A. Juste Rozas,[11] V. V. Kabachenko,[127] S. Kabana,[16] M. Kaci,[166] A. Kaczmarska,[38] P. Kadlecik,[35] M. Kado,[114] H. Kagan,[108] M. Kagan,[56] S. Kaiser,[98] E. Kajomovitz,[151] S. Kalinin,[173] L. V. Kalinovskaya,[64] S. Kama,[39] N. Kanaya,[154] M. Kaneda,[29] S. Kaneti,[27] T. Kanno,[156] V. A. Kantserov,[95] J. Kanzaki,[65] B. Kaplan,[174] A. Kapliy,[30] J. Kaplon,[29] D. Kar,[43] M. Karagounis,[20] M. Karagoz,[117] M. Karnevskiy,[41] K. Karr,[5] V. Kartvelishvili,[70] A. N. Karyukhin,[127] L. Kashif,[171] G. Kasieczka,[57b] R. D. Kass,[108] A. Kastanas,[13] M. Kataoka,[4] Y. Kataoka,[154] E. Katsoufis,[9] J. Katzy,[41] V. Kaushik,[6] K. Kawagoe,[66] T. Kawamoto,[154] G. Kawamura,[80] M. S. Kayl,[104] V. A. Kazanin,[106] M. Y. Kazarinov,[64] J. R. Keates,[81] R. Keeler,[168] R. Kehoe,[39] M. Keil,[53] G. D. Kekelidze,[64] J. Kennedy,[97] C. J. Kenney,[142] M. Kenyon,[52] O. Kepka,[124] N. Kerschen,[29] B. P. Kerševan,[73] S. Kersten,[173] K. Kessoku,[154] J. Keung,[157] F. Khalil-zada,[10] H. Khandanyan,[164] A. Khanov,[111] D. Kharchenko,[64] A. Khodinov,[95] A. G. Kholodenko,[127] A. Khomich,[57a] T. J. Khoo,[27] G. Khoriauli,[20] A. Khoroshilov,[173] N. Khovanskiy,[64] V. Khovanskiy,[94] E. Khramov,[64] J. Khubua,[50b] H. Kim,[145a,145b] M. S. Kim,[2] P. C. Kim,[142] S. H. Kim,[159] N. Kimura,[169] O. Kind,[15] B. T. King,[72] M. King,[66] R. S. B. King,[117] J. Kirk,[128] L. E. Kirsch,[22] A. E. Kiryunin,[98] T. Kishimoto,[66] D. Kisielewska,[37] T. Kittelmann,[122] A. M. Kiver,[127] E. Kladiva,[143b] J. Klaiber-Lodewigs,[42] M. Klein,[72] U. Klein,[72] K. Kleinknecht,[80] M. Klemetti,[84] A. Klier,[170] P. Klimek,[145a,145b] A. Klimentov,[24] R. Klingenberg,[42] E. B. Klinkby,[35] T. Klioutchnikova,[29] P. F. Klok,[103] S. Klous,[104] E.-E. Kluge,[57a] T. Kluge,[72] P. Kluit,[104] S. Kluth,[98] N. S. Knecht,[157] E. Kneringer,[61] J. Knobloch,[29] E. B. F. G. Knoops,[82] A. Knue,[53] B. R. Ko,[44] T. Kobayashi,[154] M. Kobel,[43] M. Kocian,[142] P. Kodys,[125] K. Köneke,[29] A. C. König,[103] S. Koenig,[80] L. Köpke,[80] F. Koetsveld,[103] P. Koevesarki,[20] T. Koffas,[28] E. Koffeman,[104] F. Kohn,[53] Z. Kohout,[126] T. Kohriki,[65] T. Koi,[142] T. Kokott,[20] G. M. Kolachev,[106] H. Kolanoski,[15] V. Kolesnikov,[64] I. Koletsou,[88a] J. Koll,[87] D. Kollar,[29] M. Kollefrath,[47] S. D. Kolya,[81] A. A. Komar,[93] Y. Komori,[154] T. Kondo,[65] T. Kono,[41,q] A. I. Kononov,[47] R. Konoplich,[107,r] N. Konstantinidis,[76] A. Kootz,[173] S. Koperny,[37] K. Korcyl,[38] K. Kordas,[153] V. Koreshev,[127] A. Korn,[117] A. Korol,[106] I. Korolkov,[11] E. V. Korolkova,[138] V. A. Korotkov,[127] O. Kortner,[98] S. Kortner,[98] V. V. Kostyukhin,[20] M. J. Kotamäki,[29] S. Kotov,[98] V. M. Kotov,[64] A. Kotwal,[44] C. Kourkoumelis,[8] V. Kouskoura,[153] A. Koutsman,[158a] R. Kowalewski,[168] T. Z. Kowalski,[37] W. Kozanecki,[135] A. S. Kozhin,[127] V. Kral,[126] V. A. Kramarenko,[96] G. Kramberger,[73] M. W. Krasny,[77] A. Krasznahorkay,[107] J. Kraus,[87] J. K. Kraus,[20] A. Kreisel,[152] F. Krejci,[126] J. Kretzschmar,[72] N. Krieger,[53] P. Krieger,[157] K. Kroeninger,[53] H. Kroha,[98] J. Kroll,[119] J. Kroseberg,[20] J. Krstic,[12a] U. Kruchonak,[64] H. Krüger,[20] T. Kruker,[16] N. Krumnack,[63] Z. V. Krumshteyn,[64] A. Kruth,[20] T. Kubota,[85] S. Kuehn,[47] A. Kugel,[57c] T. Kuhl,[41] D. Kuhn,[61] V. Kukhtin,[64] Y. Kulchitsky,[89] S. Kuleshov,[31b] C. Kummer,[97] M. Kuna,[77] N. Kundu,[117] J. Kunkle,[119] A. Kupco,[124] H. Kurashige,[66] M. Kurata,[159] Y. A. Kurochkin,[89] V. Kus,[124] M. Kuze,[156] J. Kvita,[141] R. Kwee,[15] A. La Rosa,[48] L. La Rotonda,[36a,36b] L. Labarga,[79] J. Labbe,[4] S. Lablak,[134a] C. Lacasta,[166] F. Lacava,[131a,131b] H. Lacker,[15] D. Lacour,[77] V. R. Lacuesta,[166] E. Ladygin,[64] R. Lafaye,[4] B. Laforge,[77] T. Lagouri,[79] S. Lai,[47] E. Laisne,[54] M. Lamanna,[29] C. L. Lampen,[6] W. Lampl,[6] E. Lancon,[135] U. Landgraf,[47] M. P. J. Landon,[74] H. Landsman,[151] J. L. Lane,[81] C. Lange,[41] A. J. Lankford,[162] F. Lanni,[24] K. Lantzsch,[173] S. Laplace,[77] C. Lapoire,[20] J. F. Laporte,[135] T. Lari,[88a] A. V. Larionov,[127] A. Larner,[117] C. Lasseur,[29] M. Lassnig,[29] P. Laurelli,[46] W. Lavrijsen,[14] P. Laycock,[72] A. B. Lazarev,[64] O. Le Dortz,[77] E. Le Guirriec,[82] C. Le Maner,[157] E. Le Menedeu,[9] C. Lebel,[92] T. LeCompte,[5] F. Ledroit-Guillon,[54] H. Lee,[104] J. S. H. Lee,[115] S. C. Lee,[150] L. Lee,[174] M. Lefebvre,[168] M. Legendre,[135] A. Leger,[48] B. C. LeGeyt,[119] F. Legger,[97] C. Leggett,[14] M. Lehmacher,[20] G. Lehmann Miotto,[29] X. Lei,[6] M. A. L. Leite,[23d]

R. Leitner,[125] D. Lellouch,[170] M. Leltchouk,[34] B. Lemmer,[53] V. Lendermann,[57a] K. J. C. Leney,[144b] T. Lenz,[104] G. Lenzen,[173] B. Lenzi,[29] K. Leonhardt,[43] S. Leontsinis,[9] C. Leroy,[92] J-R. Lessard,[168] J. Lesser,[145a] C. G. Lester,[27] A. Leung Fook Cheong,[171] J. Levêque,[4] D. Levin,[86] L. J. Levinson,[170] M. S. Levitski,[127] A. Lewis,[117] G. H. Lewis,[107] A. M. Leyko,[20] M. Leyton,[15] B. Li,[82] H. Li,[171,32d] S. Li,[32b,s] X. Li,[86] Z. Liang,[117,t] H. Liao,[33] B. Liberti,[132a] P. Lichard,[29] M. Lichtnecker,[97] K. Lie,[164] W. Liebig,[13] R. Lifshitz,[151] C. Limbach,[20] A. Limosani,[85] M. Limper,[62] S. C. Lin,[150,u] F. Linde,[104] J. T. Linnemann,[87] E. Lipeles,[119] L. Lipinsky,[124] A. Lipniacka,[13] T. M. Liss,[164] D. Lissauer,[24] A. Lister,[48] A. M. Litke,[136] C. Liu,[28] D. Liu,[150] H. Liu,[86] J. B. Liu,[86] M. Liu,[32b] S. Liu,[2] Y. Liu,[32b] M. Livan,[118a,118b] S. S. A. Livermore,[117] A. Lleres,[54] J. Llorente Merino,[79] S. L. Lloyd,[74] E. Lobodzinska,[41] P. Loch,[6] W. S. Lockman,[136] T. Loddenkoetter,[20] F. K. Loebinger,[81] A. Loginov,[174] C. W. Loh,[167] T. Lohse,[15] K. Lohwasser,[47] M. Lokajicek,[124] J. Loken,[117] V. P. Lombardo,[4] R. E. Long,[70] L. Lopes,[123a,c] D. Lopez Mateos,[56] J. Lorenz,[97] M. Losada,[161] P. Loscutoff,[14] F. Lo Sterzo,[131a,131b] M. J. Losty,[158a] X. Lou,[40] A. Lounis,[114] K. F. Loureiro,[161] J. Love,[21] P. A. Love,[70] A. J. Lowe,[142,f] F. Lu,[32a] H. J. Lubatti,[137] C. Luci,[131a,131b] A. Lucotte,[54] A. Ludwig,[43] D. Ludwig,[41] I. Ludwig,[47] J. Ludwig,[47] F. Luehring,[60] G. Luijckx,[104] D. Lumb,[47] L. Luminari,[131a] E. Lund,[116] B. Lund-Jensen,[146] B. Lundberg,[78] J. Lundberg,[145a,145b] J. Lundquist,[35] M. Lungwitz,[80] G. Lutz,[98] D. Lynn,[24] J. Lys,[14] E. Lytken,[78] H. Ma,[24] L. L. Ma,[171] J. A. Macana Goia,[92] G. Maccarrone,[46] A. Macchiolo,[98] B. Maček,[73] J. Machado Miguens,[123a] R. Mackeprang,[35] R. J. Madaras,[14] W. F. Mader,[43] R. Maenner,[57c] T. Maeno,[24] P. Mättig,[173] S. Mättig,[41] L. Magnoni,[29] E. Magradze,[53] Y. Mahalalel,[152] K. Mahboubi,[47] G. Mahout,[17] C. Maiani,[131a,131b] C. Maidantchik,[23a] A. Maio,[123a,c] S. Majewski,[24] Y. Makida,[65] N. Makovec,[114] P. Mal,[135] B. Malaescu,[29] Pa. Malecki,[38] P. Malecki,[38] V. P. Maleev,[120] F. Malek,[54] U. Mallik,[62] D. Malon,[5] C. Malone,[142] S. Maltezos,[9] V. Malyshev,[106] S. Malyukov,[29] R. Mameghani,[97] J. Mamuzic,[12b] A. Manabe,[65] L. Mandelli,[88a] I. Mandić,[73] R. Mandrysch,[15] J. Maneira,[123a] P. S. Mangeard,[87] I. D. Manjavidze,[64] A. Mann,[53] P. M. Manning,[136] A. Manousakis-Katsikakis,[8] B. Mansoulie,[135] A. Manz,[98] A. Mapelli,[29] L. Mapelli,[29] L. March,[79] J. F. Marchand,[28] F. Marchese,[132a,132b] G. Marchiori,[77] M. Marcisovsky,[124] A. Marin,[21,a] C. P. Marino,[168] F. Marroquim,[23a] R. Marshall,[81] Z. Marshall,[29] F. K. Martens,[157] S. Marti-Garcia,[166] A. J. Martin,[174] B. Martin,[29] B. Martin,[87] F. F. Martin,[119] J. P. Martin,[92] Ph. Martin,[54] T. A. Martin,[17] V. J. Martin,[45] B. Martin dit Latour,[48] S. Martin-Haugh,[148] M. Martinez,[11] V. Martinez Outschoorn,[56] A. C. Martyniuk,[168] M. Marx,[81] F. Marzano,[131a] A. Marzin,[110] L. Masetti,[80] T. Mashimo,[154] R. Mashinistov,[93] J. Masik,[81] A. L. Maslennikov,[106] I. Massa,[19a,19b] G. Massaro,[104] N. Massol,[4] P. Mastrandrea,[131a,131b] A. Mastroberardino,[36a,36b] T. Masubuchi,[154] M. Mathes,[20] P. Matricon,[114] H. Matsumoto,[154] H. Matsunaga,[154] T. Matsushita,[66] C. Mattravers,[117,d] J. M. Maugain,[29] J. Maurer,[82] S. J. Maxfield,[72] D. A. Maximov,[106,g] E. N. May,[5] A. Mayne,[138] R. Mazini,[150] M. Mazur,[20] M. Mazzanti,[88a] E. Mazzoni,[121a,121b] S. P. Mc Kee,[86] A. McCarn,[164] R. L. McCarthy,[147] T. G. McCarthy,[28] N. A. McCubbin,[128] K. W. McFarlane,[55] J. A. Mcfayden,[138] H. McGlone,[52] G. Mchedlidze,[50b] R. A. McLaren,[29] T. Mclaughlan,[17] S. J. McMahon,[128] R. A. McPherson,[168,k] A. Meade,[83] J. Mechnich,[104] M. Mechtel,[173] M. Medinnis,[41] R. Meera-Lebbai,[110] T. Meguro,[115] R. Mehdiyev,[92] S. Mehlhase,[35] A. Mehta,[72] K. Meier,[57a] B. Meirose,[78] C. Melachrinos,[30] B. R. Mellado Garcia,[171] L. Mendoza Navas,[161] Z. Meng,[150,v] A. Mengarelli,[19a,19b] S. Menke,[98] C. Menot,[29] E. Meoni,[11] K. M. Mercurio,[56] P. Mermod,[48] L. Merola,[101a,101b] C. Meroni,[88a] F. S. Merritt,[30] A. Messina,[29] J. Metcalfe,[102] A. S. Mete,[63] C. Meyer,[80] C. Meyer,[30] J-P. Meyer,[135] J. Meyer,[172] J. Meyer,[53] T. C. Meyer,[29] W. T. Meyer,[63] J. Miao,[32d] S. Michal,[29] L. Micu,[25a] R. P. Middleton,[128] S. Migas,[72] L. Mijović,[41] G. Mikenberg,[170] M. Mikestikova,[124] M. Mikuž,[73] D. W. Miller,[30] R. J. Miller,[87] W. J. Mills,[167] C. Mills,[56] A. Milov,[170] D. A. Milstead,[145a,145b] D. Milstein,[170] A. A. Minaenko,[127] M. Miñano Moya,[166] I. A. Minashvili,[64] A. I. Mincer,[107] B. Mindur,[37] M. Mineev,[64] Y. Ming,[171] L. M. Mir,[11] G. Mirabelli,[131a] L. Miralles Verge,[11] A. Misiejuk,[75] J. Mitrevski,[136] G. Y. Mitrofanov,[127] V. A. Mitsou,[166] S. Mitsui,[65] P. S. Miyagawa,[138] K. Miyazaki,[66] J. U. Mjörnmark,[78] T. Moa,[145a,145b] P. Mockett,[137] S. Moed,[56] V. Moeller,[27] K. Mönig,[41] N. Möser,[20] S. Mohapatra,[147] W. Mohr,[47] S. Mohrdieck-Möck,[98] A. M. Moisseev,[127,a] R. Moles-Valls,[166] J. Molina-Perez,[29] J. Monk,[76] E. Monnier,[82] S. Montesano,[88a,88b] F. Monticelli,[69] S. Monzani,[19a,19b] R. W. Moore,[2] G. F. Moorhead,[85] C. Mora Herrera,[48] A. Moraes,[52] N. Morange,[135] J. Morel,[53] G. Morello,[36a,36b] D. Moreno,[80] M. Moreno Llácer,[166] P. Morettini,[49a] M. Morii,[56] J. Morin,[74] A. K. Morley,[29] G. Mornacchi,[29] S. V. Morozov,[95] J. D. Morris,[74] L. Morvaj,[100] H. G. Moser,[98] M. Mosidze,[50b] J. Moss,[108] R. Mount,[142] E. Mountricha,[9,w] S. V. Mouraviev,[93] E. J. W. Moyse,[83] M. Mudrinic,[12b] F. Mueller,[57a] J. Mueller,[122] K. Mueller,[20] T. A. Müller,[97] T. Mueller,[80] D. Muenstermann,[29] A. Muir,[167] Y. Munwes,[152] W. J. Murray,[128] I. Mussche,[104] E. Musto,[101a,101b] A. G. Myagkov,[127] M. Myska,[124] J. Nadal,[11] K. Nagai,[159] K. Nagano,[65] Y. Nagasaka,[59] M. Nagel,[98] A. M. Nairz,[29] Y. Nakahama,[29]

K. Nakamura,[154] T. Nakamura,[154] I. Nakano,[109] G. Nanava,[20] A. Napier,[160] M. Nash,[76,d] N. R. Nation,[21] T. Nattermann,[20] T. Naumann,[41] G. Navarro,[161] H. A. Neal,[86] E. Nebot,[79] P. Yu. Nechaeva,[93] A. Negri,[118a,118b] G. Negri,[29] S. Nektarijevic,[48] A. Nelson,[162] S. Nelson,[142] T. K. Nelson,[142] S. Nemecek,[124] P. Nemethy,[107] A. A. Nepomuceno,[23a] M. Nessi,[29,x] M. S. Neubauer,[164] A. Neusiedl,[80] R. M. Neves,[107] P. Nevski,[24] P. R. Newman,[17] V. Nguyen Thi Hong,[135] R. B. Nickerson,[117] R. Nicolaidou,[135] L. Nicolas,[138] B. Nicquevert,[29] F. Niedercorn,[114] J. Nielsen,[136] T. Niinikoski,[29] N. Nikiforou,[34] A. Nikiforov,[15] V. Nikolaenko,[127] K. Nikolaev,[64] I. Nikolic-Audit,[77] K. Nikolics,[48] K. Nikolopoulos,[24] H. Nilsen,[47] P. Nilsson,[7] Y. Ninomiya,[154] A. Nisati,[131a] T. Nishiyama,[66] R. Nisius,[98] L. Nodulman,[5] M. Nomachi,[115] I. Nomidis,[153] M. Nordberg,[29] B. Nordkvist,[145a,145b] P. R. Norton,[128] J. Novakova,[125] M. Nozaki,[65] L. Nozka,[112] I. M. Nugent,[158a] A.-E. Nuncio-Quiroz,[20] G. Nunes Hanninger,[85] T. Nunnemann,[97] E. Nurse,[76] T. Nyman,[29] B. J. O'Brien,[45] S. W. O'Neale,[17,a] D. C. O'Neil,[141] V. O'Shea,[52] L. B. Oakes,[97] F. G. Oakham,[28,e] H. Oberlack,[98] J. Ocariz,[77] A. Ochi,[66] S. Oda,[154] S. Odaka,[65] J. Odier,[82] H. Ogren,[60] A. Oh,[81] S. H. Oh,[44] C. C. Ohm,[145a,145b] T. Ohshima,[100] H. Ohshita,[139] T. Ohsugi,[58] S. Okada,[66] H. Okawa,[162] Y. Okumura,[100] T. Okuyama,[154] A. Olariu,[25a] M. Olcese,[49a] A. G. Olchevski,[64] M. Oliveira,[123a,i] D. Oliveira Damazio,[24] E. Oliver Garcia,[166] D. Olivito,[119] A. Olszewski,[38] J. Olszowska,[38] C. Omachi,[66] A. Onofre,[123a,y] P. U. E. Onyisi,[30] C. J. Oram,[158a] M. J. Oreglia,[30] Y. Oren,[152] D. Orestano,[133a,133b] I. Orlov,[106] C. Oropeza Barrera,[52] R. S. Orr,[157] B. Osculati,[49a,49b] R. Ospanov,[119] C. Osuna,[11] G. Otero y Garzon,[26] J. P. Ottersbach,[104] M. Ouchrif,[134d] F. Ould-Saada,[116] A. Ouraou,[135] Q. Ouyang,[32a] A. Ovcharova,[14] M. Owen,[81] S. Owen,[138] V. E. Ozcan,[18a] N. Ozturk,[7] A. Pacheco Pages,[11] C. Padilla Aranda,[11] S. Pagan Griso,[14] E. Paganis,[138] F. Paige,[24] P. Pais,[83] K. Pajchel,[116] G. Palacino,[158b] C. P. Paleari,[6] S. Palestini,[29] D. Pallin,[33] A. Palma,[123a] J. D. Palmer,[17] Y. B. Pan,[171] E. Panagiotopoulou,[9] B. Panes,[31a] N. Panikashvili,[86] S. Panitkin,[24] D. Pantea,[25a] M. Panuskova,[124] V. Paolone,[122] A. Papadelis,[145a] Th. D. Papadopoulou,[9] A. Paramonov,[5] W. Park,[24,z] M. A. Parker,[27] F. Parodi,[49a,49b] J. A. Parsons,[34] U. Parzefall,[47] E. Pasqualucci,[131a] S. Passaggio,[49a] A. Passeri,[133a] F. Pastore,[133a,133b] Fr. Pastore,[75] G. Pásztor,[48,aa] S. Pataraia,[173] N. Patel,[149] J. R. Pater,[81] S. Patricelli,[101a,101b] T. Pauly,[29] M. Pecsy,[143a] M. I. Pedraza Morales,[171] S. V. Peleganchuk,[106] H. Peng,[32b] R. Pengo,[29] A. Penson,[34] J. Penwell,[60] M. Perantoni,[23a] K. Perez,[34,bb] T. Perez Cavalcanti,[41] E. Perez Codina,[11] M. T. Pérez García-Estañ,[166] V. Perez Reale,[34] L. Perini,[88a,88b] H. Pernegger,[29] R. Perrino,[71a] P. Perrodo,[4] S. Persembe,[3a] A. Perus,[114] V. D. Peshekhonov,[64] B. A. Petersen,[29] J. Petersen,[29] T. C. Petersen,[35] E. Petit,[4] A. Petridis,[153] C. Petridou,[153] E. Petrolo,[131a] F. Petrucci,[133a,133b] D. Petschull,[41] M. Petteni,[141] R. Pezoa,[31b] A. Phan,[85] P. W. Phillips,[128] G. Piacquadio,[29] E. Piccaro,[74] M. Piccinini,[19a,19b] S. M. Piec,[41] R. Piegaia,[26] D. T. Pignotti,[108] J. E. Pilcher,[30] A. D. Pilkington,[81] J. Pina,[123a,c] M. Pinamonti,[163a,163c] A. Pinder,[117] J. L. Pinfold,[2] J. Ping,[32c] B. Pinto,[123a,c] O. Pirotte,[29] C. Pizio,[88a,88b] M. Plamondon,[168] M.-A. Pleier,[24] A. V. Pleskach,[127] A. Poblaguev,[24] S. Poddar,[57a] F. Podlyski,[33] L. Poggioli,[114] T. Poghosyan,[20] M. Pohl,[48] F. Polci,[54] G. Polesello,[118a] A. Policicchio,[36a,36b] A. Polini,[19a] J. Poll,[74] V. Polychronakos,[24] D. M. Pomarede,[135] D. Pomeroy,[22] K. Pommès,[29] L. Pontecorvo,[131a] B. G. Pope,[87] G. A. Popeneciu,[25a] D. S. Popovic,[12a] A. Poppleton,[29] X. Portell Bueso,[29] C. Posch,[21] G. E. Pospelov,[98] S. Pospisil,[126] I. N. Potrap,[98] C. J. Potter,[148] C. T. Potter,[113] G. Poulard,[29] J. Poveda,[171] R. Prabhu,[76] P. Pralavorio,[82] A. Pranko,[14] S. Prasad,[56] R. Pravahan,[7] S. Prell,[63] K. Pretzl,[16] L. Pribyl,[29] D. Price,[60] J. Price,[72] L. E. Price,[5] M. J. Price,[29] D. Prieur,[122] M. Primavera,[71a] K. Prokofiev,[107] F. Prokoshin,[31b] S. Protopopescu,[24] J. Proudfoot,[5] X. Prudent,[43] M. Przybycien,[37] H. Przysiezniak,[4] S. Psoroulas,[20] E. Ptacek,[113] E. Pueschel,[83] J. Purdham,[86] M. Purohit,[24,z] P. Puzo,[114] Y. Pylypchenko,[62] J. Qian,[86] Z. Qian,[82] Z. Qin,[41] A. Quadt,[53] D. R. Quarrie,[14] W. B. Quayle,[171] F. Quinonez,[31a] M. Raas,[103] V. Radescu,[57b] B. Radics,[20] T. Rador,[18a] F. Ragusa,[88a,88b] G. Rahal,[176] A. M. Rahimi,[108] D. Rahm,[24] S. Rajagopalan,[24] M. Rammensee,[47] M. Rammes,[140] A. S. Randle-Conde,[39] K. Randrianarivony,[28] P. N. Ratoff,[70] F. Rauscher,[97] M. Raymond,[29] A. L. Read,[116] D. M. Rebuzzi,[118a,118b] A. Redelbach,[172] G. Redlinger,[24] R. Reece,[119] K. Reeves,[40] A. Reichold,[104] E. Reinherz-Aronis,[152] A. Reinsch,[113] I. Reisinger,[42] D. Reljic,[12a] C. Rembser,[29] Z. L. Ren,[150] A. Renaud,[114] P. Renkel,[39] M. Rescigno,[131a] S. Resconi,[88a] B. Resende,[135] P. Reznicek,[97] R. Rezvani,[157] A. Richards,[76] R. Richter,[98] E. Richter-Was,[4,cc] M. Ridel,[77] M. Rijpstra,[104] M. Rijssenbeek,[147] A. Rimoldi,[118a,118b] L. Rinaldi,[19a] R. R. Rios,[39] I. Riu,[11] G. Rivoltella,[88a,88b] F. Rizatdinova,[111] E. Rizvi,[74] S. H. Robertson,[84,k] A. Robichaud-Veronneau,[117] D. Robinson,[27] J. E. M. Robinson,[76] M. Robinson,[113] A. Robson,[52] J. G. Rocha de Lima,[105] C. Roda,[121a,121b] D. Roda Dos Santos,[29] D. Rodriguez,[161] Y. Rodriguez Garcia,[161] A. Roe,[53] S. Roe,[29] O. Røhne,[116] V. Rojo,[1] S. Rolli,[160] A. Romaniouk,[95] M. Romano,[19a,19b] V. M. Romanov,[64] G. Romeo,[26] L. Roos,[77] E. Ros,[166] S. Rosati,[131a] K. Rosbach,[48] A. Rose,[148] M. Rose,[75] G. A. Rosenbaum,[157] E. I. Rosenberg,[63] P. L. Rosendahl,[13] O. Rosenthal,[140] L. Rosselet,[48] V. Rossetti,[11]

E. Rossi,[131a,131b] L. P. Rossi,[49a] M. Rotaru,[25a] I. Roth,[170] J. Rothberg,[137] D. Rousseau,[114] C. R. Royon,[135] A. Rozanov,[82] Y. Rozen,[151] X. Ruan,[114,dd] I. Rubinskiy,[41] B. Ruckert,[97] N. Ruckstuhl,[104] V. I. Rud,[96] C. Rudolph,[43] G. Rudolph,[61] F. Rühr,[6] F. Ruggieri,[133a,133b] A. Ruiz-Martinez,[63] V. Rumiantsev,[90,a] L. Rumyantsev,[64] K. Runge,[47] Z. Rurikova,[47] N. A. Rusakovich,[64] D. R. Rust,[60] J. P. Rutherfoord,[6] C. Ruwiedel,[14] P. Ruzicka,[124] Y. F. Ryabov,[120] V. Ryadovikov,[127] P. Ryan,[87] M. Rybar,[125] G. Rybkin,[114] N. C. Ryder,[117] S. Rzaeva,[10] A. F. Saavedra,[149] I. Sadeh,[152] H. F-W. Sadrozinski,[136] R. Sadykov,[64] F. Safai Tehrani,[131a] H. Sakamoto,[154] G. Salamanna,[74] A. Salamon,[132a] M. Saleem,[110] D. Salihagic,[98] A. Salnikov,[142] J. Salt,[166] B. M. Salvachua Ferrando,[5] D. Salvatore,[36a,36b] F. Salvatore,[148] A. Salvucci,[103] A. Salzburger,[29] D. Sampsonidis,[153] B. H. Samset,[116] A. Sanchez,[101a,101b] H. Sandaker,[13] H. G. Sander,[80] M. P. Sanders,[97] M. Sandhoff,[173] T. Sandoval,[27] C. Sandoval,[161] R. Sandstroem,[98] S. Sandvoss,[173] D. P. C. Sankey,[128] A. Sansoni,[46] C. Santamarina Rios,[84] C. Santoni,[33] R. Santonico,[132a,132b] H. Santos,[123a] J. G. Saraiva,[123a] T. Sarangi,[171] E. Sarkisyan-Grinbaum,[7] F. Sarri,[121a,121b] G. Sartisohn,[173] O. Sasaki,[65] N. Sasao,[67] I. Satsounkevitch,[89] G. Sauvage,[4] E. Sauvan,[4] J. B. Sauvan,[114] P. Savard,[157,e] V. Savinov,[122] D. O. Savu,[29] L. Sawyer,[24,m] D. H. Saxon,[52] L. P. Says,[33] C. Sbarra,[19a] A. Sbrizzi,[19a,19b] O. Scallon,[92] D. A. Scannicchio,[162] M. Scarcella,[149] J. Schaarschmidt,[114] P. Schacht,[98] U. Schäfer,[80] S. Schaepe,[20] S. Schaetzel,[57b] A. C. Schaffer,[114] D. Schaile,[97] R. D. Schamberger,[147] A. G. Schamov,[106] V. Scharf,[57a] V. A. Schegelsky,[120] D. Scheirich,[86] M. Schernau,[162] M. I. Scherzer,[34] C. Schiavi,[49a,49b] J. Schieck,[97] M. Schioppa,[36a,36b] S. Schlenker,[29] J. L. Schlereth,[5] E. Schmidt,[47] K. Schmieden,[20] C. Schmitt,[80] S. Schmitt,[57b] M. Schmitz,[20] A. Schöning,[57b] M. Schott,[29] D. Schouten,[158a] J. Schovancova,[124] M. Schram,[84] C. Schroeder,[80] N. Schroer,[57c] S. Schuh,[29] G. Schuler,[29] J. Schultes,[173] H.-C. Schultz-Coulon,[57a] H. Schulz,[15] J. W. Schumacher,[20] M. Schumacher,[47] B. A. Schumm,[136] Ph. Schune,[135] C. Schwanenberger,[81] A. Schwartzman,[142] Ph. Schwemling,[77] R. Schwienhorst,[87] R. Schwierz,[43] J. Schwindling,[135] T. Schwindt,[20] M. Schwoerer,[4] W. G. Scott,[128] J. Searcy,[113] G. Sedov,[41] E. Sedykh,[120] E. Segura,[11] S. C. Seidel,[102] A. Seiden,[136] F. Seifert,[43] J. M. Seixas,[23a] G. Sekhniaidze,[101a] D. M. Seliverstov,[120] B. Sellden,[145a] G. Sellers,[72] M. Seman,[143b] N. Semprini-Cesari,[19a,19b] C. Serfon,[97] L. Serin,[114] R. Seuster,[98] H. Severini,[110] M. E. Sevior,[85] A. Sfyrla,[29] E. Shabalina,[53] M. Shamim,[113] L. Y. Shan,[32a] J. T. Shank,[21] Q. T. Shao,[85] M. Shapiro,[14] P. B. Shatalov,[94] L. Shaver,[6] K. Shaw,[163a,163c] D. Sherman,[174] P. Sherwood,[76] A. Shibata,[107] H. Shichi,[100] S. Shimizu,[29] M. Shimojima,[99] T. Shin,[55] M. Shiyakova,[64] A. Shmeleva,[93] M. J. Shochet,[30] D. Short,[117] S. Shrestha,[63] M. A. Shupe,[6] P. Sicho,[124] A. Sidoti,[131a,131b] F. Siegert,[47] Dj. Sijacki,[12a] O. Silbert,[170] J. Silva,[123a,c] Y. Silver,[152] D. Silverstein,[142] S. B. Silverstein,[145a] V. Simak,[126] O. Simard,[135] Lj. Simic,[12a] S. Simion,[114] B. Simmons,[76] M. Simonyan,[35] P. Sinervo,[157] N. B. Sinev,[113] V. Sipica,[140] G. Siragusa,[172] A. Sircar,[24] A. N. Sisakyan,[64] S. Yu. Sivoklokov,[96] J. Sjölin,[145a,145b] T. B. Sjursen,[13] L. A. Skinnari,[14] H. P. Skottowe,[56] K. Skovpen,[106] P. Skubic,[110] N. Skvorodnev,[22] M. Slater,[17] T. Slavicek,[126] K. Sliwa,[160] J. Sloper,[29] V. Smakhtin,[170] S.Yu. Smirnov,[95] L. N. Smirnova,[96] O. Smirnova,[78] B. C. Smith,[56] D. Smith,[142] K. M. Smith,[52] M. Smizanska,[70] K. Smolek,[126] A. A. Snesarev,[93] S. W. Snow,[81] J. Snow,[110] J. Snuverink,[104] S. Snyder,[24] M. Soares,[123a] R. Sobie,[168,k] J. Sodomka,[126] A. Soffer,[152] C. A. Solans,[166] M. Solar,[126] J. Solc,[126] E. Soldatov,[95] U. Soldevila,[166] E. Solfaroli Camillocci,[131a,131b] A. A. Solodkov,[127] O. V. Solovyanov,[127] J. Sondericker,[24] N. Soni,[2] V. Sopko,[126] B. Sopko,[126] M. Sosebee,[7] R. Soualah,[163a,163c] A. Soukharev,[106] S. Spagnolo,[71a,71b] F. Spanò,[75] R. Spighi,[19a] G. Spigo,[29] F. Spila,[131a,131b] R. Spiwoks,[29] M. Spousta,[125] T. Spreitzer,[157] B. Spurlock,[7] R. D. St. Denis,[52] T. Stahl,[140] J. Stahlman,[119] R. Stamen,[57a] E. Stanecka,[38] R. W. Stanek,[5] C. Stanescu,[133a] S. Stapnes,[116] E. A. Starchenko,[127] J. Stark,[54] P. Staroba,[124] P. Starovoitov,[90] A. Staude,[97] P. Stavina,[143a] G. Stavropoulos,[14] G. Steele,[52] P. Steinbach,[43] P. Steinberg,[24] I. Stekl,[126] B. Stelzer,[141] H. J. Stelzer,[87] O. Stelzer-Chilton,[158a] H. Stenzel,[51] S. Stern,[98] K. Stevenson,[74] G. A. Stewart,[29] J. A. Stillings,[20] M. C. Stockton,[29] K. Stoerig,[47] G. Stoicea,[25a] S. Stonjek,[98] P. Strachota,[125] A. R. Stradling,[7] A. Straessner,[43] J. Strandberg,[146] S. Strandberg,[145a,145b] A. Strandlie,[116] M. Strang,[108] E. Strauss,[142] M. Strauss,[110] P. Strizenec,[143b] R. Ströhmer,[172] D. M. Strom,[113] J. A. Strong,[75,a] R. Stroynowski,[39] J. Strube,[128] B. Stugu,[13] I. Stumer,[24,a] J. Stupak,[147] P. Sturm,[173] N. A. Styles,[41] D. A. Soh,[150,t] D. Su,[142] HS. Subramania,[2] A. Succurro,[11] Y. Sugaya,[115] T. Sugimoto,[100] C. Suhr,[105] K. Suita,[66] M. Suk,[125] V. V. Sulin,[93] S. Sultansoy,[3d] T. Sumida,[67] X. Sun,[54] J. E. Sundermann,[47] K. Suruliz,[138] S. Sushkov,[11] G. Susinno,[36a,36b] M. R. Sutton,[148] Y. Suzuki,[65] Y. Suzuki,[66] M. Svatos,[124] Yu. M. Sviridov,[127] S. Swedish,[167] I. Sykora,[143a] T. Sykora,[125] B. Szeless,[29] J. Sánchez,[166] D. Ta,[104] K. Tackmann,[41] A. Taffard,[162] R. Tafirout,[158a] N. Taiblum,[152] Y. Takahashi,[100] H. Takai,[24] R. Takashima,[68] H. Takeda,[66] T. Takeshita,[139] M. Talby,[82] A. Talyshev,[106,g] M. C. Tamsett,[24] J. Tanaka,[154] R. Tanaka,[114] S. Tanaka,[130] S. Tanaka,[65] Y. Tanaka,[99] K. Tani,[66] N. Tannoury,[82] G. P. Tappern,[29] S. Tapprogge,[80] D. Tardif,[157] S. Tarem,[151] F. Tarrade,[28] G. F. Tartarelli,[88a] P. Tas,[125]

M. Tasevsky,[124] E. Tassi,[36a,36b] M. Tatarkhanov,[14] Y. Tayalati,[134d] C. Taylor,[76] F. E. Taylor,[91] G. N. Taylor,[85] W. Taylor,[158b] M. Teinturier,[114] M. Teixeira Dias Castanheira,[74] P. Teixeira-Dias,[75] K. K. Temming,[47] H. Ten Kate,[29] P. K. Teng,[150] S. Terada,[65] K. Terashi,[154] J. Terron,[79] M. Testa,[46] R. J. Teuscher,[157,k] J. Thadome,[173] J. Therhaag,[20] T. Theveneaux-Pelzer,[77] M. Thioye,[174] S. Thoma,[47] J. P. Thomas,[17] E. N. Thompson,[34] P. D. Thompson,[17] P. D. Thompson,[157] A. S. Thompson,[52] E. Thomson,[119] M. Thomson,[27] R. P. Thun,[86] F. Tian,[34] M. J. Tibbetts,[14] T. Tic,[124] V. O. Tikhomirov,[93] Y. A. Tikhonov,[106,g] S. Timoshenko,[95] P. Tipton,[174] F. J. Tique Aires Viegas,[29] S. Tisserant,[82] B. Toczek,[37] T. Todorov,[4] S. Todorova-Nova,[160] B. Toggerson,[162] J. Tojo,[65] S. Tokár,[143a] K. Tokunaga,[66] K. Tokushuku,[65] K. Tollefson,[87] M. Tomoto,[100] L. Tompkins,[30] K. Toms,[102] G. Tong,[32a] A. Tonoyan,[13] C. Topfel,[16] N. D. Topilin,[64] I. Torchiani,[29] E. Torrence,[113] H. Torres,[77] E. Torró Pastor,[166] J. Toth,[82,aa] F. Touchard,[82] D. R. Tovey,[138] T. Trefzger,[172] L. Tremblet,[29] A. Tricoli,[29] I. M. Trigger,[158a] S. Trincaz-Duvoid,[77] T. N. Trinh,[77] M. F. Tripiana,[69] W. Trischuk,[157] A. Trivedi,[24,z] B. Trocmé,[54] C. Troncon,[88a] M. Trottier-McDonald,[141] M. Trzebinski,[38] A. Trzupek,[38] C. Tsarouchas,[29] J. C-L. Tseng,[117] M. Tsiakiris,[104] P. V. Tsiareshka,[89] D. Tsionou,[4,ee] G. Tsipolitis,[9] V. Tsiskaridze,[47] E. G. Tskhadadze,[50a] I. I. Tsukerman,[94] V. Tsulaia,[14] J.-W. Tsung,[20] S. Tsuno,[65] D. Tsybychev,[147] A. Tua,[138] A. Tudorache,[25a] V. Tudorache,[25a] J. M. Tuggle,[30] M. Turala,[38] D. Turecek,[126] I. Turk Cakir,[3e] E. Turlay,[104] R. Turra,[88a,88b] P. M. Tuts,[34] A. Tykhonov,[73] M. Tylmad,[145a,145b] M. Tyndel,[128] G. Tzanakos,[8] K. Uchida,[20] I. Ueda,[154] R. Ueno,[28] M. Ugland,[13] M. Uhlenbrock,[20] M. Uhrmacher,[53] F. Ukegawa,[159] G. Unal,[29] D. G. Underwood,[5] A. Undrus,[24] G. Unel,[162] Y. Unno,[65] D. Urbaniec,[34] G. Usai,[7] M. Uslenghi,[118a,118b] L. Vacavant,[82] V. Vacek,[126] B. Vachon,[84] S. Vahsen,[14] J. Valenta,[124] P. Valente,[131a] S. Valentinetti,[19a,19b] S. Valkar,[125] E. Valladolid Gallego,[166] S. Vallecorsa,[151] J. A. Valls Ferrer,[166] H. van der Graaf,[104] E. van der Kraaij,[104] R. Van Der Leeuw,[104] E. van der Poel,[104] D. van der Ster,[29] N. van Eldik,[83] P. van Gemmeren,[5] Z. van Kesteren,[104] I. van Vulpen,[104] M. Vanadia,[98] W. Vandelli,[29] G. Vandoni,[29] A. Vaniachine,[5] P. Vankov,[41] F. Vannucci,[77] F. Varela Rodriguez,[29] R. Vari,[131a] E. W. Varnes,[6] D. Varouchas,[14] A. Vartapetian,[7] K. E. Varvell,[149] V. I. Vassilakopoulos,[55] F. Vazeille,[33] G. Vegni,[88a,88b] J. J. Veillet,[114] C. Vellidis,[8] F. Veloso,[123a] R. Veness,[29] S. Veneziano,[131a] A. Ventura,[71a,71b] D. Ventura,[137] M. Venturi,[47] N. Venturi,[157] V. Vercesi,[118a] M. Verducci,[137] W. Verkerke,[104] J. C. Vermeulen,[104] A. Vest,[43] M. C. Vetterli,[141,e] I. Vichou,[164] T. Vickey,[144b,ff] O. E. Vickey Boeriu,[144b] G. H. A. Viehhauser,[117] S. Viel,[167] M. Villa,[19a,19b] M. Villaplana Perez,[166] E. Vilucchi,[46] M. G. Vincter,[28] E. Vinek,[29] V. B. Vinogradov,[64] M. Virchaux,[135,a] J. Virzi,[14] O. Vitells,[170] M. Viti,[41] I. Vivarelli,[47] F. Vives Vaque,[2] S. Vlachos,[9] D. Vladoiu,[97] M. Vlasak,[126] N. Vlasov,[20] A. Vogel,[20] P. Vokac,[126] G. Volpi,[46] M. Volpi,[85] G. Volpini,[88a] H. von der Schmitt,[98] J. von Loeben,[98] H. von Radziewski,[47] E. von Toerne,[20] V. Vorobel,[125] A. P. Vorobiev,[127] V. Vorwerk,[11] M. Vos,[166] R. Voss,[29] T. T. Voss,[173] J. H. Vossebeld,[72] N. Vranjes,[12a] M. Vranjes Milosavljevic,[104] V. Vrba,[124] M. Vreeswijk,[104] T. Vu Anh,[80] R. Vuillermet,[29] I. Vukotic,[114] W. Wagner,[173] P. Wagner,[119] H. Wahlen,[173] J. Wakabayashi,[100] J. Walbersloh,[42] S. Walch,[86] J. Walder,[70] R. Walker,[97] W. Walkowiak,[140] R. Wall,[174] P. Waller,[72] C. Wang,[44] H. Wang,[171] H. Wang,[32b,gg] J. Wang,[150] J. Wang,[54] J. C. Wang,[137] R. Wang,[102] S. M. Wang,[150] A. Warburton,[84] C. P. Ward,[27] M. Warsinsky,[47] R. Wastie,[117] P. M. Watkins,[17] A. T. Watson,[17] I. J. Watson,[149] M. F. Watson,[17] G. Watts,[137] S. Watts,[81] A. T. Waugh,[149] B. M. Waugh,[76] M. Weber,[128] M. S. Weber,[16] P. Weber,[53] A. R. Weidberg,[117] P. Weigell,[98] J. Weingarten,[53] C. Weiser,[47] H. Wellenstein,[22] P. S. Wells,[29] M. Wen,[46] T. Wenaus,[24] S. Wendler,[122] Z. Weng,[150,t] T. Wengler,[29] S. Wenig,[29] N. Wermes,[20] M. Werner,[47] P. Werner,[29] M. Werth,[162] M. Wessels,[57a] C. Weydert,[54] K. Whalen,[28] S. J. Wheeler-Ellis,[162] S. P. Whitaker,[21] A. White,[7] M. J. White,[85] S. R. Whitehead,[117] D. Whiteson,[162] D. Whittington,[60] D. Wicke,[173] F. Wicek,[114] F. J. Wickens,[128] W. Wiedenmann,[171] M. Wielers,[128] P. Wienemann,[20] C. Wiglesworth,[74] L. A. M. Wiik-Fuchs,[47] P. A. Wijeratne,[76] A. Wildauer,[166] M. A. Wildt,[41,q] I. Wilhelm,[125] H. G. Wilkens,[29] J. Z. Will,[97] E. Williams,[34] H. H. Williams,[119] W. Willis,[34] S. Willocq,[83] J. A. Wilson,[17] M. G. Wilson,[142] A. Wilson,[86] I. Wingerter-Seez,[4] S. Winkelmann,[47] F. Winklmeier,[29] M. Wittgen,[142] M. W. Wolter,[38] H. Wolters,[123a,i] W. C. Wong,[40] G. Wooden,[86] B. K. Wosiek,[38] J. Wotschack,[29] M. J. Woudstra,[83] K. W. Wozniak,[38] K. Wraight,[52] C. Wright,[52] M. Wright,[52] B. Wrona,[72] S. L. Wu,[171] X. Wu,[48] Y. Wu,[32b,hh] E. Wulf,[34] R. Wunstorf,[42] B. M. Wynne,[45] S. Xella,[35] M. Xiao,[135] S. Xie,[47] Y. Xie,[32a] C. Xu,[32b,w] D. Xu,[138] G. Xu,[32a] B. Yabsley,[149] S. Yacoob,[144b] M. Yamada,[65] H. Yamaguchi,[154] A. Yamamoto,[65] K. Yamamoto,[63] S. Yamamoto,[154] T. Yamamura,[154] T. Yamanaka,[154] J. Yamaoka,[44] T. Yamazaki,[154] Y. Yamazaki,[66] Z. Yan,[21] H. Yang,[86] U. K. Yang,[81] Y. Yang,[60] Y. Yang,[32a] Z. Yang,[145a,145b] S. Yanush,[90] Y. Yao,[14] Y. Yasu,[65] G. V. Ybeles Smit,[129] J. Ye,[39] S. Ye,[24] M. Yilmaz,[3c] R. Yoosoofmiya,[122] K. Yorita,[169] R. Yoshida,[5] C. Young,[142] S. Youssef,[21] D. Yu,[24] J. Yu,[7] J. Yu,[111] L. Yuan,[32a,ii] A. Yurkewicz,[105] B. Zabinski,[38] V. G. Zaets,[127] R. Zaidan,[62]

A. M. Zaitsev,[127] Z. Zajacova,[29] L. Zanello,[131a,131b] P. Zarzhitsky,[39] A. Zaytsev,[106] C. Zeitnitz,[173] M. Zeller,[174] M. Zeman,[124] A. Zemla,[38] C. Zendler,[20] O. Zenin,[127] T. Ženiš,[143a] Z. Zinonos,[121a,121b] S. Zenz,[14] D. Zerwas,[114] G. Zevi della Porta,[56] Z. Zhan,[32d] D. Zhang,[32b,gg] H. Zhang,[87] J. Zhang,[5] X. Zhang,[32d] Z. Zhang,[114] L. Zhao,[107] T. Zhao,[137] Z. Zhao,[32b] A. Zhemchugov,[64] S. Zheng,[32a] J. Zhong,[117] B. Zhou,[86] N. Zhou,[162] Y. Zhou,[150] C. G. Zhu,[32d] H. Zhu,[41] J. Zhu,[86] Y. Zhu,[32b] X. Zhuang,[97] V. Zhuravlov,[98] D. Zieminska,[60] R. Zimmermann,[20] S. Zimmermann,[20] S. Zimmermann,[47] M. Ziolkowski,[140] R. Zitoun,[4] L. Živković,[34] V. V. Zmouchko,[127,a] G. Zobernig,[171] A. Zoccoli,[19a,19b] Y. Zolnierowski,[4] A. Zsenei,[29] M. zur Nedden,[15] V. Zutshi,[105] and L. Zwalinski[29]

(ATLAS Collaboration)

[1]*University at Albany, Albany, New York, USA*
[2]*Department of Physics, University of Alberta, Edmonton, Alberta, Canada*
[3a]*Department of Physics, Ankara University, Ankara, Turkey*
[3b]*Department of Physics, Dumlupinar University, Kutahya, Turkey*
[3c]*Department of Physics, Gazi University, Ankara, Turkey*
[3d]*Division of Physics, TOBB University of Economics and Technology, Ankara, Turkey*
[3e]*Turkish Atomic Energy Authority, Ankara, Turkey*
[4]*LAPP, CNRS/IN2P3 and Université de Savoie, Annecy-le-Vieux, France*
[5]*High Energy Physics Division, Argonne National Laboratory, Argonne, Illinois, USA*
[6]*Department of Physics, University of Arizona, Tucson, Arizona, USA*
[7]*Department of Physics, The University of Texas at Arlington, Arlington, Texas, USA*
[8]*Physics Department, University of Athens, Athens, Greece*
[9]*Physics Department, National Technical University of Athens, Zografou, Greece*
[10]*Institute of Physics, Azerbaijan Academy of Sciences, Baku, Azerbaijan*
[11]*Institut de Física d'Altes Energies and Departament de Física de la Universitat Autònoma de Barcelona and ICREA, Barcelona, Spain*
[12a]*Institute of Physics, University of Belgrade, Belgrade, Serbia*
[12b]*Vinca Institute of Nuclear Sciences, Belgrade, Serbia*
[13]*Department for Physics and Technology, University of Bergen, Bergen, Norway*
[14]*Physics Division, Lawrence Berkeley National Laboratory and University of California, Berkeley, California, USA*
[15]*Department of Physics, Humboldt University, Berlin, Germany*
[16]*Albert Einstein Center for Fundamental Physics and Laboratory for High Energy Physics, University of Bern, Bern, Switzerland*
[17]*School of Physics and Astronomy, University of Birmingham, Birmingham, United Kingdom*
[18a]*Department of Physics, Bogazici University, Istanbul, Turkey*
[18b]*Division of Physics, Dogus University, Istanbul, Turkey*
[18c]*Department of Physics Engineering, Gaziantep University, Gaziantep, Turkey*
[18d]*Department of Physics, Istanbul Technical University, Istanbul, Turkey*
[19a]*INFN Sezione di Bologna, Italy*
[19b]*Dipartimento di Fisica, Università di Bologna, Bologna, Italy*
[20]*Physikalisches Institut, University of Bonn, Bonn, Germany*
[21]*Department of Physics, Boston University, Boston, Massachusetts, USA*
[22]*Department of Physics, Brandeis University, Waltham, Massachusetts, USA*
[23a]*Universidade Federal do Rio De Janeiro COPPE/EE/IF, Rio de Janeiro, Brazil*
[23b]*Federal University of Juiz de Fora (UFJF), Juiz de Fora, Brazil*
[23c]*Federal University of Sao Joao del Rei (UFSJ), Sao Joao del Rei, Brazil*
[23d]*Instituto de Fisica, Universidade de Sao Paulo, Sao Paulo, Brazil*
[24]*Physics Department, Brookhaven National Laboratory, Upton, New York, USA*
[25a]*National Institute of Physics and Nuclear Engineering, Bucharest, Romania*
[25b]*University Politehnica Bucharest, Bucharest, Romania*
[25c]*West University in Timisoara, Timisoara, Romania*
[26]*Departamento de Física, Universidad de Buenos Aires, Buenos Aires, Argentina*
[27]*Cavendish Laboratory, University of Cambridge, Cambridge, United Kingdom*
[28]*Department of Physics, Carleton University, Ottawa, Ontario, Canada*
[29]*CERN, Geneva, Switzerland*
[30]*Enrico Fermi Institute, University of Chicago, Chicago, Illinois, USA*
[31a]*Departamento de Fisica, Pontificia Universidad Católica de Chile, Santiago, Chile*
[31b]*Departamento de Física, Universidad Técnica Federico Santa María, Valparaíso, Chile*
[32a]*Institute of High Energy Physics, Chinese Academy of Sciences, Beijing, China*

[32b]Department of Modern Physics, University of Science and Technology of China, Anhui, China
[32c]Department of Physics, Nanjing University, Jiangsu, China
[32d]High Energy Physics Group, Shandong University, Shandong, China
[33]Laboratoire de Physique Corpusculaire, Clermont Université and Université Blaise Pascal and CNRS/IN2P3, Aubiere Cedex, France
[34]Nevis Laboratory, Columbia University, Irvington, New York, USA
[35]Niels Bohr Institute, University of Copenhagen, Kobenhavn, Denmark
[36a]INFN Gruppo Collegato di Cosenza, Italy
[36b]Dipartimento di Fisica, Università della Calabria, Arcavata di Rende, Italy
[37]Faculty of Physics and Applied Computer Science, AGH-University of Science and Technology, Krakow, Poland
[38]The Henryk Niewodniczanski Institute of Nuclear Physics, Polish Academy of Sciences, Krakow, Poland
[39]Physics Department, Southern Methodist University, Dallas, Texas, USA
[40]Physics Department, University of Texas at Dallas, Richardson, Texas, USA
[41]DESY, Hamburg and Zeuthen, Germany
[42]Institut für Experimentelle Physik IV, Technische Universität Dortmund, Dortmund, Germany
[43]Institut für Kern-und Teilchenphysik, Technical University Dresden, Dresden, Germany
[44]Department of Physics, Duke University, Durham, North Carolina, USA
[45]SUPA-School of Physics and Astronomy, University of Edinburgh, Edinburgh, United Kingdom
[46]INFN Laboratori Nazionali di Frascati, Frascati, Italy
[47]Fakultät für Mathematik und Physik, Albert-Ludwigs-Universität, Freiburg i.Br., Germany
[48]Section de Physique, Université de Genève, Geneva, Switzerland
[49a]INFN Sezione di Genova, Italy
[49b]Dipartimento di Fisica, Università di Genova, Genova, Italy
[50a]E.Andronikashvili Institute of Physics, Georgian Academy of Sciences, Tbilisi, Georgia
[50b]High Energy Physics Institute, Tbilisi State University, Tbilisi, Georgia
[51]II Physikalisches Institut, Justus-Liebig-Universität Giessen, Giessen, Germany
[52]SUPA-School of Physics and Astronomy, University of Glasgow, Glasgow, United Kingdom
[53]II Physikalisches Institut, Georg-August-Universität, Göttingen, Germany
[54]Laboratoire de Physique Subatomique et de Cosmologie, Université Joseph Fourier and CNRS/IN2P3 and Institut National Polytechnique de Grenoble, Grenoble, France
[55]Department of Physics, Hampton University, Hampton, Virginia, USA
[56]Laboratory for Particle Physics and Cosmology, Harvard University, Cambridge, Massachusetts, USA
[57a]Kirchhoff-Institut für Physik, Ruprecht-Karls-Universität Heidelberg, Heidelberg, Germany
[57b]Physikalisches Institut, Ruprecht-Karls-Universität Heidelberg, Heidelberg, Germany
[57c]ZITI Institut für technische Informatik, Ruprecht-Karls-Universität Heidelberg, Mannheim, Germany
[58]Faculty of Science, Hiroshima University, Hiroshima, Japan
[59]Faculty of Applied Information Science, Hiroshima Institute of Technology, Hiroshima, Japan
[60]Department of Physics, Indiana University, Bloomington, Indiana, USA
[61]Institut für Astro- und Teilchenphysik, Leopold-Franzens-Universität, Innsbruck, Austria
[62]University of Iowa, Iowa City, Iowa, USA
[63]Department of Physics and Astronomy, Iowa State University, Ames, Iowa, USA
[64]Joint Institute for Nuclear Research, JINR Dubna, Dubna, Russia
[65]KEK, High Energy Accelerator Research Organization, Tsukuba, Japan
[66]Graduate School of Science, Kobe University, Kobe, Japan
[67]Faculty of Science, Kyoto University, Kyoto, Japan
[68]Kyoto University of Education, Kyoto, Japan
[69]Instituto de Física La Plata, Universidad Nacional de La Plata and CONICET, La Plata, Argentina
[70]Physics Department, Lancaster University, Lancaster, United Kingdom
[71a]INFN Sezione di Lecce, Italy
[71b]Dipartimento di Fisica, Università del Salento, Lecce, Italy
[72]Oliver Lodge Laboratory, University of Liverpool, Liverpool, United Kingdom
[73]Department of Physics, Jožef Stefan Institute and University of Ljubljana, Ljubljana, Slovenia
[74]School of Physics and Astronomy, Queen Mary University of London, London, United Kingdom
[75]Department of Physics, Royal Holloway University of London, Surrey, United Kingdom
[76]Department of Physics and Astronomy, University College London, London, United Kingdom
[77]Laboratoire de Physique Nucléaire et de Hautes Energies, UPMC and Université Paris-Diderot and CNRS/IN2P3, Paris, France
[78]Fysiska institutionen, Lunds universitet, Lund, Sweden
[79]Departamento de Fisica Teorica C-15, Universidad Autonoma de Madrid, Madrid, Spain
[80]Institut für Physik, Universität Mainz, Mainz, Germany

[81]*School of Physics and Astronomy, University of Manchester, Manchester, United Kingdom*
[82]*CPPM, Aix-Marseille Université and CNRS/IN2P3, Marseille, France*
[83]*Department of Physics, University of Massachusetts, Amherst, Massachusetts, USA*
[84]*Department of Physics, McGill University, Montreal, Quebec, Canada*
[85]*School of Physics, University of Melbourne, Victoria, Australia*
[86]*Department of Physics, The University of Michigan, Ann Arbor, Michigan, USA*
[87]*Department of Physics and Astronomy, Michigan State University, East Lansing, Michigan, USA*
[88a]*INFN Sezione di Milano, Italy*
[88b]*Dipartimento di Fisica, Università di Milano, Milano, Italy*
[89]*B.I. Stepanov Institute of Physics, National Academy of Sciences of Belarus, Minsk, Republic of Belarus*
[90]*National Scientific and Educational Centre for Particle and High Energy Physics, Minsk, Republic of Belarus*
[91]*Department of Physics, Massachusetts Institute of Technology, Cambridge, Massachusetts, USA*
[92]*Group of Particle Physics, University of Montreal, Montreal, Quebec, Canada*
[93]*P.N. Lebedev Institute of Physics, Academy of Sciences, Moscow, Russia*
[94]*Institute for Theoretical and Experimental Physics (ITEP), Moscow, Russia*
[95]*Moscow Engineering and Physics Institute (MEPhI), Moscow, Russia*
[96]*Skobeltsyn Institute of Nuclear Physics, Lomonosov Moscow State University, Moscow, Russia*
[97]*Fakultät für Physik, Ludwig-Maximilians-Universität München, München, Germany*
[98]*Max-Planck-Institut für Physik (Werner-Heisenberg-Institut), München, Germany*
[99]*Nagasaki Institute of Applied Science, Nagasaki, Japan*
[100]*Graduate School of Science, Nagoya University, Nagoya, Japan*
[101a]*INFN Sezione di Napoli, Italy*
[101b]*Dipartimento di Scienze Fisiche, Università di Napoli, Napoli, Italy*
[102]*Department of Physics and Astronomy, University of New Mexico, Albuquerque, New Mexico, USA*
[103]*Institute for Mathematics, Astrophysics and Particle Physics, Radboud University Nijmegen/Nikhef, Nijmegen, Netherlands*
[104]*Nikhef National Institute for Subatomic Physics and University of Amsterdam, Amsterdam, Netherlands*
[105]*Department of Physics, Northern Illinois University, DeKalb, Illinois, USA*
[106]*Budker Institute of Nuclear Physics, SB RAS, Novosibirsk, Russia*
[107]*Department of Physics, New York University, New York, New York, USA*
[108]*Ohio State University, Columbus, Ohio, USA*
[109]*Faculty of Science, Okayama University, Okayama, Japan*
[110]*Homer L. Dodge Department of Physics and Astronomy, University of Oklahoma, Norman, Oklahoma, USA*
[111]*Department of Physics, Oklahoma State University, Stillwater, Oklahoma, USA*
[112]*Palacký University, RCPTM, Olomouc, Czech Republic*
[113]*Center for High Energy Physics, University of Oregon, Eugene, Oregon, USA*
[114]*LAL, Univ. Paris-Sud and CNRS/IN2P3, Orsay, France*
[115]*Graduate School of Science, Osaka University, Osaka, Japan*
[116]*Department of Physics, University of Oslo, Oslo, Norway*
[117]*Department of Physics, Oxford University, Oxford, United Kingdom*
[118a]*INFN Sezione di Pavia, Italy*
[118b]*Dipartimento di Fisica Nucleare e Teorica, Università di Pavia, Pavia, Italy*
[119]*Department of Physics, University of Pennsylvania, Philadelphia, Pennsylvania, USA*
[120]*Petersburg Nuclear Physics Institute, Gatchina, Russia*
[121a]*INFN Sezione di Pisa, Italy*
[121b]*Dipartimento di Fisica E. Fermi, Università di Pisa, Pisa, Italy*
[122]*Department of Physics and Astronomy, University of Pittsburgh, Pittsburgh, Pennsylvania, USA*
[123a]*Laboratorio de Instrumentacao e Fisica Experimental de Particulas-LIP, Lisboa, Portugal*
[123b]*Departamento de Fisica Teorica y del Cosmos and CAFPE, Universidad de Granada, Granada, Spain*
[124]*Institute of Physics, Academy of Sciences of the Czech Republic, Praha, Czech Republic*
[125]*Faculty of Mathematics and Physics, Charles University in Prague, Praha, Czech Republic*
[126]*Czech Technical University in Prague, Praha, Czech Republic*
[127]*State Research Center Institute for High Energy Physics, Protvino, Russia*
[128]*Particle Physics Department, Rutherford Appleton Laboratory, Didcot, United Kingdom*
[129]*Physics Department, University of Regina, Regina, Saskatchewan, Canada*
[130]*Ritsumeikan University, Kusatsu, Shiga, Japan*
[131a]*INFN Sezione di Roma I, Italy*
[131b]*Dipartimento di Fisica, Università La Sapienza, Roma, Italy*
[132a]*INFN Sezione di Roma Tor Vergata, Italy*
[132b]*Dipartimento di Fisica, Università di Roma Tor Vergata, Roma, Italy*
[133a]*INFN Sezione di Roma Tre, Italy*

[133b]Dipartimento di Fisica, Università Roma Tre, Roma, Italy
[134a]Faculté des Sciences Ain Chock, Réseau Universitaire de Physique des Hautes Energies-Université Hassan II, Casablanca, Morocco
[134b]Centre National de l'Energie des Sciences Techniques Nucleaires, Rabat, Morocco
[134c]Université Cadi Ayyad, Faculté des sciences Semlalia Département de Physique, B.P. 2390 Marrakech 40000, Morocco
[134d]Faculté des Sciences, Université Mohamed Premier and LPTPM, Oujda, Morocco
[134e]Faculté des Sciences, Université Mohammed V, Rabat, Morocco
[135]DSM/IRFU (Institut de Recherches sur les Lois Fondamentales de l'Univers), CEA Saclay (Commissariat a l'Energie Atomique), Gif-sur-Yvette, France
[136]Santa Cruz Institute for Particle Physics, University of California Santa Cruz, Santa Cruz, California, USA
[137]Department of Physics, University of Washington, Seattle, Washington, USA
[138]Department of Physics and Astronomy, University of Sheffield, Sheffield, United Kingdom
[139]Department of Physics, Shinshu University, Nagano, Japan
[140]Fachbereich Physik, Universität Siegen, Siegen, Germany
[141]Department of Physics, Simon Fraser University, Burnaby, British Columbia, Canada
[142]SLAC National Accelerator Laboratory, Stanford, California, USA
[143a]Faculty of Mathematics, Physics & Informatics, Comenius University, Bratislava, Slovak Republic
[143b]Department of Subnuclear Physics, Institute of Experimental Physics of the Slovak Academy of Sciences, Kosice, Slovak Republic
[144a]Department of Physics, University of Johannesburg, Johannesburg, South Africa
[144b]School of Physics, University of the Witwatersrand, Johannesburg, South Africa
[145a]Department of Physics, Stockholm University, Sweden
[145b]The Oskar Klein Centre, Stockholm, Sweden
[146]Physics Department, Royal Institute of Technology, Stockholm, Sweden
[147]Department of Physics and Astronomy, Stony Brook University, Stony Brook, New York, USA
[148]Department of Physics and Astronomy, University of Sussex, Brighton, United Kingdom
[149]School of Physics, University of Sydney, Sydney, Australia
[150]Institute of Physics, Academia Sinica, Taipei, Taiwan
[151]Department of Physics, Technion: Israel Inst. of Technology, Haifa, Israel
[152]Raymond and Beverly Sackler School of Physics and Astronomy, Tel Aviv University, Tel Aviv, Israel
[153]Department of Physics, Aristotle University of Thessaloniki, Thessaloniki, Greece
[154]International Center for Elementary Particle Physics and Department of Physics, The University of Tokyo, Tokyo, Japan
[155]Graduate School of Science and Technology, Tokyo Metropolitan University, Tokyo, Japan
[156]Department of Physics, Tokyo Institute of Technology, Tokyo, Japan
[157]Department of Physics, University of Toronto, Toronto, Ontario, Canada
[158a]TRIUMF, Vancouver, British Columbia, Canada
[158b]Department of Physics and Astronomy, York University, Toronto, Ontario, Canada
[159]Institute of Pure and Applied Sciences, University of Tsukuba, 1-1-1 Tennodai,Tsukuba, Ibaraki 305-8571, Japan
[160]Science and Technology Center, Tufts University, Medford, Massachusetts, USA
[161]Centro de Investigaciones, Universidad Antonio Narino, Bogota, Colombia
[162]Department of Physics and Astronomy, University of California Irvine, Irvine, California, USA
[163a]INFN Gruppo Collegato di Udine, Italy
[163b]ICTP, Trieste, Italy
[163c]Dipartimento di Chimica, Fisica e Ambiente, Università di Udine, Udine, Italy
[164]Department of Physics, University of Illinois, Urbana, Illinois, USA
[165]Department of Physics and Astronomy, University of Uppsala, Uppsala, Sweden
[166]Instituto de Física Corpuscular (IFIC) and Departamento de Física Atómica, Molecular y Nuclear and Departamento de Ingenierá Electrónica and Instituto de Microelectrónica de Barcelona (IMB-CNM), University of Valencia and CSIC, Valencia, Spain
[167]Department of Physics, University of British Columbia, Vancouver, British Columbia, Canada
[168]Department of Physics and Astronomy, University of Victoria, Victoria, British Columbia, Canada
[169]Waseda University, Tokyo, Japan
[170]Department of Particle Physics, The Weizmann Institute of Science, Rehovot, Israel
[171]Department of Physics, University of Wisconsin, Madison, Wisconsin, USA
[172]Fakultät für Physik und Astronomie, Julius-Maximilians-Universität, Würzburg, Germany
[173]Fachbereich C Physik, Bergische Universität Wuppertal, Wuppertal, Germany
[174]Department of Physics, Yale University, New Haven, Connecticut, USA
[175]Yerevan Physics Institute, Yerevan, Armenia
[176]Domaine scientifique de la Doua, Centre de Calcul CNRS/IN2P3, Villeurbanne Cedex, France

[a]Deceased.
[b]Also at Laboratorio de Instrumentacao e Fisica Experimental de Particulas-LIP, Lisboa, Portugal.
[c]Also at Faculdade de Ciencias and CFNUL, Universidade de Lisboa, Lisboa, Portugal.
[d]Also at Particle Physics Department, Rutherford Appleton Laboratory, Didcot, United Kingdom.
[e]Also at TRIUMF, Vancouver, BC, Canada.
[f]Also at Department of Physics, California State University, Fresno, CA, USA.
[g]Also at Novosibirsk State University, Novosibirsk, Russia.
[h]Also at Fermilab, Batavia, IL, USA.
[i]Also at Department of Physics, University of Coimbra, Coimbra, Portugal.
[j]Also at Università di Napoli Parthenope, Napoli, Italy.
[k]Also at Institute of Particle Physics (IPP), Canada.
[l]Also at Department of Physics, Middle East Technical University, Ankara, Turkey.
[m]Also at Louisiana Tech University, Ruston, LA, USA.
[n]Also at Department of Physics and Astronomy, University College London, London, United Kingdom.
[o]Also at Group of Particle Physics, University of Montreal, Montreal, QC, Canada.
[p]Also at Institute of Physics, Azerbaijan Academy of Sciences, Baku, Azerbaijan.
[q]Also at Institut für Experimentalphysik, Universität Hamburg, Hamburg, Germany.
[r]Also at Manhattan College, New York, NY, USA.
[s]Also at CPPM, Aix-Marseille Université and CNRS/IN2P3, Marseille, France.
[t]Also at School of Physics and Engineering, Sun Yat-sen University, Guanzhou, China.
[u]Also at Academia Sinica Grid Computing, Institute of Physics, Academia Sinica, Taipei, Taiwan.
[y]Also at High Energy Physics Group, Shandong University, Shandong, China.
[w]Also at DSM/IRFU (Institut de Recherches sur les Lois Fondamentales de l'Univers), CEA Saclay (Commissariat a l'Energie Atomique), Gif-sur-Yvette, France.
[x]Also at Section de Physique, Université de Genève, Geneva, Switzerland.
[y]Also at Departamento de Fisica, Universidade de Minho, Braga, Portugal.
[z]Also at Department of Physics and Astronomy, University of South Carolina, Columbia, SC, USA.
[aa]Also at KFKI Research Institute for Particle and Nuclear Physics, Budapest, Hungary.
[bb]Also at California Institute of Technology, Pasadena, CA, USA.
[cc]Also at Institute of Physics, Jagiellonian University, Krakow, Poland.
[dd]Also at Institute of High Energy Physics, Chinese Academy of Sciences, Beijing, China.
[ee]Also at Department of Physics and Astronomy, University of Sheffield, Sheffield, United Kingdom.
[ff]Also at Department of Physics, Oxford University, Oxford, United Kingdom.
[gg]Also at Institute of Physics, Academia Sinica, Taipei, Taiwan.
[hh]Also at Department of Physics, The University of Michigan, Ann Arbor. MI, USA.
[ii]Also at Laboratoire de Physique Nucléaire et de Hautes Energies, UPMC and Université Paris-Diderot and CNRS/IN2P3, Paris, France.